Master's thesis

NTNU
Norwegian University of Science and Technology
Faculty of Natural Sciences
Department of Biotechnology and Food Science

Hilde Kristoffersen

β-1,3-glucan and β-1,3-glucan-based diblock polysaccharides: Preparation, characterization, and solution behavior

Master's thesis in Biotechnology
Supervisor: Bjørn E. Christensen
Co-supervisor: Amalie Solberg
June 2021

NTNU
Norwegian University of Science and Technology

Hilde Kristoffersen

β-1,3-glucan and β-1,3-glucan-based diblock polysaccharides: Preparation, characterization, and solution behavior

Master's thesis in Biotechnology
Supervisor: Bjørn E. Christensen
Co-supervisor: Amalie Solberg
June 2021

Norwegian University of Science and Technology
Faculty of Natural Sciences
Department of Biotechnology and Food Science

NTNU
Norwegian University of
Science and Technology

Preface

This master thesis was conducted at the Department of Biotechnology and Food Science at the Norwegian University of Science and Technology (NTNU) in the time period September 2020 to June 2021.

First of all, I would like to thank my supervisor Bjørn E. Christensen for guidance and discussions throughout the course of this work. Secondly, I wish to express my gratitude to my co-supervisor and PhD candidate Amalie Solberg for all the invaluable help and advice during the laboratory work and the writing process of this thesis. I would also like to thank Olav A. Aarstad for technical support and guidance in the laboratory.

A big thank you to my fellow master students Mina Gravdahl, Trine Muren, and Marianne Von Krogh for support and encouragement.

Last but not least, I would like to thank my family and friends for all the love and support during these five years at NTNU.

Trondheim, June 21th, 2021

Hilde Kristoffersen

Abstract

β-1,3-glucans are one of the most widely reported bioactive polysaccharides with potential use in various industries. A water-soluble preparation of β-1,3-glucan with 1,6-linked branches (SBG), originally isolated from the cell walls of *Saccharomyces cerevisiae* was studied in this thesis. Although being water-soluble, SBG tend to aggregate strongly in aqueous solution. The aim of this master thesis was to prepare samples of fully soluble SBG by terminal activation with the bifunctional dioxyamine propanediylbishydroxylamine (PDHA) and preparation of SBG-based block polysaccharides.

SBG was first activated by terminal conjugation to PDHA. Conjugation of the dioxyamine resulted in a mixture of (*E*)- and (*Z*)-oximes and β-*N*-pyranoside. Stable secondary amines were obtained by reduction with 2-picoline borane (PB). PDHA-activated SBG (SBG-PDHA) was further separated and fractionated by size exclusion chromatography (SEC) to obtain samples of narrower molar mass distributions. Fractions of SBG-PDHA collected from the separation were studied by SEC with multiangle light-scattering (SEC-MALS) detector and a viscosity detector both with and without pretreatment at high temperature. The strongly aggregating material could not be dispersed as single chains in water following terminal activation with PDHA. However, aggregating SBG-PDHA could be dispersed as single chains in dimethylacetamide (DMAc) containing 0.9 % LiCl.

Block polysaccharides were prepared from PDHA-activated SBG by attaching dextran and alginate as the second block. Coupling of the blocks through their reducing ends ensures retention and allow combination of their intrinsic properties. Kinetic studies for the conjugation of dextran and alginate to PDHA-activated SBG are presented. Attachment of alginate turned out to be faster and resulted in higher yields of diblocks compared to the attachment of dextran. Protocols established for the preparation of short SBG-*b*-dextran and SBG-*b*-alginate diblock oligosaccharides were used to prepare diblocks of longer chain lengths. Attachment of dextran and alginate to PDHA-activated SBG in this case did not appear to increase the solubility enough to counter the aggregation of SBG. Increasing the chain length of the second block might be the answer to obtain fully soluble SBG.

Sammendrag

β-glukaner er en av de mest rapporterte biologisk aktive polysakkaridene og anses å ha et stort potensial i ulike industrier. Et vannløselig preparat av β-1,3-glukan med forgreninger koblet via 1,6-bindinger (SBG), opprinnelig isolert fra celleveggene til *Saccharomyces cerevisiae*, ble studert i denne oppgaven. Selv om SBG er vannløselig, har det en tendens til å aggregere sterkt i vandig løsning. Målet med denne masteroppgaven var å fremstille prøver av fullt løselig SBG ved terminal aktivering med det bifunksjonelle dioksyaminet propandiylbishydroksylamin (PDHA) og fremstilling av SBG-baserte blokkpolysakkarider.

SBG ble først aktivert ved terminal kobling til PDHA. Koblingen av dioksyaminet resulterte i en blanding av (*E*)- og (*Z*)-oksimer og β-*N*-pyranosid. Stabile sekundære aminer ble oppnådd ved reduksjon med 2-pikolinboran (PB). PDHA-aktivert SBG (SBG-PDHA) ble ytterligere separert og fraksjonert ved eksklusjonskromatografi (SEC) for å oppnå prøver med smalere molar massefordeling. Fraksjoner av SBG-PDHA samlet fra separasjonen ble studert ved SEC med fler-vinklet lysspredningsdetektor (SEC-MALS) og en viskositetsdetektor både med og uten forbehandling med høy temperatur. Det sterkt aggregerende materialet kunne ikke løses opp som enkeltkjeder i vann etter terminal aktivering med PDHA. Imidlertid kunne aggregerende SBG-PDHA løses opp som enkeltkjeder i dimetylacetamid (DMAc) som inneholdt 0.9 % LiCl.

Blokkpolysakkarider ble fremstilt fra PDHA-aktivert SBG ved å feste på dekstran og alginat som den andre blokken. Kobling av blokkende gjennom deres reduserende ende sikrer opprettholdelse og tillater kombinasjon av deres iboende egenskaper. Kinetiske studier for koblingen av dekstran og alginat til PDHA-aktivert SBG er presentert. Koblingen av alginat viste seg å være raskere og ga et høyere utbytte av diblokker sammenlignet med koblingen av dekstran. Protokollene etablert for framstilling av korte SBG-*b*-dekstran og SBG-*b*-alginat diblokk-oligosakkarider ble brukt til å fremstille diblokker med lengre kjedelengder. Kobling av dekstran og alginat til PDHA-aktivert SBG i dette tilfellet viste seg å ikke øke løseligheten til SBG nok til å motvirke aggregeringen. Å øke kjedelengden til den andre blokken kan være svaret for å oppnå fullt løselig SBG.

Abbreviations

AmAc	Ammonium acetate
DMAc/LiCl	Dimethylacetamide/lithium chloride
DMSO	Dimethyl sulfoxide
DP	Degree of polymerization
DP_n	Number average degree of polymerization
^{1}H-NMR	Proton nuclear magnetic resonance
M_n	Number average molecular weight
MQ-water	MilliQ-water (ultrapure water)
M_w	Weight average molecular weight
MWCO	Molecular weight cut-off
NaAc	Sodium acetate
PB	2-methylpyridine borane complex
PDHA	*O,O*'-1,3-propanediylboshydroxylamine
pK_a	Acid dissociation constant
SBG	Water-soluble β-1,3-glucan
SEC	Size exclusion chromatography
SEC-MALS	Size exclusion chromatography with multiangle light scattering
TSP	3-(Trimethylsilyl)-propionic-2,2,3,3-d4 acid sodium salt

Contents

1 Introduction

Polysaccharides are one of the most abundant biopolymers in nature and considered key compounds in the field of sustainable chemistry [1]. They are renewable, ultra-lightweight, inexpensive, and they comprise a diversity of monomer units of different configurations covalently linked by various linkages, giving rise to structures of high complexity with a wide range of physical and chemical properties. Their natural products have attracted great attention in fields such as health food and medicine during the past decades due to their general safety, biocompatibility, and biodegradability in vivo [2].

Since the early 1970s, polysaccharides with significant biological activities have been discovered from a variety of sources [3]. One of the most widely reported bioactive polysaccharides are β-1,3-glucans. β-1,3-glucans derived from fungi are currently of large interest due to their ability to interact with specific receptors located on immune cells stimulating signaling pathways to enhance immune responses [4, 5]. The significance of their bioactivities is assumed to be closely correlated with specific physiochemical parameters. However, the detailed physical and chemical properties determining their biological effects has not been clarified in detail [6]. It is suggested that the branching pattern, the chain length distribution, as well as the extent and mode of aggregation greatly influences their biological activity [7]. The aggregation behavior may be an important and potential useful property in terms of many biological functions and applications. However, from a fundamental perspective and for regulatory approval the aggregation behavior must be accurately known [7, 8]. Several derivation procedures have been applied in order to obtain fully soluble β-1,3-glucans under neutral conditions. Many β-1,3-glucans are reported to dissolve as single, un-associated chains in aqueous solution following carboxymethylation or phosphorylation [7, 9]. However, methods avoiding lateral modification are sometimes more beneficial to fully preserve the integrity of the polysaccharide and therefore better preserve its chemical and biological properties [1, 10]. Thus, methods to prepare fully soluble β-1,3-glucan with optimal retention of their intrinsic properties are necessary.

The short supply of raw material for synthetic polymers and drugs have made the synthesis processes of chemical products by renewable material one of the new frontiers in basic chemistry [3]. Polysaccharide block copolymers represent a new class of sustainable engineered polymers with an enormous potential in both material science and drug delivery [1, 11].

Literature on linear block polysaccharides based on β-1,3-glucans is scarcely. However, incorporation of β-1,3-glucans in polysaccharide block copolymers promotes the possibility to extend both their properties and applications.

A water-soluble preparation of β-1,3-glucan (SBG) originally isolated from the cell wall of *S. cerevisiae* and optimized for biological activity has been developed as a possible medical device or drug [7]. As for many other β-1,3-glucans, SBG tend to aggregate strongly in aqueous solution. The aim of this master thesis was to prepare samples of fully soluble SBG of defined chain length by terminal activation with the bifunctional dioxyamine propanediylboshydroxylamine (PDHA) and by preparation of SBG-based diblock polysaccharides.

2 Theory

2.1 β-1,3-glucan

β-1,3-glucans are a group of high-molecular weight glucose polymers naturally occurring in the cell wall of many different organisms including plants, bacteria, and fungi, where they serve as important structural or skeletal elements [12]. They are neutral polysaccharides with a main chain consisting of β-1,3-linked glycopyranosyl residues with various amounts of side chains attached to the backbone through β-1,6 linkages (Figure 2.1) [3, 7].

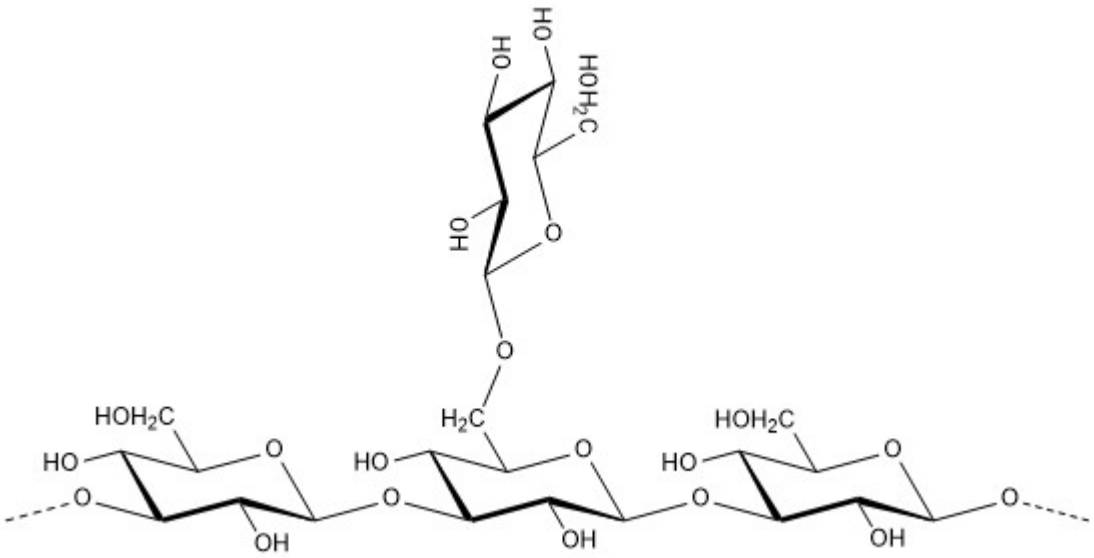

Figure 2.1: Structure of β-1,3-glucan with side chains attached through β-1,6 linkages.

2.1.1 Solution properties of β-1,3-glucans

β-1,3-glucans display a variety of solution properties depending on the molecular size and chemistry of the polysaccharide, as well as the thermal and solvent histories of the extracted polysaccharide [12]. The combination of these variables leads to a diversity of physiochemical properties of β-1,3-glucans with apparently similar structure. Not only does these properties influence the structuring in solutions, but they also influence the cellular interactions that underlie some of the promising therapeutic properties of β-1,3-glucans. Their different solubility properties have been explained based on differences in chain length or degree of polymerization (DP) as well as the frequency and distribution of side-chain branches [13]. In general, linear β-1,3-glucans without or with few branched glucose residues such as curdlan and yeast glucan are insoluble in water, while the β-1,3-glucans with higher degree of

branching such as schizophyllan, scleroglucan, and lentinan can be dissolved in water [3]. The increased water solubility of branched β-1,3-glucans can be explained by the crucial role the hydroxyl groups on the side chains play in the interaction with water.

2.1.2 Soluble β-1,3-glucan (SBG)

A water-soluble preparation of β-1,3-glucan (SBG) originally isolated from the cell wall of *S. cerevisiae* and optimized for biological activity has been developed as a possible medical device or drug [7]. Early methylation studies suggest that it contains approximately 5 branch points per 100 units in the β-1,3-glucan main chain [14]. SBG differ from other fungal branched β-1,3-glucan such as scleroglucan, schizophyllan and lentinan which are characterized by extremely high molecular weights and consistent branching patterns [8]. However, chain association or aggregation in aqueous solution is a recurrent theme despite their differences. β-1,3-glucans exhibit hydrophobicity in terms of the hydrophobic carbon rings in the polysaccharide chain which leads to limited water-solubility and self-aggregation [3]. Association between uncharged polysaccharides is stabilized by a hydrogen bond exchange reaction [12]. When the interaction or hydrogen bonding between polysaccharide chains becomes stronger than the interaction between polysaccharides and solvent, association will occur. The mode of association between β-1,3-glucans varies, from soluble triple helices as observed in scleroglucan and schizophyllan, to large soluble aggregates as observed for SBG, to water-insoluble materials as observed for curdlan [8, 15]. SBG tend to aggregate strongly in aqueous solution. The aggregation of SBG can for example be manifested by characteristically high molecular weights, but low intrinsic viscosities. This aggregating behavior complicates the characterization, including determination of chain length, of SBG in aqueous solution [10]. However, many β-1,3-glucans can dissociate as single, un-aggregated chains at in organic solvents such as DMAc/LiCl and DMSO, in dilute alkali, or at sufficiently high temperatures [8, 10, 16, 17]. Another possible strategy to obtain fully soluble SBG is to “build in” this particular property, namely solubility, by joining SBG together with another component having this desirable property [18]. Block copolymers allow for the combination of the inherent physicochemical properties of different polymers. Hence the possibility of increasing the solubility of SBG lies within the block copolymer framework.

2.2 Block copolymers

Block copolymers are structures composed of two or more constitutionally different polymer segments covalently linked at their chain termini [1]. The blocks are usually conjugated through a non-repeating atom or group of atoms called a junction unit or a linker. The blocks differ from each other in which they comprise constitutionally units derived from different species of monomer of from the same species but with a different composition or sequence distribution [19]. The construction of new block copolymer structures is an active field of research and with the advancement within polymer synthetic strategies and techniques it has become possible to create block copolymers with architectures of various complexity and well-defined composition [20, 21]. Linear block copolymers composed of two blocks in sequence are among the simplest block copolymers (Figure 2.2). Despite of their simplicity, these are the structures most studied. This is due to their ability to form a plethora of nanoscale ordered structures [20].

Figure 2.2: Block copolymer composed of two blocks in sequence conjugated at their chain termini by a bivalent linker.

2.2.1 Polysaccharide block copolymers

Following the evolvement of block copolymer chemistry, the motivation for incorporating natural polymers has increased due to the growing interest in polymers as biomaterials [20]. Block copolymers based on polysaccharides represent a new class of engineered polymers [11]. Polysaccharides are naturally abundant, biosynthesized, renewable, and generally nontoxic polymers that offers a wide structural variety, yielding divers materials with a wide range of properties and application potential [22]. They are major components of biological systems with structure- and storage-related functions as well as they play important roles in fundamental biological processes such as cell-cell communication, host-pathogen interactions, and immune responses [20, 23]. Compared to synthetic polymers, polysaccharides present beneficial properties including increased biodegradability, biocompatibility, and diverse bioactivities depending on their structure. Their benign nature and distinctive properties make them attractive building blocks in the construction of functional biomaterials and key compounds in the field of sustainable chemistry [1, 24].

2.2.2 Physicochemical properties of polysaccharide block copolymers

Polysaccharide block copolymers are relatively novel structures. Most studies performed on these structures are focused on their chemical aspects and only a few of them describe their physiochemical properties at the macromolecular level [20]. The conformation of a triblock copolymer consisting of two stiff amylose tricarbanilite chains conjugated by a flexible linker composed of a short polymethylene or poly(ethylene oxide) chain was investigated by Pfannemüller *et al*. [25]. Their goal was to determine whether the flexible linkers influenced the geometric and hydrodynamic molecular dimensions of the helical amylose tricarbanilate chains. The study showed that the linkers were not capable of changing the overall flexibility of the stiff chain. However, an unambiguous differentiation from pure amylose tricarbanilate chains was evidenced. Reibel *et al*. studied the conformation of triblock copolymers consisting of two stiff poly(γ-L-glutamate) blocks of variable lengths built around a central flexible block of poly(ethylene oxide) and they stated similar conclusions [26]. Another study investigates the solution properties of a diblock copolymer comprised of chitosan conjugated to highly water-soluble polyethylene glycol (PEG) [27]. The diblock was shown to be soluble under conditions where unmodified chitosan normally precipitates (pH > 6.5). Hence incorporation of polysaccharides with limited solubility into block copolymers can be used as a strategy to increase their solubility [27].

2.2.3 Pathway to polysaccharide block copolymers

Polysaccharides contain a large number of hydroxyl groups with relatively low reactivity. Fortunately, the saccharide residue at the ω-chain termini has higher reactivity compared to the others [22]. This enhanced reactivity is due to the equilibrium between open and closed ring form, where in open chain form a free electrophilic aldehyde group is available and can serve as a reducing agent (Figure 2.3). This unique part of the polysaccharide creates a potential site for selective derivatization and modification through chemoselective reactions [23].

Figure 2.3: Depiction of the of the open and closed ring forms of a glucose reducing end saccharide, displaying the aldehyde functional group available for further reactions.

Modern synthetic strategies for construction of polysaccharide block copolymers rely on functionalization of the reducing end in one way or another. A great advantage with end-functionalization compared to functionalization of side groups within the polymer chain is that the intrinsic chemical and biological properties of the polymer chains are better preserved as none of their lateral functions are altered [20]. One of the main synthetic strategies for the preparation of linear polysaccharide-containing block copolymers described in literature is end-to-end conjugation reactions where the polymer blocks are covalently linked at their ends due to antagonistic functions. An example of this approach is reductive amination where the reducing end of carbohydrates can be linked to amines [20].

2.3 Reductive amination

Reductive amination is a commonly used method to functionalize polysaccharide end-chains [20]. It is a two-step reaction where the reducing-end aldehyde of the polysaccharide is reacted with an amine to form an imine intermediate which is further reduced to a secondary amine in the presence of a selective reducing agent [22]. Reductive amination is an acid catalyzed reaction. The carbonyl oxygen of the aldehyde is protonated which makes it susceptible to nucleophilic attack by the amino group of the amine. Subsequent elimination of water leads to the formation of an imine or Schiff base [28, 29]. As imines have a carbon-nitrogen double bond, the imine can form as a mixture of (*E*) and (*Z*) isomers depending on the priority of the groups attached to the atoms at the double bond. The group with the atom of a higher atomic number is given the highest priority. The isomer is (*Z*) if the two groups of higher priority are on the same side of the double bond, and (*E*) if they are on opposite sides of the double bond. The (*Z*) isomer is usually less stable than the (*E*) isomer due to greater strain caused by steric arrangements [30]. Furthermore, protonation of the imine intermediate to an iminium ion promotes the hydride transfer from the reducing agent to the iminium ion and the formation of a stable secondary amine [29]. While polysaccharide block copolymers may be created using reductive amination alone, a more powerful approach involves the coupling of reductive amination with click chemistry [22].

2.3.1 Click reactions

Click chemistry is an immensely potent approach for the efficient coupling of molecular entities through reactions characterized by simple methodology and mild experimental conditions, high yields and tolerance of functional groups [20, 31]. The copper-catalyzed azide-alkyne

cycloaddition (CuAAC) reaction is the most commonly used click reaction. This technique includes the use of reductive amination to introduce the click active functionality. An alternative click reaction for the construction of polysaccharide-containing block copolymers was presented by Novoa-Carballal and Müller. This reaction involves the formation of oximes through reacting an aldehyde with an aminooxy group and was termed oxime click or oxime ligation [1]. A major advantage with this strategy is that it avoids any previous modifications to the reducing end aldehyde of the polysaccharide. This is a more effective method for direct coupling reactions compared to reductive amination as the oxyamines have higher nucleophilicity compared to amines due to the alpha effect [22]. The oxime ligation is a reversible process that proceeds under mildly acidic conditions and generates a tautomeric mixture of ligation products [32]. The aldehyde present in the open-chain form at the reducing end of the polysaccharide is attacked by oxyamines to give an hemiaminal. Subsequent water elimination leads to the formation of an equilibrium mixture composed of predominantly diastereomeric acyclic oximes in (*E*)- and (*Z*)-configuration and a small quantity cyclic *N*-glycosides (Figure 2.4) [23, 32].

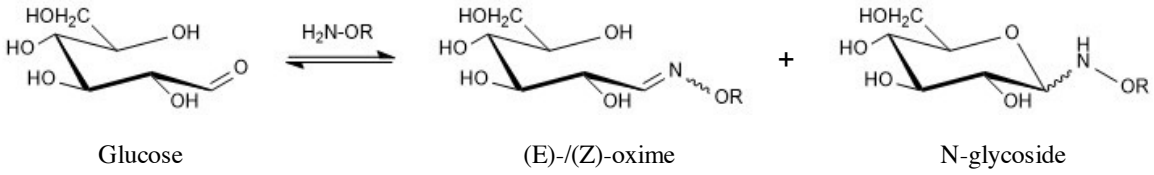

Figure 2.4: General reaction between reducing glucose and oxyamines, showing the formation of acyclic oximes in (*E*)- and (*Z*)-configuration and cyclic *N*-glycosides.

2.4 Oxyamines

Oxyamines have become very useful and efficient tools for various applications, including the construction of new glycoconjugates [33]. The reducing-end conjugation of unprotected carbohydrates with oxyamines is a highly chemo-selective reaction which take advantage of the high nucleophilicity of oxyamines. The use of oxyamines allows for the facile introduction of a variety of functionalized linkers without affecting the structural integrity of the reducing end sugar and has become a powerful method for site-specific linking of biomacromolecules [34, 35].

2.4.1 PDHA as linker molecule

O,*O*'-1,3-propanediylbishydroxylamine (PDHA) is a symmetrical molecule with a C3 backbone and reactive oxyamine groups at both ends of the molecule (Figure 2.5). The bifunctional nature of PDHA makes it a good candidate for the cross-linking of biomolecules providing a 7-atom bridge between the conjugated molecules. The pK_a of the terminal amino groups of PDHA is 4.2 [36]. PDHA has for example been used in the activation of chitooligosaccharides and as a linker molecule in the preparation of diblock oligosaccharides consisting of chitin and dextran [11, 36].

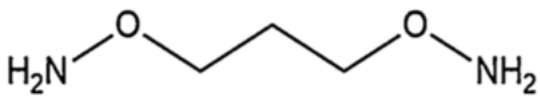

Figure 2.5: Chemical structure of the oxyamine O,O'-1,3-propanediylboshydroxylamine (PDHA).

2.5 2-picoline borane as reducing agent for oxime ligation

Reductive amination of polysaccharides requires a reducing agent to transform the imines formed during the amination reaction to a stable secondary amine. For a successful reaction it is essential to choose a reducing agent that selectively reduces the imines intermediates over the aldehydes of the saccharide. Sodium cyanoborohydride ($NaCNBH_3$) is the reagent most commonly used as reducing agent for the reductive amination of carbohydrates [37]. However, due to the generation of highly toxic by-products during the reaction several environment-friendly alternatives have been developed. The use of 2-picoline borane (PB) as reducing agent for the reductive amination reaction of aldehydes and ketones was introduced by Sato *et al*. as a greener and less toxic alternative to sodium cyanoborohydride [38]. PB (Figure 2.6) is more stable and less solvent-selective, generates no toxic waste, has high selectivity towards imines as well as it is commercially available and comes at low cost [39]. It has proven to have equal or better reducing efficacies in labelling of oligosaccharides by reductive amination compared to $NaCNBH_3$ and it can also be employed under both aqueous and non-aqueous condition which is beneficial for reactions with carbohydrates [36].

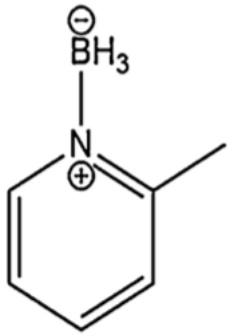

Figure 2.6: Chemical structure of the reducing agent 2-picoline borane (PB).

2.6 Dextran

Dextran is an example of a polysaccharide previously utilized in the construction of polysaccharide block copolymers [11]. Dextran is a neutral polysaccharide synthesized from sucrose by different bacterial strains, the best known being *Leuconostoc mesenteroides* [40]. It has a backbone composed of glucose monomers linked by α-1,6-glycosidic bonds with varying amounts of branches attached to the main chain by α-1,3 linkages. The α-1,6-linkages includes three bonds in the glycosidic linkages which allows much greater conformational freedom compared to the usual two-bond linkages as in 1,3- and 1,4-linked polysaccharides [12]. This provides an increased chain mobility and flexibility which is responsible for the solubility in various solvents including water, DMSO, DMAc/LiCl, among others [40].

2.7 Alginate

Alginate is another possible polysaccharide to use as a component in polysaccharide block copolymers. Alginates comprise a family of linear polysaccharides produced by brown algae and a few bacteria [41]. They can be described as binary copolymers consisting of 1,4-linked β-D-mannuronic acid (M) and α-L-guluronic acid (G) residues. Alginates are initially synthesized as homopolymeric mannuronan and G residues are enzymatically introduced through the action of C5-epimerases [42]. Stretches of continuous G residues are referred to as oligoguluronat or G-blocks. These residues adopt a $^{1}C_{4}$ conformation with diaxial linkages between G-residues resulting in a more rigid structure due to hindered rotation around the glycosidic linkage [43]. The electrostatic repulsion between the charged groups on the polymer chain will also increase the chain extension [44]. Alginates of monovalent ions are soluble in water; however, the solubility of alginates is largely dependent on the pH of the solvent as it influences the presence of electrostatic charges on the uronic acid residues.

2.8 Analytical methods

2.8.1 Nuclear magnetic resonance (NMR) spectroscopy

Nuclear magnetic resonance (NMR) spectroscopy is one of the most powerful analytical tools for structural characterization of organic compounds [45]. It has also been widely employed for structural and conformational analysis of polysaccharides. NMR spectroscopy is a method based on quantum mechanical properties of atom nuclei and their characteristic behavior when exposed to an external magnetic field. These behaviors can be detected and processed to obtain useful quantitative and qualitative data about the compound of interest [46].

All atomic nuclei carry a charge, and several nuclides have nuclear spin. A spinning charge leads to the formation of a magnetic dipole with a magnitude proportional to the nuclear spin. The intrinsic magnitude of the dipole is proportional to the nuclear spin and is expressed in terms of the nuclear magnetic moment (μ). The nuclear spin is described by a nuclear spin quantum number (I) which is determined based on nuclear mass and atomic number of the nuclei. Nuclei with I = 0 possesses no spin and cannot be observed by NMR. Furthermore, nuclei with I = ½ such as the common isotopes ^{1}H and ^{13}C are ideal for NMR as they have a uniform spherical charge distribution [45].

When magnetic nuclei are exposed to an external magnetic field, they may assume a certain number of quantum mechanical states determined by the nuclear spin number. A nucleus with spin I can assume $2I + 1$ possible states or energy levels denoted by a second quantum number (m). for nuclei with I = ½ there are two energy levels (m = ½ and m = -½). The energy difference between them (ΔE) is given by:

$$\Delta E = \left(\frac{h\gamma}{2\pi}\right)\boldsymbol{B}_0 \tag{2.1}$$

where γ and π are constants and h is Plank's constant [45]. This equation states that the energy difference is proportional to the strength of the magnetic field ($\boldsymbol{B}_0$). A transition from the lower to the higher energy level requires applied radiation with energy corresponding to ΔE:

$$\Delta E = h\nu \tag{2.2}$$

where v is the frequency of the radiation [45]. Consequently, each nucleus at a given magnetic field strength ($\boldsymbol{B}_0$) has a characteristic resonance frequency:

$$v = \frac{\gamma B_0}{2\pi} \tag{2.3}$$

NMR instruments provide short pulses of high-power radiofrequency energy that excites all nuclei of a given type. The frequency is usually on the order of mega-hertz (MHz). When the nuclei relax back to equilibrium it releases energy that is detected by the NMR instrument [45].

An ^{1}H-NMR spectrum consists of a plot of peak intensity versus frequency or chemical shift. Chemical shifts are given in ppm (10^{-6}) and are assigned relative to the chemical shift of a reference compound and is defined as:

$$\delta = \frac{v - v_{ref}}{v_{ref}} \tag{2.4}$$

where v is the frequency of the peak of interest in the compound under study, and v_{ref} is the frequency of the resonance of the reference compound which its chemical shift is designated zero. Tetramethylsilane (TMS) is a common reference compound for ^{1}H-NMR. In addition to chemical shifts, NMR also provide information about spin-spin coupling. Spin-spin coupling is a phenomenon that leads to the splitting of peaks due to coupling of proton spins through the intervening bonding electrons. Where there is no coupling, equivalent protons appear as one single peak in the NMR spectrum. However, where there are coupling between a pair of proton spins, the resonance frequency of each spin is slightly affected by the two possible spin states of the other. Each individual peak will then appear as a doublet where the center of the doublet defines the chemical shift. When there are coupling between several proton spins, further splitting or peaks appear. The frequency difference, expressed in Hz, between adjacent peaks in a split signal is denoted by a coupling constant (J) [45].

Characterization of polysaccharides by ^{1}H-NMR

^{1}H NMR is commonly employed in polysaccharide characterization. Despite the fact that most resonances of carbohydrate protons are clustered in the 3.4-4.0 ppm region, the ^{1}H spectra do comprise some well-resolved signals [47]. This includes the resonances of the reducing end anomeric protons. The anomeric protons in α- and β-configuration are usually found in the chemical shift region between 5.1-5.8 ppm and 4.3-4.8, respectively [48]. Anomeric

configurations are normally assigned based on the magnitude of the coupling constant, with values between 2-4 Hz for the equatorial-axial coupling associated with the α-anomer and 7-9 Hz indicative of the diaxial coupling of the β-anomer [47]. Apart from this, the number of saccharide residues or the degree of polymerization (DP) can be estimated by comparison of the integrated intensities of all the anomeric protons in the saccharide chain.

2.8.2 Size exclusion chromatography (SEC)

Many biopolymers, especially polysaccharides, are composed of chains with different molecular weights [46]. A classical technique widely used to define the molecular weight distribution of biopolymers is chromatography. Chromatography is an important laboratory technique that covers a variety of separation methods [49]. It is essentially a method in which components of a sample are separated based on their distribution between two phases, a stationary phase and a mobile phase that percolates through the stationary phase in a definite direction [50]. The separation occurs as a result of different retention of the sample components by the stationary phase as the mobile phase transports the components through the chromatographic system [51].

Size-exclusion chromatography (SEC) is a chromatographic method where macromolecules are separated on the basis of molecular size, or more accurately, molecular hydrodynamic volume [52]. A typical SEC-system is composed of a solvent reservoir, a pump to deliver solvent into the system within a given flow range, an injector to introduce the sample into the system, a column, or columns, where the separation of sample components occurs, a detector and a data handling device [51].

The sample of interest is normally dissolved in the SEC mobile phase before it is injected into the column. The column is packed with a stationary phase composed of inert porous particles of defined pore size selectively chosen for the molecules to be separated [46]. Stagnant mobile phase trapped within the pores of the particles is also considered to be a part of the stationary phase [53]. The mobile phase transports the sample components of different sizes throughout the column in contact with the stationary phase. Molecules too large to penetrate into the pores of the particles are excluded from the stationary phase and transported with the mobile phase through spaces between the particles [51]. These molecules will elute in the interstitial or void volume, V_0, of the column, the volume of mobile phase located between the particles, due to little or no retention. Molecules small enough, relatively to the pore size, to freely diffuse into

all of the pores will elute at the total elution volume, V_i, of the packed SEC column [52]. Molecules of intermediate size will elute in between with elution volume V_e [51]. The elution volume of any sample component is given by

$$V_e = V_0 + KV_i \tag{2.5}$$

where K is the distribution coefficient which corresponds to the ratio of the average concentration of molecules in the stationary phase to the mobile phase at equilibrium [54]. It is constrained to values between 0 and 1. The concentration or relative amount of the eluting components is measured by a detector (e.g. a refractive index (RI) detector) and the information acquired from the chromatographic experiment is contained in a chromatogram. The chromatogram usually consists of a plot of detector response as a continuous function of time or volume of mobile phase passed through the column(s) [53]. Furthermore, coupling SEC to a multiplicity of detection methods allows additional information about the physiochemical properties of the polymers of interest [54].

Size exclusion chromatography with multiangle light-scattering (SEC-MALS)

SEC combined with on-line multiangle light-scattering detection (SEC-MALS) is considered a benchmark approach to determine molecular weight averages and distributions of polymers. The molecular weight distribution of polymers is characterized by a series of statistical averages [54]. Two of the most common of these averages are the number average (M_n) and weight average (M_w) molecular weights. The width of the distribution, or the polydispersity, is described by the ratio of M_w/M_n [52]. For a polydisperse polymer, $M_w > M_n$, whereas $M_w = M_n$ for monodisperse polymers [54]. In SEC-MALS the chromatographic set-up is based on the use of two on-line detectors, a concentration-sensitive detector and a light-scattering detector measuring scattered light at a multiplicity of angles simultaneously [46]. Combining MALS and a concentration-sensitive detector (e.g. RI detector) to SEC allows for the determination of molecular weight averages and distribution [54].

Adding an on-line viscometry detector to the SEC-MALS system allows additional determination of the viscosity of the polymer in solution. The viscometer measures the specific viscosity $[\eta_{sp}]$ and the RI detector measures the concentration c. As the intrinsic viscosity $[\eta]$ is defined as

$$[\eta] \equiv \lim_{c \to 0} \frac{\eta_{sp}}{c} \tag{2.6}$$

the ratio of the signals from the viscometer and the RI detector provides continuous measure of intrinsic viscosity across the chromatogram [54]. $[\eta]$ provides additional information about the shape and extension of the polymer [46].

3 Materials and methods

3.1 Materials

Water-soluble β-1,3-glucan (SBG, M_w = 35 kDa, M_n = 9.1 kDa, DP_n = 56) isolated from the cell wall of *Saccharomyces cerevisiae* was provided by Biotec BetaGlucans AS (Tromsø, Norway) as freeze-dried materials. The molar mass distribution of SBG is presented in Figure 3.1. Dextran T-2000 (M_w = 2000 kDa) was obtained from Pharmacia Fine Chemicals. *O,O*'-1,3-propanediylboshydroxylamine dihydrochloride (PDHA) and 2-methylpyridine borane complex (PB) were obtained from Sigma-Aldrich.

3-(Trimethylsilyl)-propionic-2,2,3,3-d4 acid sodium salt (TSP), deuterium oxide (D_2O), dimethyl sufoxide-d6 ($DMSO_{d6}$), and acetic acid-d4 ($AcOH_{d4}$) used in ^{1}H-NMR were purchased from Sigma-Aldrich. All other chemicals were obtained from commercial sources and were of analytical grade.

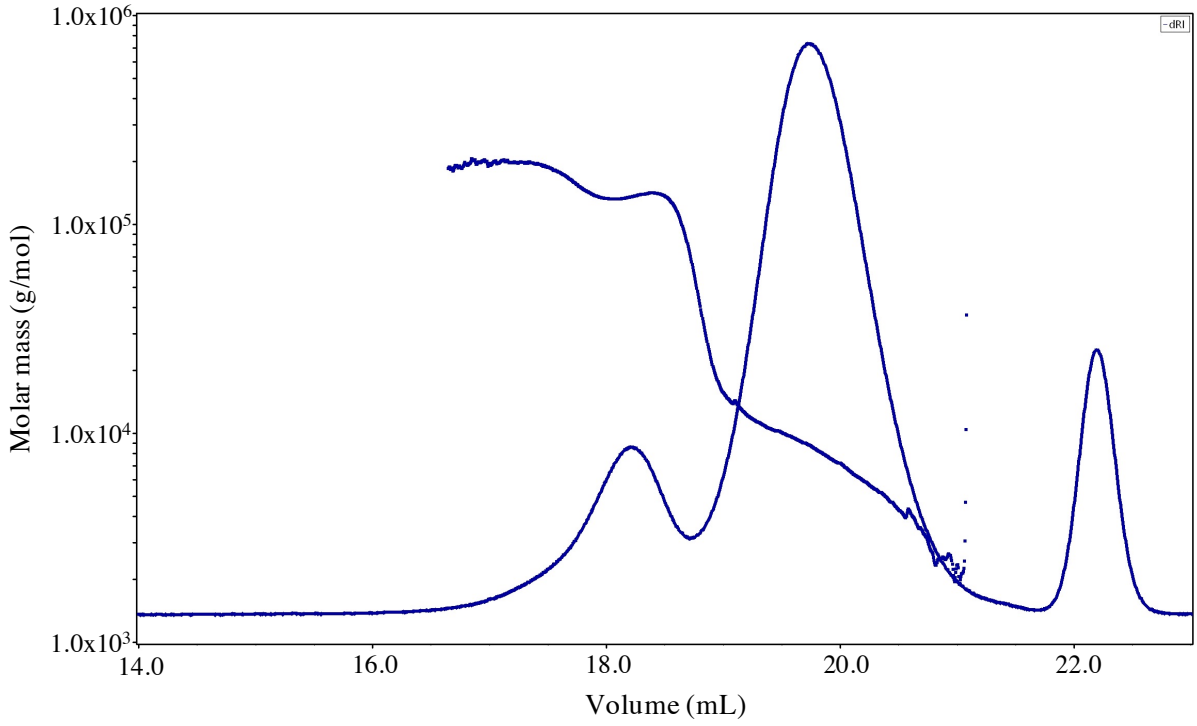

Figure 3.1: SEC-MALS chromatogram of molar mass vs elution volume for SBG.

3.2 Proton nuclear magnetic resonance (^{1}H-NMR) spectroscopy

Samples were dissolved in D_2O (475-600 μL, approx. 4-10 mg/mL) and transferred to 5 mm NMR tubes. Samples for time-course NMR experiments were prepared in deuterated sodium

acetate (NaAc) buffer (500 mM, pD 4.0, 2 mM TSP). All NMR experiments were carried out on a Bruker Ascend NEO 600 MHz spectrometer (Bruker BioSpin AG, Fällanden, Switzerland) equipped with Avance III HD electronics and a 5 mm cryogenic CP-TCI z-gradient probe. Characterization was performed by obtaining 1D ^{1}H-NMR spectra at 25 or 82 °C. Time-course experiments were performed by obtaining 1D ^{1}H-NMR spectra at specific time points at 25 °C. All spectra were recorded, processed, and analyzed using TopSpin 4.0.9 software (Bruker BioSpin).

3.3 Size exclusion chromatography (SEC)

Samples were separated and fractionated by size exclusion chromatography (SEC). Two different semi-preparative SEC systems were utilized. System 1 was composed of a Superdex 75 column (HiLoad 26/600, Cytiva) continuously eluting ammonium acetate (AmAc) buffer (0.15 M, pH 4.5) with a flow rate of 2.0 mL/min. System 2 was composed of three Superdex 30 columns (HiLoad™ 26/60, GE Healthcare Bio-Science) connected in series, continuously eluting AmAc (0.1 M, pH 6.9) buffer with a flow rate of 0.8 mL/min. The samples (50-200 mg) were dissolved in buffer (4 mL) and filtered (0.45 μm) prior to the injection into the SEC system. A refractive index (RI) detector (Shodex RI-101) was used to monitor the separation of both systems and the fractions were collected by a fraction collector (System 1: LKB 2211 SuperRac; System 2: Frac-100, Pharmacia Fine Chemicals). Fractions were pooled according to elution times, dialyzed against MQ-water until the conductivity of the water was below 2 μS/cm, and freeze-dried.

3.4 Size exclusion chromatography with multiangle light-scattering (SEC-MALS)

3.4.1 SEC-MALS in aqueous solvent

Samples (2-5 mg/mL) were dissolved in the mobile phase (0.15 M $NaNO_3$ with 0.01 M EDTA, pH 6.0) and filtered (0.45 μm) prior to injection (100 μL). The system was composed of a mobile phase reservoir, an on-line degasser, and HPLA isocratic pump, an autoinjector, a guard column, and two TSK gel columns 4000 and 2500 PWXL connected in series. The column outlet was connected to two serially connected detectors, a light scattering detector (Dawn HELEOS-II, Wyatt), and a refractive index detector (Shodex RI-501). An additional viscosity detector (ViscoStar III, Wyatt) was used in some experiments. The analyses were carried out at room temperature with a flow rate of 0.5 mL/min. Astra software v. 7.3.2 (Wyatt) was used to collect and process the data obtained from the detectors. Values for refractive index increment

(d*n*/d*c*) and second viral coefficient (A_2) used in the processing of data of analyzed samples are given in Table 3.1.

3.4.2 SEC-MALS in DMAc/LiCl

Samples were dissolved in the mobile phase (0.9 % LiCl/DMAc). Due to slow dissolution, heating was applied (90 °C for 15 min). The SEC-MALS system consisted of a multiangle laser light scattering detector (Dawn DSP, Wyatt), and a refractive index detector (Shodex RI-71), with automatic injection (Agilent 1200 series) and four serial columns (PL gel mixedA ALS, 20 μm, 7.5x300 mm) and one guard column. The analysis was carried out at ambient temperatures with a flow rate of 1.0 mL/min. Astra software v. 7.3.2 (Wyatt) was used to process the data obtained. Values for refractive index increment (d*n*/d*c*) and second viral coefficient (A_2) used in the processing of data of analyzed samples are given in Table 3.1. SEC-MALS experiments in DMAc/LiCl was performed by A. Potthast at BOKU, Vienna.

Table 3.1: Values for refractive index increment (d*n*/d*c*) and second viral coefficient (A_2) used in the processing of data of samples analyzed by SEC-MALS in aqueous solvent and in DMAc/LiCl.

Samples	Aqueous solvent		DMAc/LiCl	
	d*n*/d*c* (mL/g)	A_2 (mL mol g^{-2})	d*n*/d*c* (mL/g)	A_2 (mL mol g^{-2})
SBG	0.148	1x10^{-4}	0.136	0
Dextran	0.150	2x10^{-4}	0.136	0

3.5 Preparation of PDHA-activated SBG

SBG (500 mg) and 10 equivalents PDHA were dissolved in acetate buffer (500 mM, pH 4.0) to a final concentration of 20.1 mM and 201 mM, respectively. The acetate buffer was prepared by dissolving required volumes of acetic acid in MQ-water (3/4 of total volume). The pH was adjusted with NaOH to the desired value and diluted with MQ-water to the final volume. The conjugation was performed at room temperature with shaking for 48 h before 20 equivalents PB (402 mM) were added, and the sample was placed in a water bath at 40 °C for another 48 h for reduction. Prior to the addition of PB, 100 μL sample was taken out, dialyzed (MCWO = 3.5 kDa) against MQ-water until the measured conductivity was below 2 μS/cm, freeze-dried, and characterized by ^{1}H-NMR. The reduction was terminated by dialysis (MCWO = 3.5 kDa) against NaCl (0.05 M) until the insoluble PB was dissolved, followed by several shifts against MQ-water until the conductivity of the water was below 2 μS/cm. The sample was freeze-dried and analyzed by ^{1}H-NMR spectroscopy.

PDHA-activated SBG was separated using SEC system 1 (Superdex 75 column, 0.15 M AmAc, pH 4.5). The sample was fractionated into three separate fractions according to elution times given in Table 3.2. Fractions were further dialyzed against MQ-water until the measured conductivity of the water was less than 2 μS/cm and freeze-dried. Molecular weight of PDHA-activated SBG fractionated by SEC was analyzed by SEC-MALS both in aqueous solvent (with additional viscosity detector) and in DMAc/LiCl.

Table 3.2: PDHA-activated SBG was separated using SEC (Superdex 75 column) and fractionated into three separate fractions according to given elution times.

Fraction	From (min)	To (min)
1	54	64
2	64	87
3	87	110

3.6 Thermal treatment of PDHA-activated SBG

PDHA-activated SBG (fraction 1) prepared as described in section 3.5 was dissolved in SEC-MALS mobile phase (0.15 M $NaNO_3$ with 0.01 M EDTA, pH 6.0) to a final concentration of 2.5 and 0.25 mg/mL. The samples were heated to 120 °C in an autoclave in 15 mL tubes with 1 mL sample for 20 min. Caps were placed on the tubes as tight as possible to avoid any evaporation. The temperature was controlled with an internal sensor. After heating, the samples were cooled to room temperature, filtered (0.45 μm), and analyzed by SEC-MALS in aqueous solvent.

3.7 PDHA-activation of SBG oligomers in DMSO

The conjugation of SBG_n oligomers (n = DP) to PDHA in DMSO was studied by time-course ^{1}H-NMR. SBG_n (10 mM) and 2 equivalents PDHA (20 mM) were dissolved separately in 1:5 v/v $AcOH_{d4}$ in $DMSO_{d6}$ and transferred to a 5 mm NMR tube. The mixing of the reagents in the NMR tube served as time zero (t = 0). ^{1}H-NMR spectra were recorded at desired time points over a period of 60 h. The same procedure was repeated with the addition of 10 % D_2O, except the reaction was only studied for 24 h.

3.8 Preparation of dextran oligomers

Dextran T-2000 (50 mg/mL) was dissolved in MQ-water overnight. HCl (0.1 M) was added to give a final concentration of 0.05 M HCl and 25 mg/mL dextran. Acid hydrolysis was

performed at 95 °C for 190 minutes. Partially hydrolyzed dextran was dialyzed (MWCO = 3.5 kDa) against MQ-water until the conductivity of the water was below 3 μS/cm, freeze-dried, and characterized by ^{1}H-NMR. This part was performed in cooperation with fellow master students.

Partially hydrolyzed dextran was separated using SEC system 2 (Superdex 30 column, 0.1 M AmAc, pH 6.9). The sample was fractionated into five separate fractions according to elution times given in Table 3.3. Fractions were further dialyzed against MQ-water until the measured conductivity of the water was less than 2 μS/cm, freeze-dried, and analyzed by SEC-MALS in aqueous solvent.

Table 3.3: Partially hydrolyzed dextran was separated using SEC (Superdex 30 column) and fractionated into five separate fractions according to given elution times.

Fraction	From (min)	To (min)
1	380	458
2	458	505
3	505	579
4	579	648
5	648	794

3.9 Preparation of diblock structures from PDHA-activated SBG of low DP

3.9.1 SBG-*b*-Dextran

In-house samples of PDHA-activated SBG oligomers with n residues (SBG$_n$-PDHA) and dextran oligomers with m residues (Dext$_m$) prepared by Ingrid V. Mo and Odin W. Haarberg (Department of Biotechnology, NTNU), respectively, was used in the preparation of SBG$_n$-PDHA-Dext$_m$ diblock structures.

SBG$_n$-PDHA (10 mM) and one molar equivalent of Dext$_m$ (10 mM) was dissolved separately in deuterated acetate buffer (500 mM, pH 4.0, 2 mM TSP) and transferred to a 5 mm NMR tube. The mixing of the reagents in the NMR tube served as time zero (t = 0). The conjugation was studied by time-course ^{1}H-NMR at room temperature where ^{1}H-NMR spectra were recorded at specific time points until equilibrium was reached. Reduction of SBG$_n$-PDHA-Dext$_m$ diblock structures was performed by adding 3 molar equivalents of PB (30 mM) to the reaction mixture. The reduction was followed by time-course ^{1}H-NMR over a period of 5 days before it was terminated by dialysis, one shift against NaCl (0.05 M) followed by several shifts

against MQ-water until the conductivity of the water was less than 2 μS/cm. The sample was freeze-dried and characterized by ^{1}H-NMR.

3.9.2 SBG-*b*-Alginate

In-house samples of SBG$_n$-PDHA and oligoguluronate with *m* residues (G$_m$) prepared by Ingrid V. Mo and Amalie Solberg (Deparment of Biotechnology, NTNU), respectively, was used in the preparation of SBG$_n$-PDHA-G$_m$ diblock structures.

The conjugation of SBG$_n$-PDHA (7 mM) to one molar equivalent of G$_m$ (7 mM) was studied by time-course ^{1}H-NMR as described in the previous section. Reduction of SBG$_n$-PDHA-G$_m$ diblock structures were performed by adding 3 molar equivalents of PB (21 mM) to the reaction mixture. The reduction was studied by time-course ^{1}H-NMR for five days before it was terminated by dialysis, one shift against NaCl (0.05 M) followed by several shifts against MQ-water until the conductivity of the water was less than 2 μS/cm. The sample was freeze-dried and characterized by ^{1}H-NMR.

3.10 Preparation of diblocks structures from PDHA-activated SBG of high DP

3.10.1 SBG-*b*-Dextran

PDHA-activated SBG (fraction 1, 5 mM) prepared as described in section 3.5 was reacted with 3 equivalents dextran (fraction 4, 15 mM) (section 3.7) in acetate buffer (500 mM, pH 4.0). The sample was left on a shaker for 12 days at room temperature. 20 equivalents PB (100 mM) was added, and the sample was placed in a water bath at 40 °C for 72 h. The reaction was terminated by dialysis against NaCl (0.05 M) until the insoluble PB was dissolved, followed by several shifts against MQ-water until the conductivity of the water was less than 2 μS/cm. The samples were freeze-dried and analyzed by SEC-MALS in aqueous solvent. PDHA-activated SBG (fraction 1) was additionally reacted with 3 equivalents dextran fractions 2 and 3 as described above.

3.10.2 SBG-*b*-Alginate

PDHA-activated SBG (fraction 1, 7 mM) prepared in section 3.5 was reacted with 3 equivalents oligoguluronate (DP$_n$ 18, 21 mM) in acetate buffer (500 mM, pH 4.0). Oligoguluronate was prepared by Amalie Solberg (Department of Biotechnology, NTNU). The sample was left on a shaker for 24 h at room temperature. 10 equivalents PB (50 mM) was added to the sample and

the sample was left on a shaker for 5 days at room temperature. The reaction was terminated by dialysis as described in the previous section, freeze-dried and analyzed by SEC-MALS in aqueous solvent.

4 Results

SBG was activated with PDHA, fractionated by SEC, and analyzed by SEC-MALS to determine the molar mass distribution of the collected fractions. PDHA-activated SBG was exposed to thermal treatment to obtain fully soluble samples for accurate determination of molar mass distribution by SEC-MALS. Activation of SBG with PDHA was also studied in DMSO. Moreover, dextran oligomers were prepared for the later preparation of SBG-*b*-dextran diblock polysaccharides. Diblock structures from PDHA-activated SBG was prepared by conjugation to dextran and oligoguluronate. The conjugation was first studied by time-course ^{1}H-NMR using saccharides of low DP to determine an optimized protocol for the preparation of diblocks. SBG-*b*-dextran and SBG-*b*-oligoguluronate of higher DP was analyzed by SEC-MALS. Taken together, the presented results were performed to obtain soluble and non-aggregating SBG-containing block polysaccharides for potential applications in the biomedical field.

4.1 Preparation and characterization of PDHA-activated SBG

Terminal modification utilizing the reducing end aldehyde group in the SBG chain allows for selective modification without affecting the rest of the functional groups in the polysaccharide chain. As a first step toward the preparation of SBG-containing diblock polysaccharides, terminal activation of SBG with the bifunctional linker PDHA was studied as detailed below. Notably, terminal conjugation to a reactive linker can also allow for other applications of SBG for example for applications in bio-orthogonal chemistry [55, 56].

4.1.1 Terminal activation of SBG with PDHA

An earlier study reported the use of PDHA for the terminal activation of SBG oligosaccharides with a DP ranging from 4-10 [57]. However, PDHA-activation of SBG for the preparation of SBG-based diblock polysaccharides has not been reported. In order to prepare diblock polysaccharides from PDHA-activated SBG, SBG_{56} (the subscript referring to DP_n) was reacted with PDHA and subsequently reduced with PB to obtain stable secondary amines. The reducing end resonances of SBG_{56} was characterized by ^{1}H-NMR prior to the reaction to be able to validate the conjugation to PDHA after the reaction. The resonances for the reducing end protons in α- and β-configuration were observed at 5.23 and 4.66 ppm, respectively (Figure 4.1).

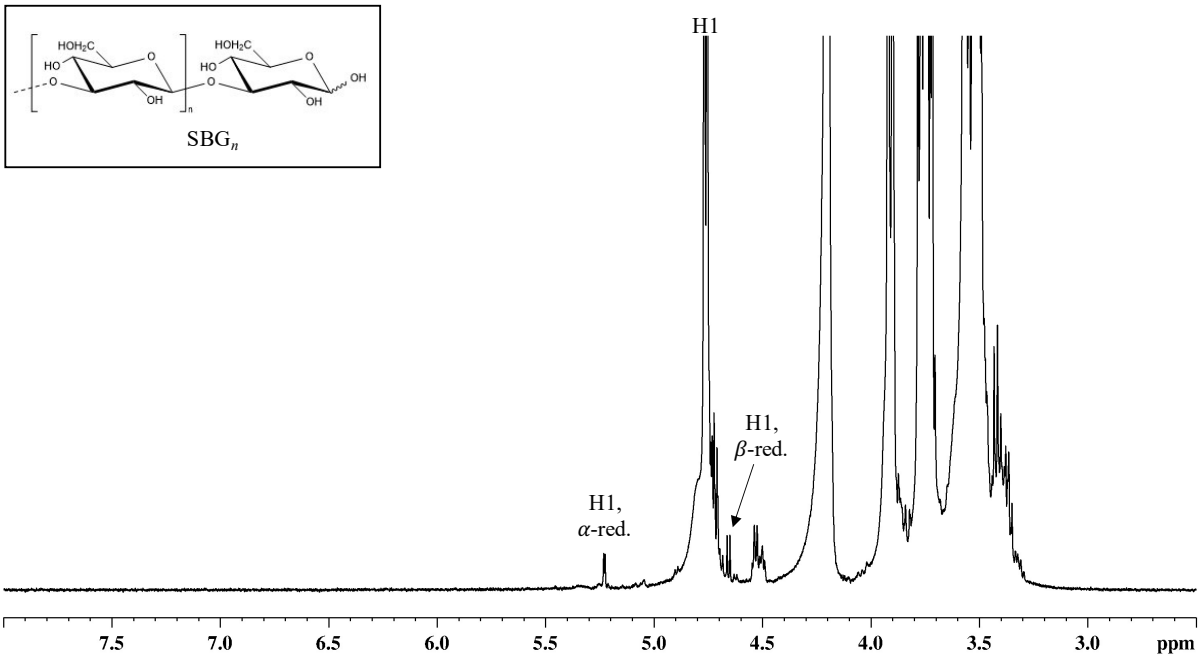

Figure 4.1: ^{1}H-NMR spectra (600 MHz, 82 °C) of SBG$_{56}$. Key resonances are assigned. General structure of SBG$_n$ is included, notably without side-chain branches.

The conjugation of PDHA to SBG$_{56}$ was verified by the appearance of resonances for (*E*)- and (*Z*)-oximes at 7.62 and 7.00 ppm, respectively (Figure 4.2).

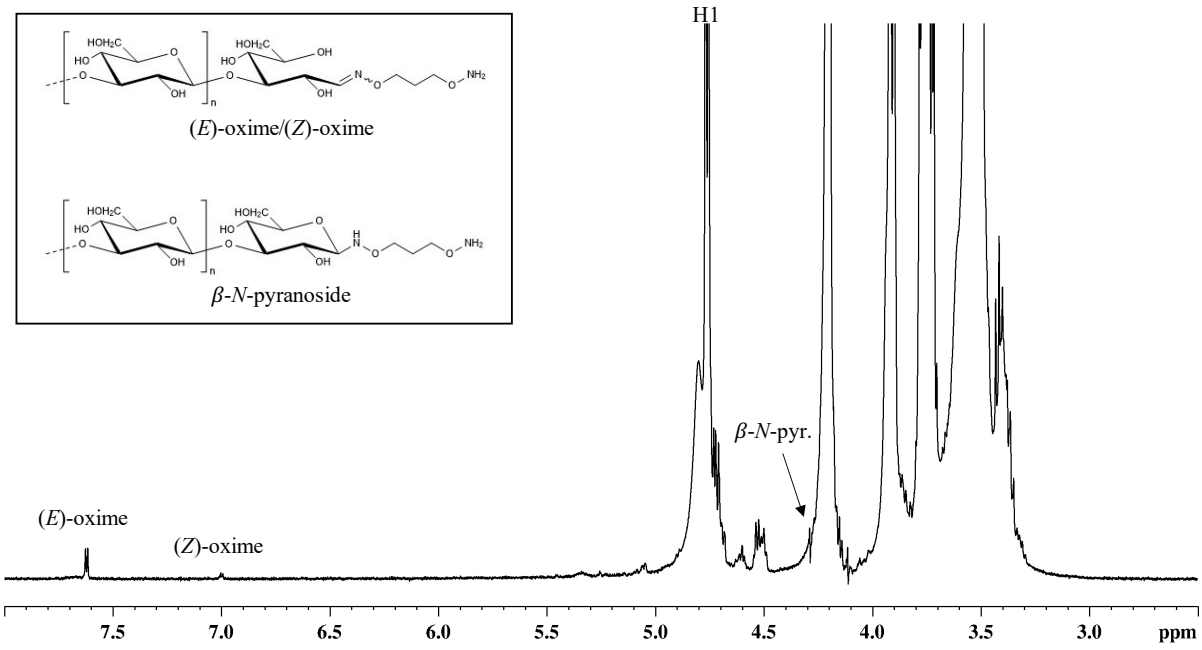

Figure 4.2: ^{1}H-NMR spectra (600 MHz, 82 °C) of PDHA conjugated to SBG$_{56}$. Key resonances are assigned. General structure of SBG$_n$ oximes in (*E*)/(*Z*)-configuration and β-*N*-pyranoside is included.

A weak signal appearing at 4.27 ppm was assigned to β-*N*-pyranoside according to literature [23]. Due to peak overlap, the combined yield could not be determined accurately by NMR. However, the absence of signals from the reducing ends indicated that SBG_{56}-PDHA conjugates had been obtained in high yields. SBG_{56}-PDHA was further irreversibly reduced to stable secondary amines by PB. Resonances for the methylene protons of the secondary amines formed after reduction was observed at 3.00 and 3.21 ppm (Figure 4.3). A weak signal for (*E*)-oximes was also observed. From integration, the yield of reduced SBG_{56}-PDHA was calculated to be 68 % (Appendix A, Figure A.1).

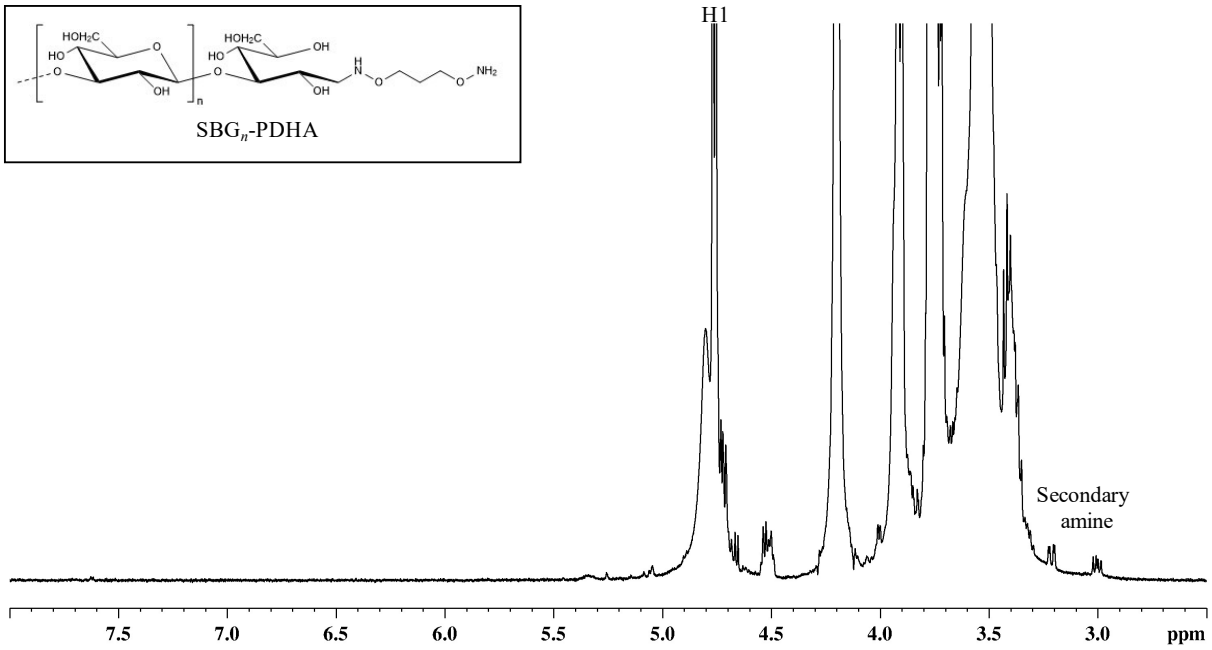

Figure 4.3: ^{1}H-NMR spectra (600 MHz, 82 °C) of reduced SBG_{56}-PDHA. Key resonances are assigned. General structure of reduced SBG_n-PDHA is included.

4.1.2 Fractionation of PDHA-activated SBG by SEC

SBG_{56}-PDHA was separated and fractionated by SEC in order to obtain samples with a narrower chain length distribution. As SBG is known to aggregate in aqueous solution, this can allow us to examine the role of chain length in the aggregation process. The chromatogram obtained from the separation is presented in Figure 4.4.

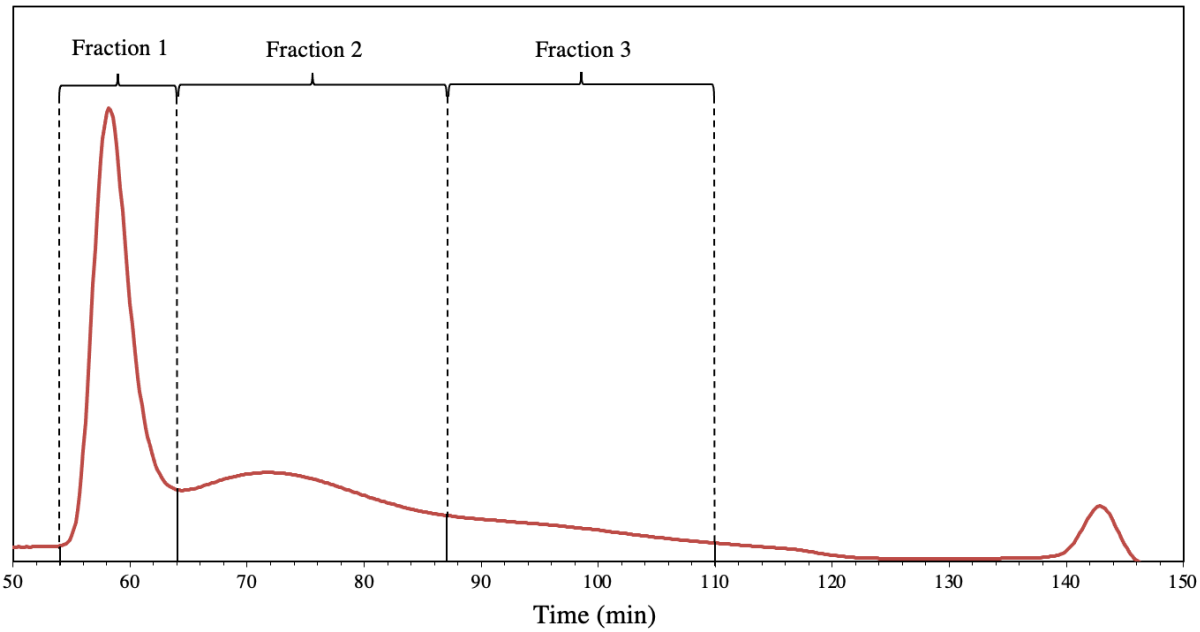

Figure 4.4: SBG-PDHA separated and fractionated into three separate fractions by SEC (Superdex G-75 column, 0.15 M AmAc, pH 4.5).

As observed from the chromatogram, the sample apparently contained a high concentration of high-molecular weight components. These molecules were too large to be retained by the stationary phase and hence too large to be separated. Since SEC separates purely on molecular size it was unclear whether the components were aggregated or not. The sample was fractionated into three separate fractions according to elution times as indicated in Figure 4.4 for further determination of molar mass distribution by SEC-MALS.

4.1.3 Determination of molar mass distribution of fractionated SBG-PDHA by SEC-MALS in aqueous solvent

The three fractions in Figure 4.4 were analyzed by SEC-MALS in aqueous solution to determine their molar mass and chain length distribution. The RI profile of fraction 1-3 together with the corresponding molecular weight is presented in Figure 4.5.

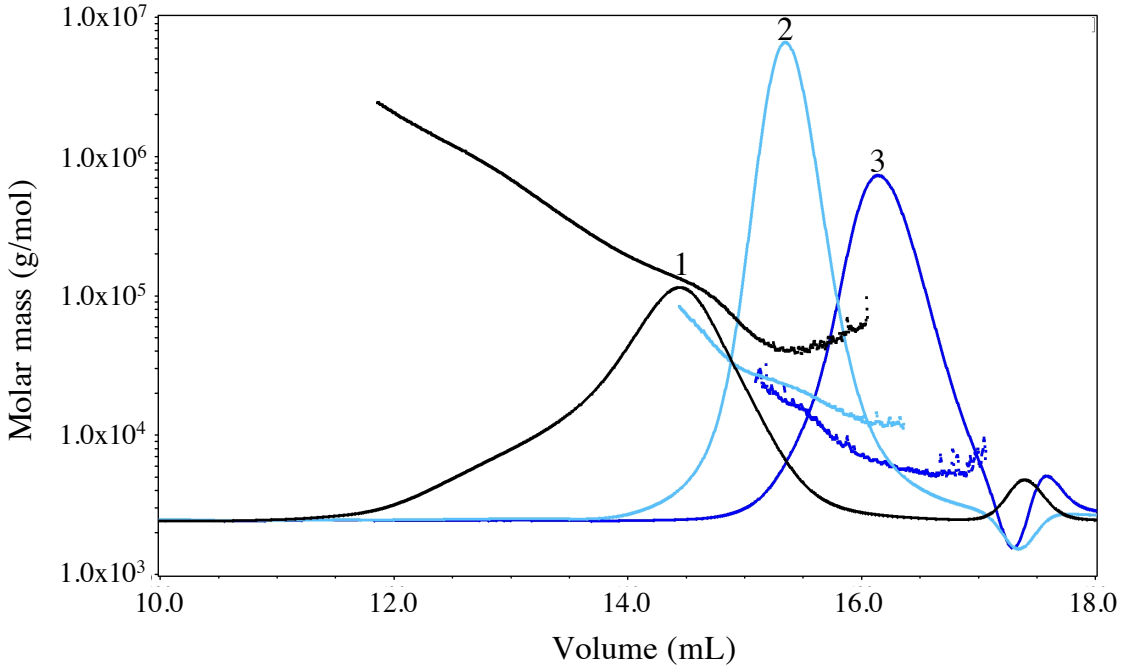

Figure 4.5: SEC-MALS data for SBG-PDHA fraction 1-3 obtained in aqueous solution at room temperature. Solid lines refer to the RI profile and dotted lines refer to the molar mass.

Chromatographic peaks appeared with increasing elution volume according to the separation on SEC. The molar mass was ranging from around 10^5 to 10^6 g/mol for fraction 1 and 10^4 to 10^5 g/mol for fraction 2. Fraction 3 showed a molar mass in the area around 10^4 g/mol. The calculated weight average (M_w) and number average (M_n) molecular weights of fraction 1 was 309 and 126 kDa, respectively. The latter value corresponded to a DP_n of 775. Values for M_w, M_n, polydispersity, and DP_n of all three fractions are summarized in Table 4.1.

Table 4.1: Weight average (M_w), number average (M_n) molecular weights, polydispersity, and calculated DP_n for SBG-PDHA fraction 1-3 obtained by SEC-MALLS in aqueous solution.

Fraction	M_w (kDa)	M_n (kDa)	Polydispersity (M_w/M_n)	DP_n
1	309	126	2.45	775
2	24.9	21.2	1.17	131
3	7.7	6.9	1.12	43

In addition to molecular weight, intrinsic viscosity data was also obtained by an on-line viscosity detector. The molecular weight dependence of the intrinsic viscosity (Mark-Houwink-Sakurada (MHS) plot) is shown in Figure 4.6. Corresponding data for water-soluble, un-aggregated carboxymethylated SBG (CM-SBG) adopted from a previous publication [7] was included for comparison.

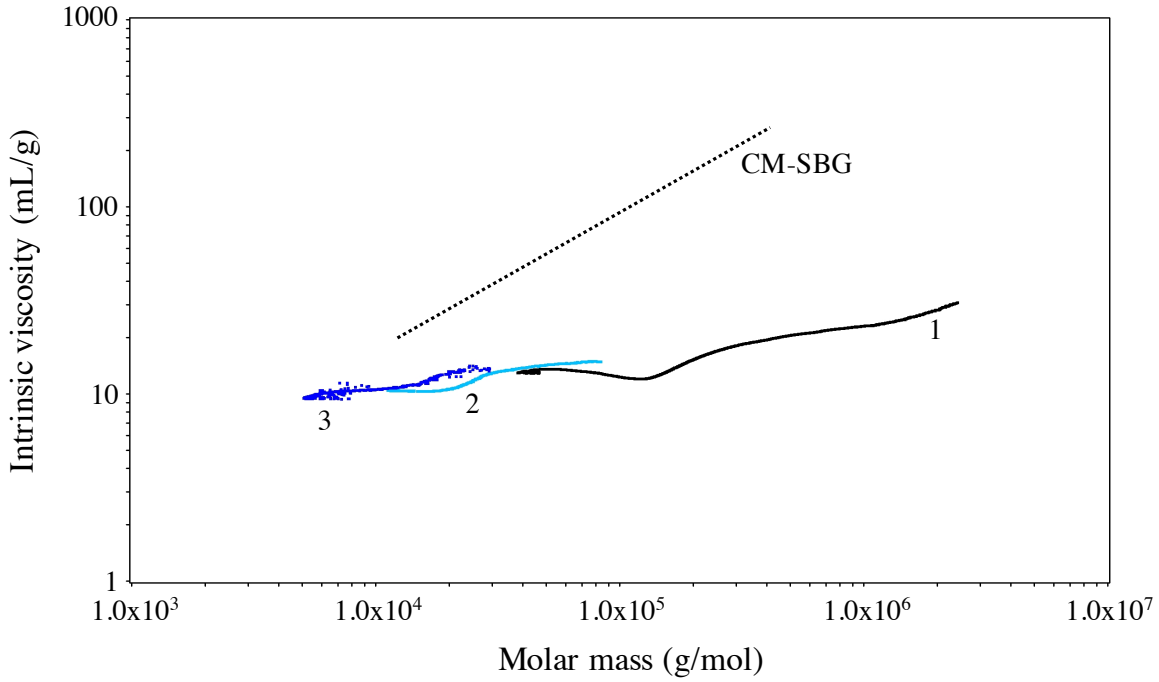

Figure 4.6: Molecular weight dependence of the intrinsic viscosity (MHS plots) of SBG-PDHA fraction 1-3 and carboxymethylated SBG (CM-SBG) (adopted from [7]) obtained by SEC-MALS in aqueous solution.

The average intrinsic viscosity for fraction 1 was calculated to be 15.6 mL/g while fractions 2 and 3 gave values of 11.4 and 10.2 mL/g, respectively. The difference in intrinsic viscosity for the three fractions was quite small. All three fractions of SBG-PDHA had viscosities below the values observed for CM-SBG with corresponding molecular weights. The data also showed some curvature. Through line fitting (not shown), the average slope of all three fractions ranged between values of 0.15 to 3.0. The high molecular weights, especially of fraction 1, together with the low intrinsic viscosities indicated aggregation. Hence determination of accurate molecular weight and chain length distribution was not possible using this system. To obtain these values we decided to turn to a non-aqueous solvent. DMAc containing 0.5-0.9% LiCl has over the past years become a widely used solvent for SEC-MALS analysis of cellulose [58]. Kivelä et al. also reported the successful use of DMAc/LiCl (0.9%, w/v) as solvent in SEC-MALLS for the determination of molecular weight distribution of mixed-linkage β-

(1→3),(1→4)-glucan extracted from oat [59]. This motivated the SEC-MALS analysis of PDHA-activated SBG in DMAc/LiCl to determine the accurate molecular weight and chain length distribution.

4.1.4 Determination of molar mass distribution of fractionated SBG-PDHA by SEC-MALS in DMAc/LiCl

Hydrogen bonds are known to play an important role in the aggregation of neutral polysaccharides [60]. Solvents with strong polarity, such as DMAc/LiCl, appear to break these hydrogen bonds and in many cases transform aggregates into single, un-associated chains [10]. SBG-PDHA was therefore analyzed by SEC-MALS in DMAc/LiCl in order to determine the accurate molar mass distribution. This would also provide additional information about the aggregation behavior of SBG. As this system was not available in our lab, the experiment was carried out by A. Potthast at BOKU, Vienna, in late April 2021. Figure 4.7 shows SEC-MALLS data of SBG-PDHA with the use of DMAc/LiCl as mobile phase. Due to lack of material, only fractions 1 and 2 (see section 4.1.2) were analyzed.

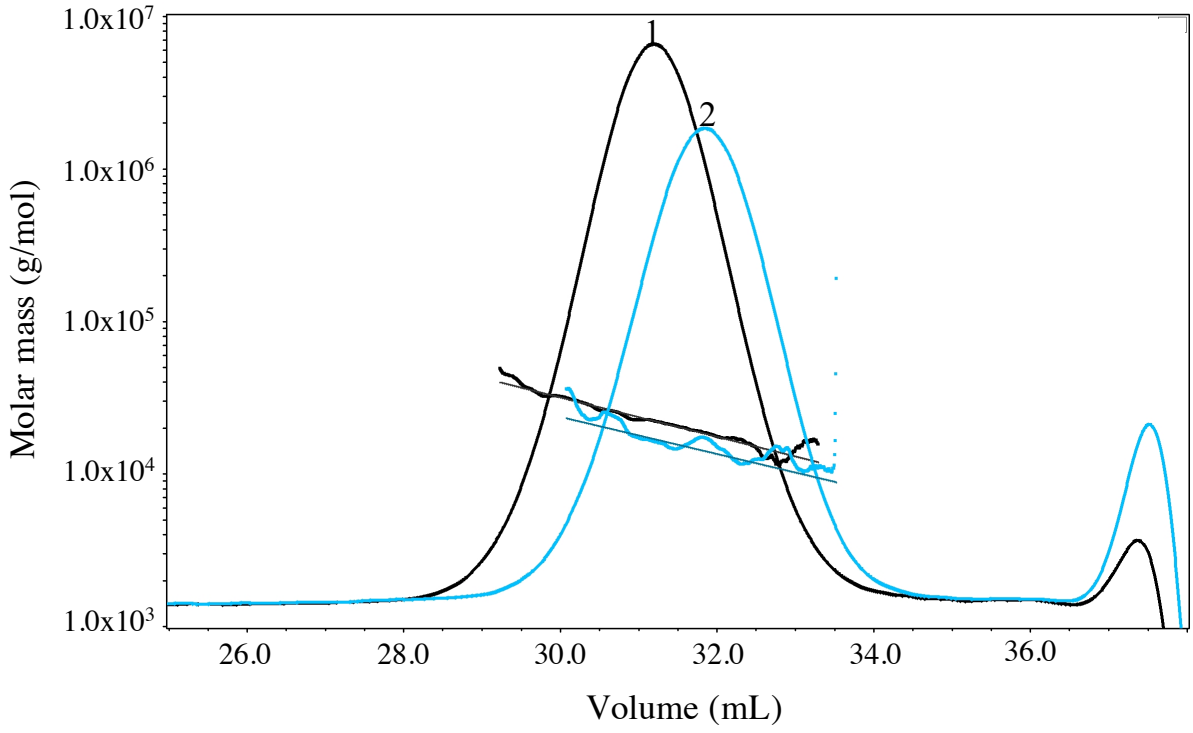

Figure 4.7: SEC-MALS data for SBG-PDHA fraction 1 and 2 obtained in DMAc/LiCl at room temperature. Solid lines refer to the RI profile and dotted lines refer to the molar mass.

The RI peak of both fractions was quite symmetrical and appeared with very similar elution volume. The molar masses were in the in the range of 10^4 g/mol which were far below the values obtained from SEC-MALS analysis in aqueous solution, especially for fraction 1. The difference in molar mass for the two fractions also appeared to be relatively small. Calculated molecular weight averages (M_w and M_n), as well as the polydispersity and DP_n values are summarized in Table 4.2.

Table 4.2: Weight average (M_w), number average (M_n) molecular weights, and calculated polydispersity and DP_n for SBG-PDHA fraction 1 and 2 obtained by SEC-MALLS in DMAc/LiCl.

Fraction	M_w (kDa)	M_n (kDa)	Polydispersity (M_w/M_n)	DP_n
1	23.0	21.5	1.07	133
2	14.6	13.9	1.05	86

Based on these results, the aggregation of SBG in aqueous solution was evident even when conjugated to the positively charged dioxyamine PDHA. Furthermore, and in accordance with previous findings [10], the dissolution of SBG-PDHA in DMAc/LiCl combined with SEC-MALS appeared to be a suitable strategy for the determination of molar mass distribution of SBG-PDHA.

4.2 Method development for studying SBG in the single chain state: Thermal treatment

As for solvents of high polarity, increasing the temperature is known to disrupt the hydrogen bonding between associated polysaccharide chains [61]. Since the SEC-MALS system in DMAc/LiCl was not available in our lab at the present time we wanted to explore the possibility of using high temperature as a simple tool to obtain un-aggregated SBG for future analyses by SEC-MALS in aqueous solution. Concentrated and diluted samples of SBG_{133}-PDHA (the subscript referring to DP_n, see Table 4.2) were exposed to thermal treatment and analyzed by SEC-MALS to determine the effect on molecular weight. Figure 4.8 shows the obtained molecular weight after heat treatment. SEC-MALS data of SBG_{133}-PDHA obtained without heat treatment and in DMAc/LiCl, both with concentration equal to that of the concentrated sample, were included for comparison.

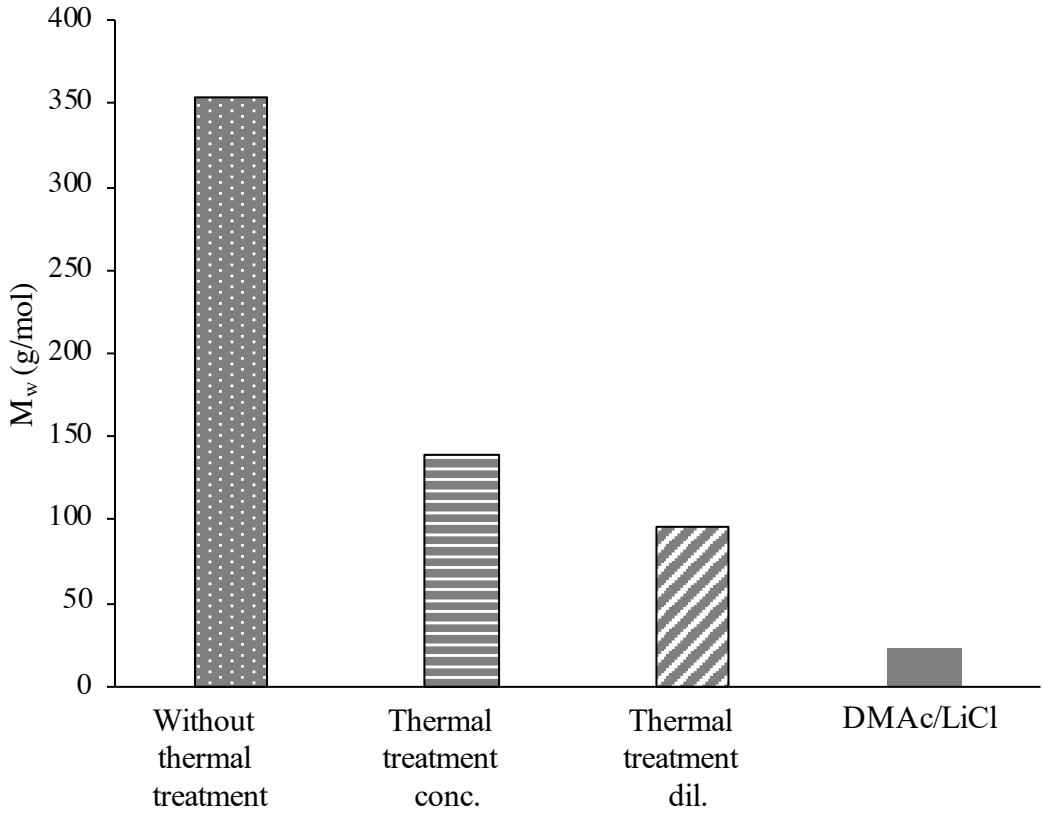

Figure 4.8: Weigh average (M_w) molecular weight of SBG_{133}-PDHA obtained by SEC-MALS analysis in aqueous solution, with and without thermal treatment, and in DMAc/LiCl.

Both the concentrated and diluted sample of SBG_{133}-PDHA showed a reduction in molecular weight after thermal treatment. Compared to the sample without thermal treatment, the molecular weight of the concentrated sample was reduced with 61 % while the molecular weight of the diluted sample was reduced with 73 %. However, neither of the samples reached a molecular weight equal to that observed in DMAc/LiCl. This indicated that SBG_{133}-PDHA did not fully dissociate into single, un-associated chains with the applied thermal treatment. Hence this strategy was not sufficient to obtain un-aggregated SBG_{133}-PDHA for SEC-MALS analysis in aqueous solution.

4.3 Method development for studying SBG in the single chain state: Organic solvent

SBG-PDHA appeared to aggregate strongly in aqueous solvent, even at elevated temperature. The use of solvents where SBG is fully soluble can be beneficial both in the preparation of PDHA-activated SBG and in the characterization process. A generally accepted solvent which can disrupt the aggregation of branched and unbranched β-1,3-glucans is DMSO [15]. DMSO has for example been widely used as mobile phase in SEC-MALS to provide the molecular weight and for structural characterization of several β-1,3-glucans [2, 10, 62]. This SEC-

MALS system was not available in our lab during the present study. However, as an initial experiment it was of interest to investigate the use of DMSO to perform chemical modification of SBG. Organic solvents have been shown to affect the reaction kinetics for certain reactions where water is a by-product. An example is the terminal modification of chitin. The reaction kinetics and yield for the terminal conjugation of PDHA to chitin oligomers was significantly increased using DMAc/LiCl as solvent compared to aqueous solvent [63]. Based on previous studies where organic solvents have been used for the successful conjugation of oxyamines to carbohydrates [64], we therefore decided to explore the use of DMSO as solvent for the terminal activation of SBG with PDHA.

4.3.1 Terminal activation of SBG with PDHA in DMSO

To investigate if using DMSO as solvent could increase the reaction efficiencies of the terminal conjugation of PDHA to SBG, the reaction was studied in detail by time-course ^{1}H-NMR. Acetic acid was added as catalyst based on a previous study [64]. SBG_6 (the subscript referring to DP) was reacted with 2 equivalents PDHA. A short oligomer was used as this simplify the NMR spectra. Spectra taken at different time points are presented in Figure 4.9.

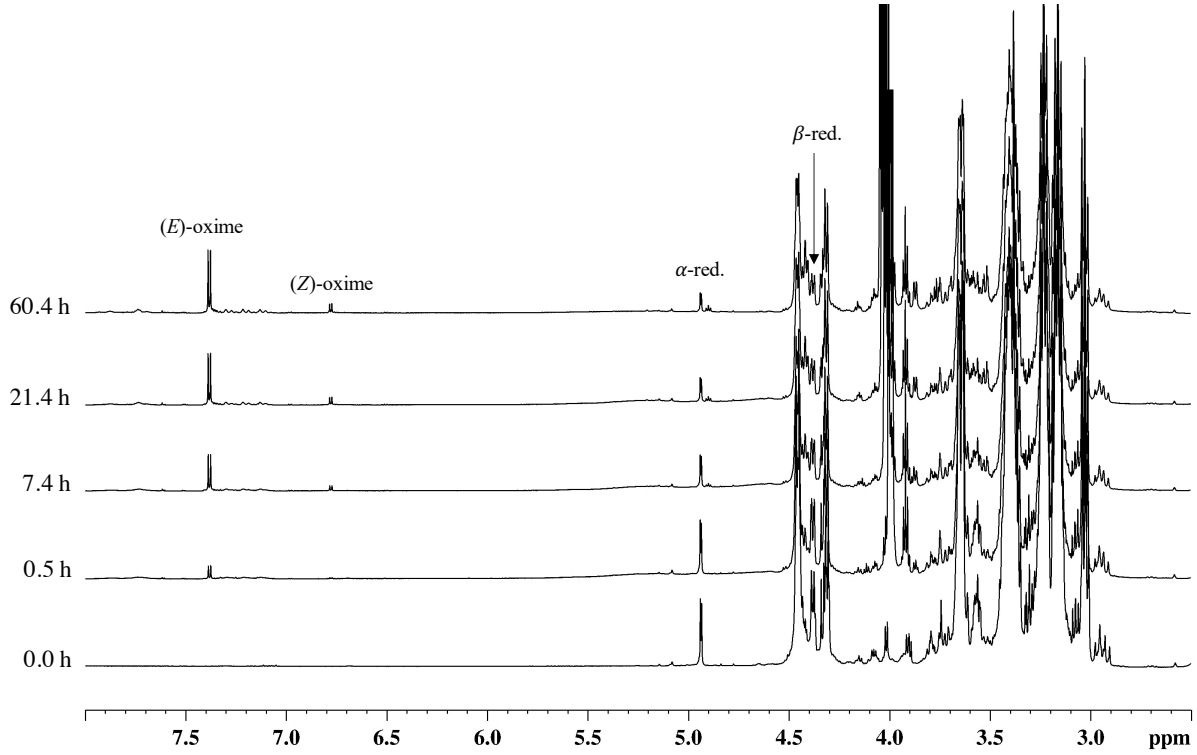

Figure 4.9: ^{1}H-NMR spectra (600 MHz, 25 °C) at given time points for the conjugation of SBG_6 to 2 equivalents PDHA in DMSO.

Formation of (*E*)- and (*Z*)-oximes was observed at 7.40 and 6.79 ppm, respectively. *β*-*N*-pyranoside was also assumed to be present based on the conjugation studied in aqueous solution [57]. However, due to overlapping peaks it was difficult to annotate its signal and hence the formation of *β*-*N*-pyranoside was assumed to be equal to that obtained in aqueous solution. By integration of the key resonances, the decrease in reactant and formation of reaction products was calculated. The yields plotted against reaction time is presented in Figure 4.10. Yields were calculated relative to the signal intensity of the anomeric protons prior to the addition of PDHA (Appendix B, Figure B.1-B.2).

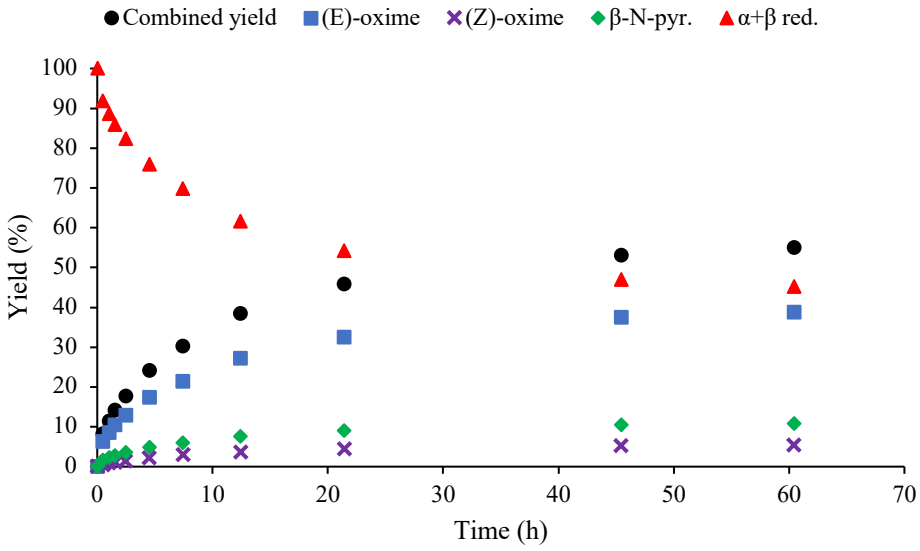

Figure 4.10: Course of the reaction of SBG_6 to 2 equivalents PDHA obtained by integration of the spectra presented in Figure 4.9.

The reduction of reactant and the formation of (*E*)-oxime, (*Z*)-oxime, and *β*-*N*-pyranoside are shown over time. The combined yield of reaction products is also included. After 60 hours the combined yield was 50 %. The obtained yield was significantly lower compared to the yield obtained in aqueous solution for the same reaction (94 % after 24 hours reaction) [57]. A plausible explanation for the low yield might be the high pK_a value of acetic acid in DMSO (pK_a = 12.6) [65]. This may prevent it to donate protons for the acid catalyzed reaction between SBG and PDHA. We therefore decided to investigate the reaction with the addition of 10 % water to increase the efficiency of the acid catalyst and thereby increase the yield and kinetics of the conjugation.

4.3.2 Terminal activation of SBG with PDHA in DMSO with the addition of water

For estimation of the yield and kinetics for the terminal conjugation of PDHA to SBG using DMSO containing 10 % water as solvent, the reaction was monitored by time-course ^{1}H-NMR. SBG_4 was conjugated to 2 equivalents PDHA. ^{1}H-NMR spectra following the reaction are shown in Figure 4.11.

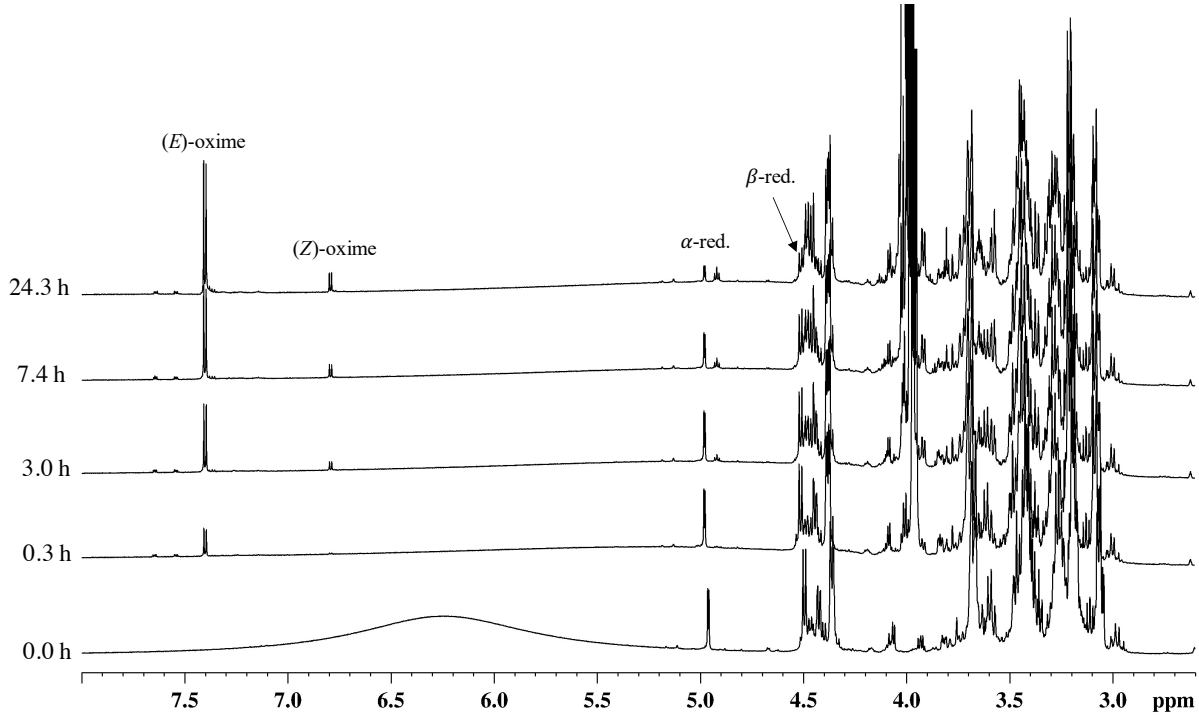

Figure 4.11: ^{1}H-NMR spectra (600 MHz, 25 °C) at given time points for the conjugation of SBG_6 to 2 equivalents PDHA in DMSO with 10 % water.

The course of the reaction was obtained by integration of the recorded spectra. Corresponding yields over time are presented in Figure 4.12. Yields were calculated relative to the signal intensity of the anomeric protons prior to the addition of PDHA (Appendix B, Figure B.3-B.4).

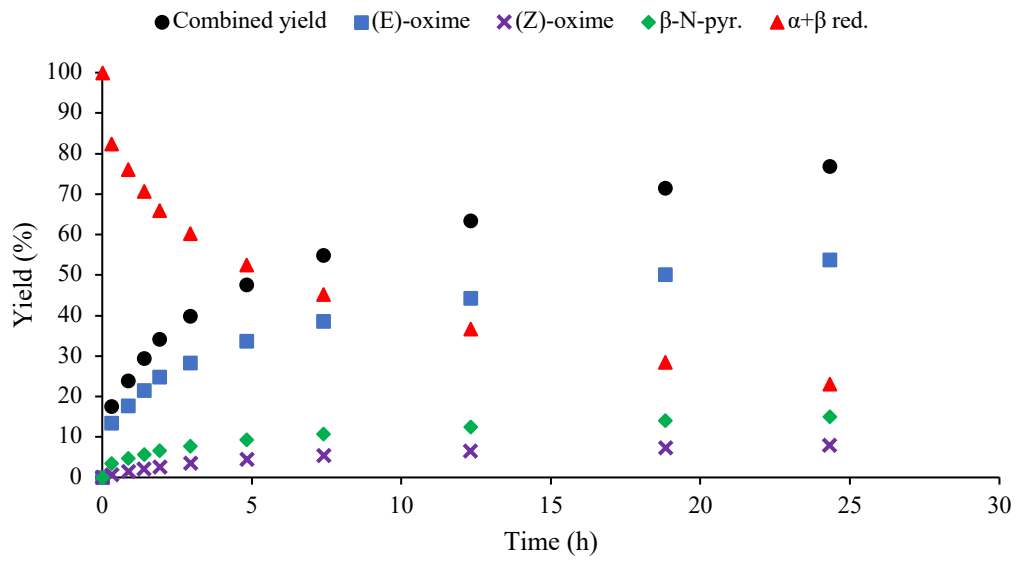

Figure 4.12: Course of the reaction of SBG_4 to 2 equivalents PDHA obtained by integration of the spectra presented in Figure 4.11.

The reduction in free reducing ends in α- and β-configuration and the formation of (*E*)-oxime, (*Z*)-oxime, and β-*N*-pyranoside are displayed over time. The combined yield of reaction products is also included. After 24 hours of reaction the obtained combined yield was calculated to be 77 %. Both the yield and reaction kinetics were improved by the addition of water. However, it was still below the values obtained in aqueous solution. We therefore decided to not work any further with this strategy.

4.4 Preparation of dextran oligomers

To the best of our knowledge, diblock structures composed of dextran conjugated to PDHA-activated SBG have not been prepared. In order to construct SBG-*b*-dextran diblock copolymers, dextran oligomers were prepared by acid hydrolysis, followed by fractionation on SEC. The molar mass distributions were subsequently determined by SEC-MALS.

4.4.1 Determination of DP of partially hydrolyzed dextran

To obtain dextran oligomers, high-molecular weight dextran was degraded by acid hydrolysis. The hydrolyzed sample had a DP_n of 28 determined by ^{1}H-NMR (Figure 4.13).

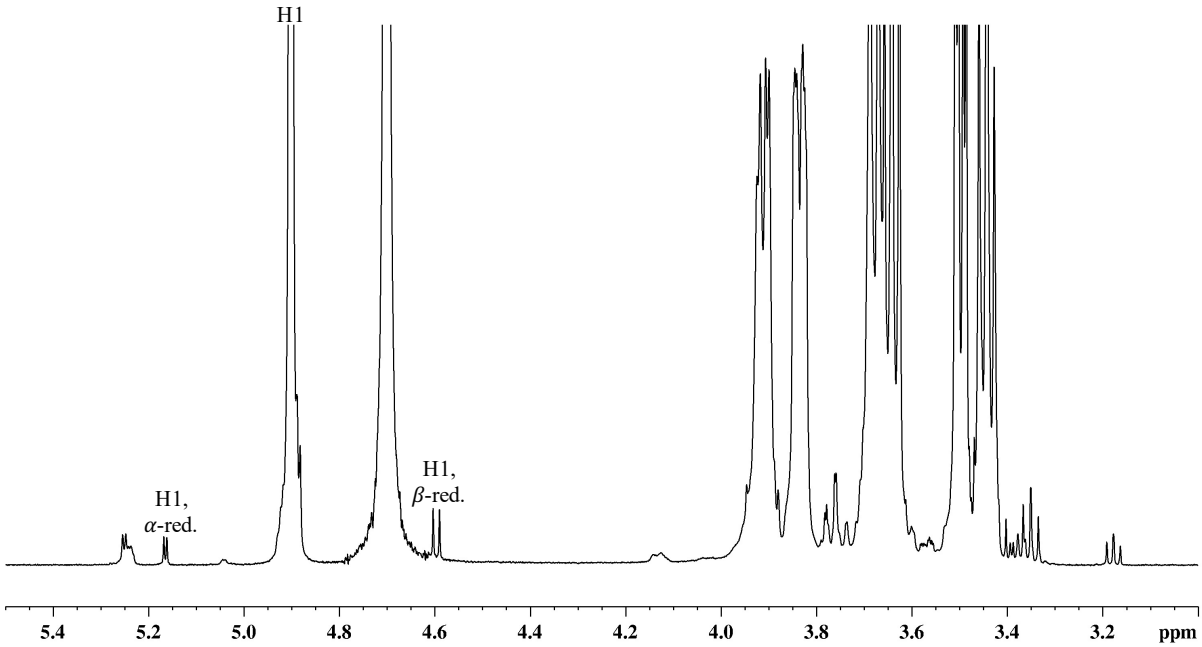

Figure 4.13: ^{1}H-NMR spectrum (600 MHz, 25 °C) of partially hydrolyzed dextran (DP_n 28). Key resonances are assigned [66].

4.4.2 Fractionation of partially hydrolyzed dextran by SEC

Partially hydrolyzed dextran was further separated and fractionated by SEC to obtain samples with narrower chain length distribution. The chromatogram obtained from the separation is presented in Figure 4.14.

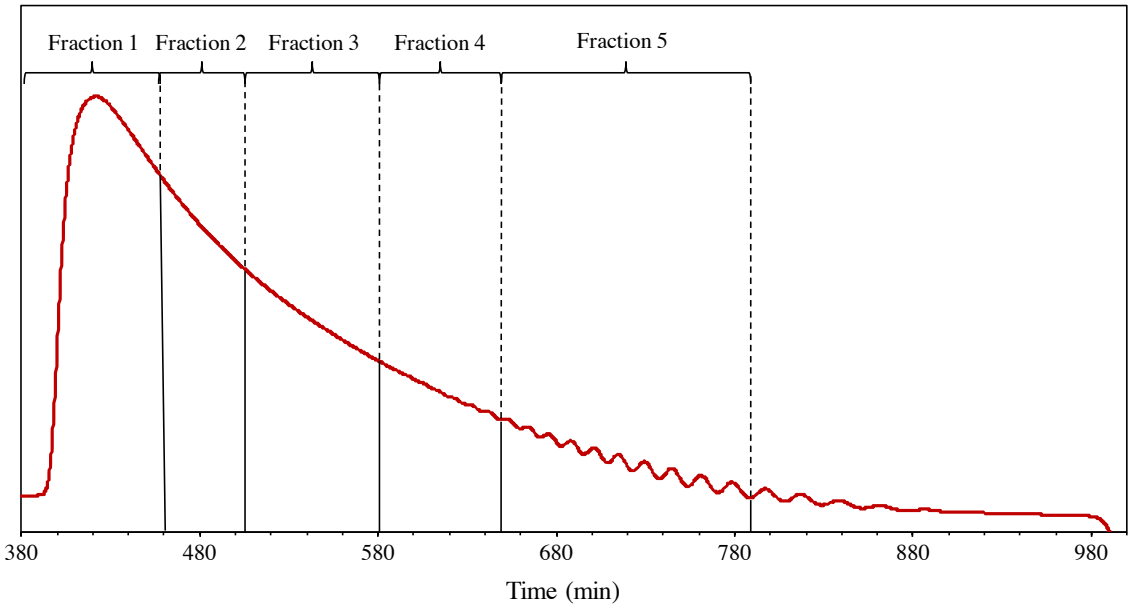

Figure 4.14: Partially hydrolyzed dextran (DP_n 28) separated and fractionated into five separate fractions by SEC (Superdex G-30, 0.1 M AmAc, pH 6.9).

The chromatogram showed good separation with discernible peaks at high elution times. The sample was fractionated into five separate fractions according to elution times as indicated in Figure 4.14 for further determination of molar mass distribution by SEC-MALS.

4.4.3 Determination of molar mass distribution of dextran fractions by SEC-MALS

The five fractions in Figure 4.14 were analyzed by SEC-MALS to determine their molar mass and chain length distribution. The RI profile of fraction 1-5 together with the corresponding molecular weight is presented in Figure 4.15.

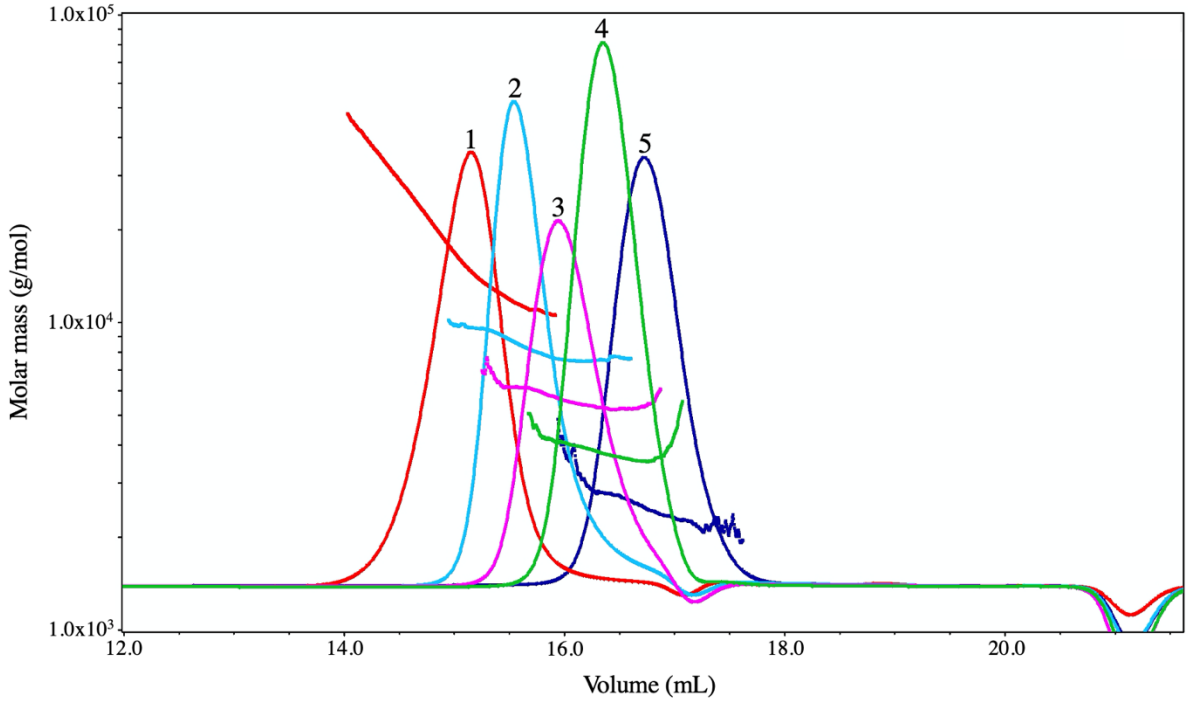

Figure 4.15: SEC-MALS data for partially hydrolyzed dextran fraction 1-5 obtained at room temperature. Solid lines refer to the RI profile and dotted lines refer to the molecular weights.

All peaks were symmetrical and eluted with increasing elution volume according to the separation on SEC. The molar mass decreased with increased elution volume, from around $2x10^4$ g/mol for fraction 1 to around $2x10^3$ g/mol for fraction 5. Values obtained for M_w and M_n are given in Table 4.3. Except for fraction 1, M_w was more or less equal to M_n for all fractions indicating quite narrow chain length distributions. DP_n were calculated from M_n and are included in Table 4.3 as well as the polydispersity.

Table 4.3: Weight average (M_w), number average (M_n) molecular weights, polydispersity, and calculated chain length distribution (DP_n) for partially hydrolyzed dextran fraction 1-5 obtained by SEC-MALLS.

Fraction	M_w (kDa)	M_n (kDa)	Polydispersity (M_w/M_n)	DP_n
1	17.0	15.6	1.09	96
2	8.4	8.4	1.00	52
3	5.6	5.6	1.00	35
4	3.8	3.8	1.00	23
5	2.5	2.5	1.00	15

4.5 Attaching a second block: SBG-*b*-Dextran diblock structures

Polysaccharide block copolymers are relatively novel structures, and the properties of diblock polysaccharides are little described. We wanted to prepare polysaccharide block copolymers from PDHA-activated SBG by attaching dextran as the second block. Dextran is a highly flexible polysaccharide and has significantly higher solubility in water compared to SBG. It was therefore of interest to explore if an SBG-*b*-dextran diblock would have increased solubility compared to pure SBG. For this reason, dextran with *m* residues ($Dext_m$) was conjugated to PDHA-activated SBG with *n* residues (SBG_n-PDHA).

4.5.1 Attachment of $Dext_m$ to SBG_n-PDHA: Kinetics and structure

The conjugation of dextran to PDHA-activated SBG was first studied by time-course ^{1}H-NMR to determine the kinetics governing the reaction. The data could further be compared to literature, as the conjugation with dextran and free PDHA has been studied using the same approach. SBG_4-PDHA was conjugated to an equimolar concentration of $Dext_5$. Oligomers with DP 4-5 were chosen for this study as short oligomers simplify the ^{1}H-NMR spectra. ^{1}H-NMR spectra following the reaction is given in Figure 4.16.

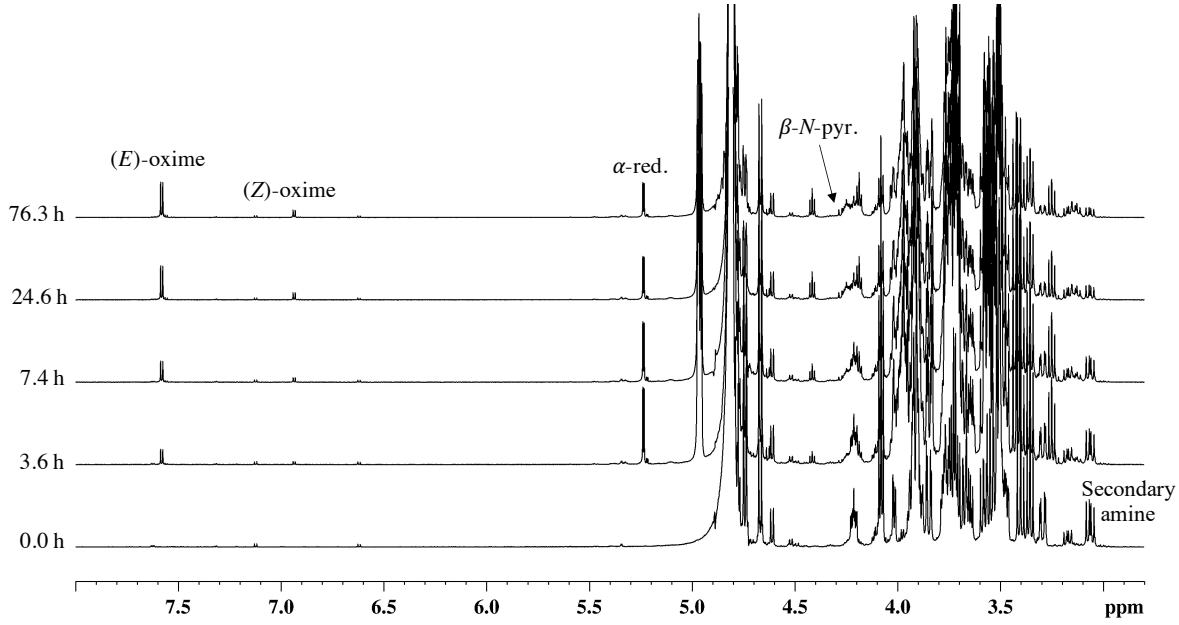

Figure 4.16: ^{1}H-NMR spectra (600 MHz, 25 °C) at given time points for the conjugation of SBG_4-PDHA to $Dext_5$.

Formation of (*E*)- and (*Z*)-oximes was observed at 7.58 and 6.94 ppm, respectively. A weak signal for *β*-*N*-pyranoside was detected at 4.28 ppm, partly overlapped by other peaks. The reducing intensity of reducing end resonances and the emergence of signals from the Schiff bases was evident from the NMR spectra taken at different timepoints. Integration was performed to determine the combined yield and kinetic parameter. Yields were calculated relative to the signal intensity of the methylene proton of SBG_4-PDHA secondary amine at 3.06 ppm before $Dext_5$ was added (Appendix C, Figure C.1-C.2). Yield plotted against reaction time is presented in Figure 4.17.

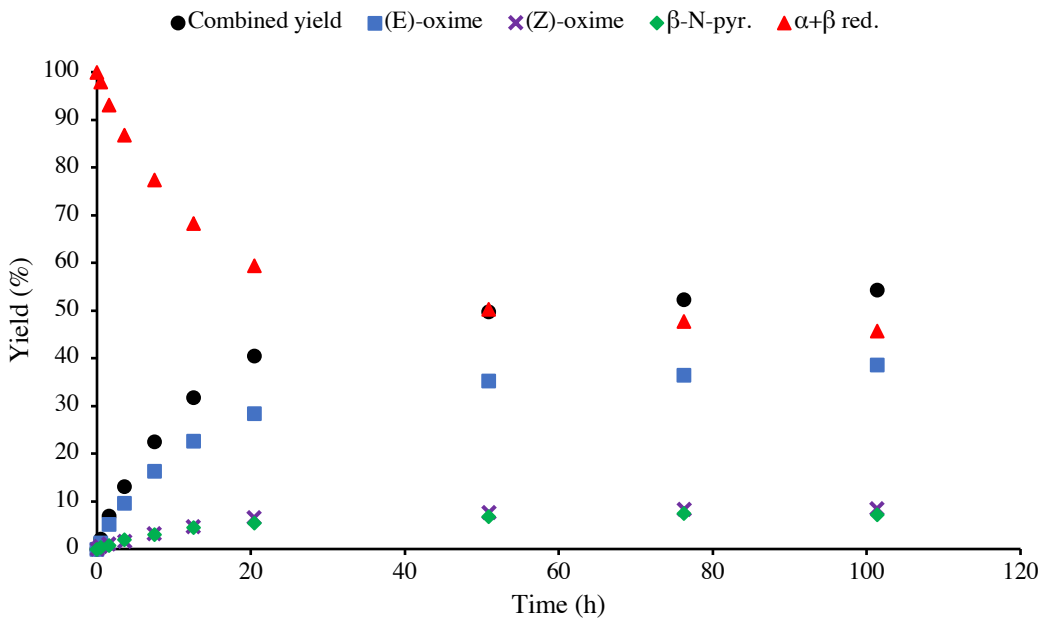

Figure 4.17: Course of the conjugation reaction of SBG_4-PDHA to $Dext_5$ obtained by integration of the spectra presented in Figure 4.16.

The reduction in free reducing end resonances and the formation of (*E*)-oxime, (*Z*)-oxime, and *β*-*N*-pyranoside are displayed over time. The calculated sum of the reaction products is also included as combined yield. By treating the combined yield as a single product, the reaction was fitted to a model of first order kinetics as described by Mo *et al*. [36]. At equilibrium, the combined yield was estimated to be 53 % for the conjugation of SBG_4-PDHA to one equivalent $Dext_5$. The reaction time required to reach 50 % ($t_{0.5}$) and 90 % ($t_{0.9}$) of the equilibrium yield were estimated by the same model to be 9.1 h and 33.4 h, respectively.

The subsequent reduction of the Schiff bases was studied by adding 3 equivalents PB and monitoring the reaction with time-course ^{1}H-NMR over a period of 5 days. The reduction yields stable SBG_4-PDHA-$Dext_5$ diblock structures. ^{1}H-NMR spectrum of the reaction mixture after ended reduction is presented in Figure 4.18.

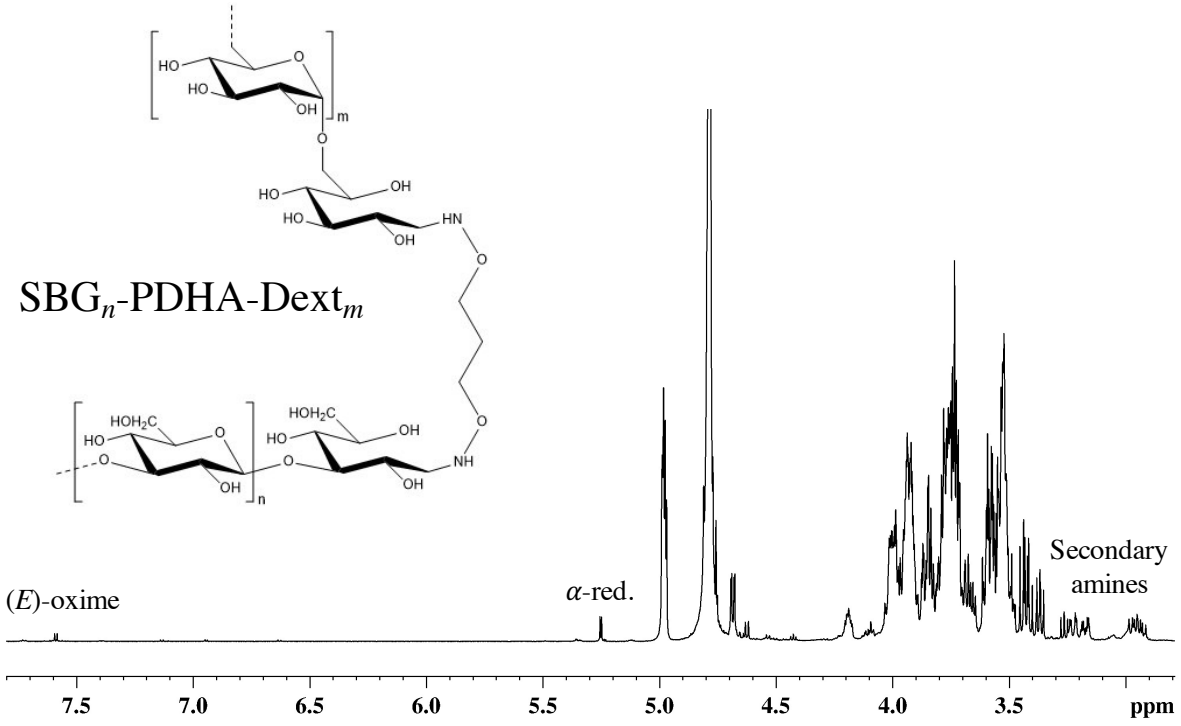

Figure 4.18: ^{1}H-NMR spectrum (600 MHz, 25 °C) of reaction mixture obtained for the preparation of SBG diblock structures by reacting SBG_4-PDHA with $Dext_5$ in an equimolar ratio followed by reduction by 3 equivalents PB over a period of 5 days. The general structure of reduced SBG_n-PDHA-$Dext_m$ diblock are included.

A weak signal for (*E*)-oximes were still detectable after 5 days of reduction whereas resonances for (*Z*)-oximes and *β*-*N*-pyanoside was not observed. Resonances for the methylene protons of the secondary amines was detected around 3.00 ppm. Due to peak overlap the combined yield could not be determined accurately by NMR. However, the detection of signals from the reducing ends and small amounts of (*E*)-oxime indicated that the reduction was incomplete.

4.5.2 Characterization of SBG-*b*-dextran diblocks of high molecular weight using SEC-MALS

Based on the protocol prepared in the previous section for the conjugation of $Dext_5$ to SBG_4-PDHA, SBG_{133}-PDHA was reacted with dextran of different chain lengths ($Dext_{23}$, $Dext_{35}$, and $Dext_{52}$, the subscripts referring to DP_n). The chains were now too long to monitor the reaction with NMR to verify the conjugation and to determine the reaction yield. The course of the reaction was instead simulated to predict the total yield using the kinetic parameters obtained in the section above (Appendix C, Table C.1) in combination with the assumption that the kinetics are independent of DP [36]. Dextran was added in excess to increase the yield as lower concentrations were used due to solubility limitations of SBG_{133}-PDHA. Hence, by reacting 5

mM SBG_{133}-PDHA with 3 equivalents dextran the simulation yielded approximately 3.6 mM of reaction products ((E)-oximes, (Z)-oximes, and β-*N*-pyranoside) which corresponded to a combined yield of 73 % diblocks (Appendix C, Figure C.3). The diblock structures were subsequently reduced with 20 equivalents PB, and as the reduction was slow at room temperature, the temperature was increased to 40 °C. The resulting structures were analyzed by SEC-MALLS to verify conjugation and to evaluate whether the conjugation affected the aggregation of SBG. Due to time considerations, excess dextran was not removed prior to the analysis. The RI profiles and the corresponding molecular weights of the diblock samples are presented in Figure 4.19. SBG_{133}-PDHA was included for comparison.

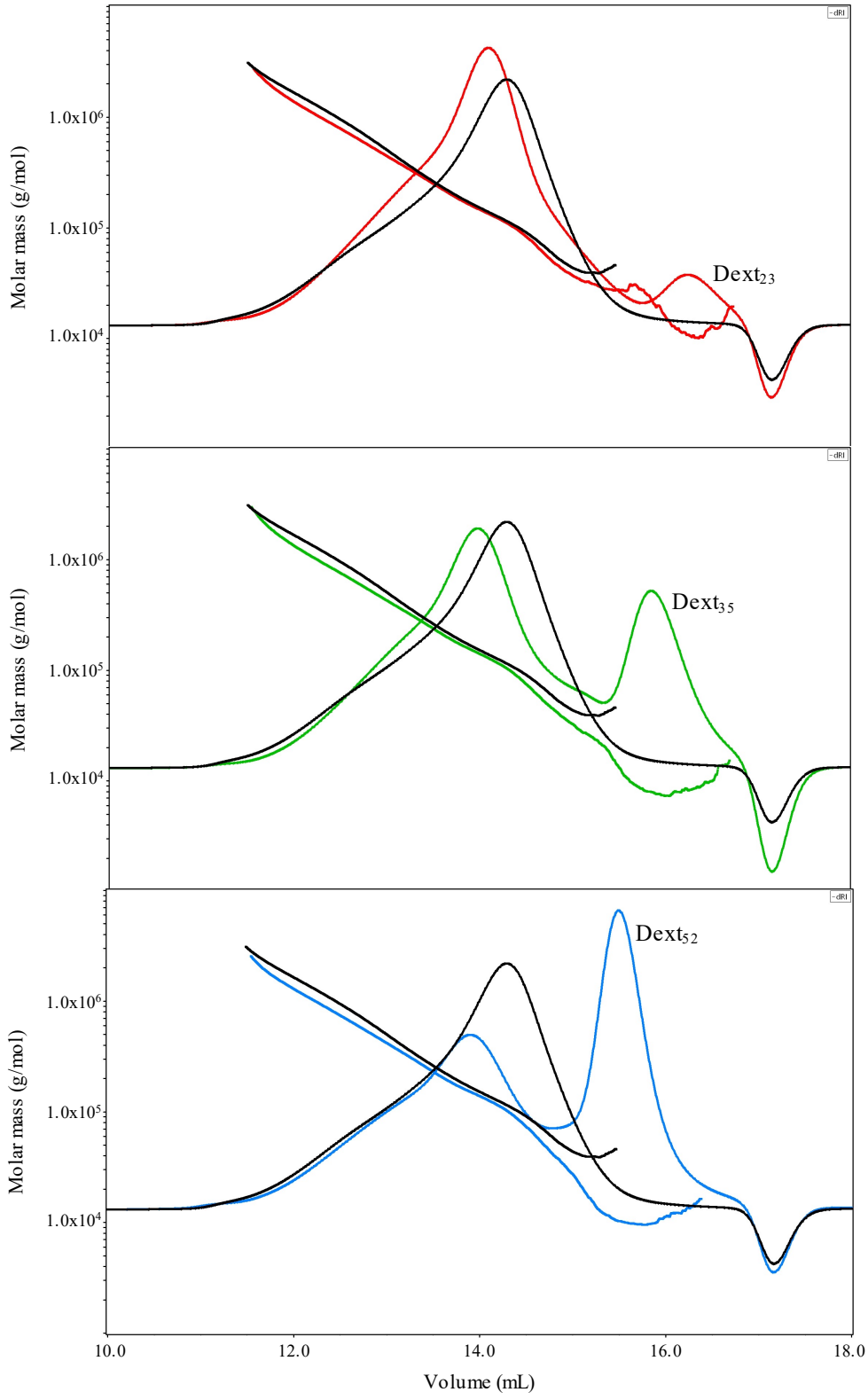

Figure 4.19: SEC-MALLS data for SBG_{133}-PDHA-$Dext_{23}$ (top, red), SBG_{133}-PDHA-$Dext_{35}$ (middle, green), and SBG_{133}-PDHA-$Dext_{52}$ (bottom, blue) samples. SBG_{133}-PDHA (black) was included for comparison in all three plots. Unreacted $Dext_{23}$, $Dext_{35}$, and $Dext_{52}$ is marked. Solid lines refer to the RI profile and dotted lines refer to the molecular weights.

As observed from the RI profiles, two peaks appeared, one broad peak and one narrower peak. The broad peak appearing at lower elution volume is largely overlapping with the peak corresponding to SBG_{133}-PDHA. The narrower peak appearing at higher elution volume corresponds to unreacted dextran. The peak for unreacted dextran is increasing in area and decreasing in elution volume in accordance with the increasing chain length. It should be noted that as the chain length distribution of SBG-PDHA was determined to be 133 after this experiment was carried out, SBG_{133}-PDHA was actually reacted with 3.25, 3,50, and 2,87 equivalents $Dext_{23}$, $Dext_{35}$, and $Dext_{52}$, respectively. Moreover, the broad peak in all three plots is shifted slightly towards lower elution volume compared to the peak of free SBG_{133}-PDHA. This indicated that SBG_{133}-PDHA had been conjugated to dextran. Conspicuously, the peak for unreacted dextran, especially $Dext_{23}$ (top plot) seemed to be disproportionally small knowing that dextran was added in excess. By integration of the chromatograms (Appendix C, Figure C.4-C.6) the peak area of unreacted $Dext_{23}$, $Dext_{35}$, and $Dext_{52}$ accounted for 7, 26, and 43 % of the total area, respectively. By calculating the weight ratio of SBG_{133}-PDHA-$Dext_m$ to unreacted $Dext_m$ (m = 23, 35, 52) at 100 % conjugation, the area of unreacted $Dext_{23}$, $Dext_{35}$, and $Dext_{52}$ would have accounted for 27, 34, and 35 % of the total area, respectively. Hence, the samples of SBG_{133}-PDHA conjugated to $Dext_{23}$ and $Dext_{35}$ corresponded to a degree of conjugation above 100 % while the sample of SBG_{133}-PDHA conjugated to $Dext_{52}$ corresponded to a degree of conjugation of 73 %. The latter was in good agreement with the theoretical yield obtained by simulation (notably without reduction). However, as the peaks were not baseline separated the degree of conjugation could not be determined accurately by SEC-MALS. Nevertheless, by assuming 73 % conjugation, the molecular weight of all the diblock samples was still essentially the same as the molecular weight observed for free SBG_{133}-PDHA, ranging from around 10^4 to 10^6 Da. This therefore suggested that the conjugation to dextran of defined chain length did not disrupt the aggregation of SBG_{133}-PDHA.

4.6 Attaching a second block: SBG-*b*-Alginate diblock structures

As the conjugation of dextran to SBG_{133}-PDHA did not appear to reduce the aggregation of SBG, we decided to explore the effects of attaching a charged polysaccharide. Oligoguluronate is a polyelectrolyte which has been reported to be highly reactive towards free PDHA [unpublished work, Solberg, A.]. For this reason, alginate oligoguluronate with m residues (G_m) was attached as the second block to SBG_n-PDHA.

4.6.1 Attachment of G_m to SBG_n-PDHA: Kinetics and structure

The conjugation of a short SBG-PDHA chain (SBG_9-PDHA) to a short oligoguluronate chain (G_3) was first investigated by time-course ^{1}H-NMR to determine the yield and the kinetics governing the reaction. SBG_9-PDHA was conjugated to an equimolar concentration of G_3. ^{1}H-NMR spectra following the conjugation is given in Figure 4.20.

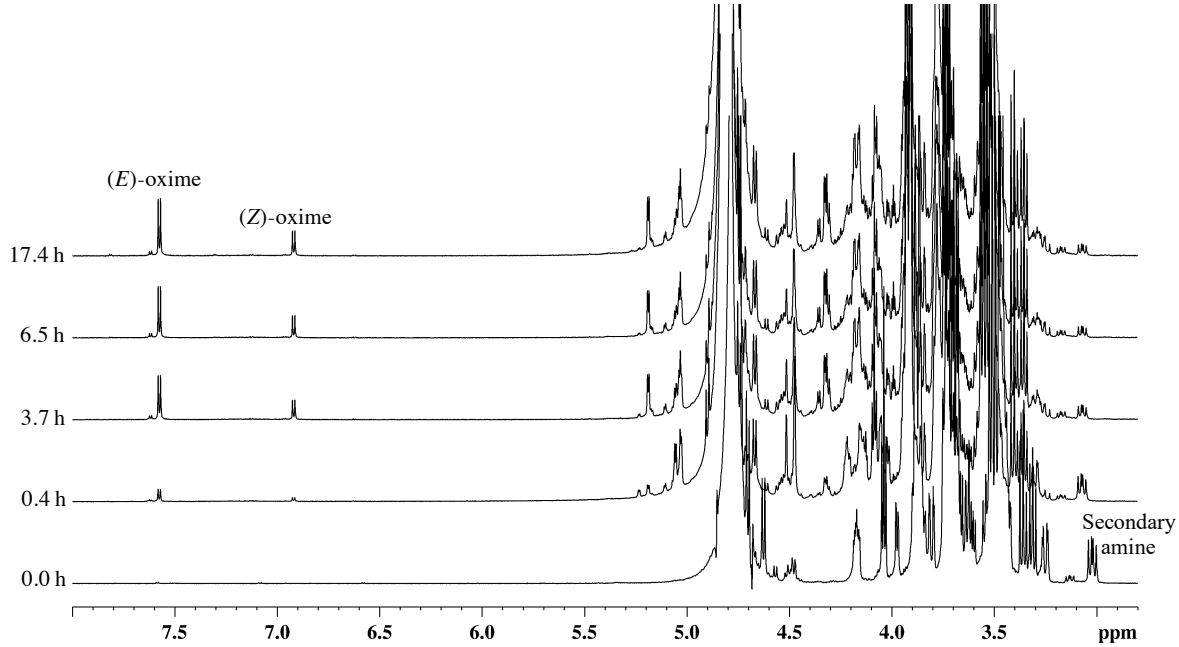

Figure 4.20: ^{1}H-NMR spectra (600 MHz, 25 °C) at given time points for the conjugation of SBG_9-PDHA to one equivalent G_3.

Resonances for (*E*)- and (*Z*)-oximes appeared at 7.58 and 6.92 ppm, respectively. From NMR spectra taken at different time points, the emergence of signals from the Schiff bases and the reducing intensity of the reducing end resonances was evident. Integration was performed to determine the combined yield of reaction products and the kinetic parameters. Yields were calculated relative to the signal intensity of the methylene proton of SBG_9-PDHA secondary amine at 3.02 ppm before G_3 was added (Appendix D, Figure D.1-D.2). The course of the reaction is presented in Figure 4.21.

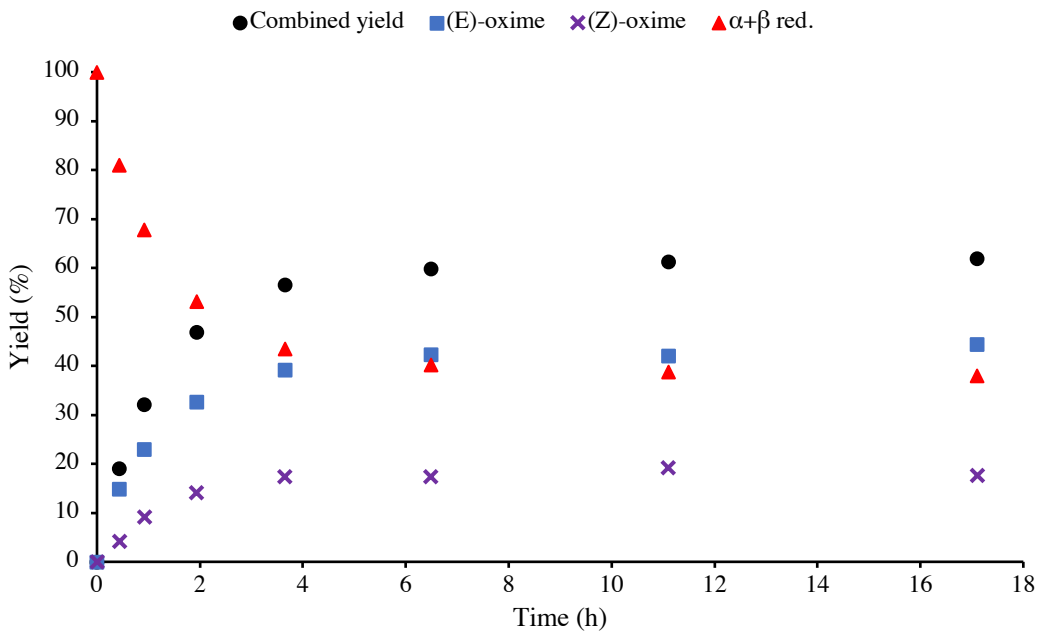

Figure 4.21: Course of the conjugation reaction of SBG_9-PDHA to G_3 obtained by integration of the spectra presented in Figure 4.20.

The reduction in free reducing end resonances and the formation of (*E*)- and (*Z*)-oxime are shown over time as well as the combined yield. Conjugation of SBG_9-PDHA to one equivalent G_3 resulted in a combined yield of 61 % conjugates at equilibrium. $t_{0.5}$ and $t_{0.9}$ were estimated to 0.85 h and 3.3 h, respectively.

The subsequent reduction of the Schiff bases was studied by adding 3 equivalents PB and monitoring the reaction with time-course ^{1}H-NMR over a period of 5 days. ^{1}H-NMR spectrum of the reaction mixture for the preparation of SBG_9-PDHA-G_3 after terminated reduction is presented in Figure 4.22.

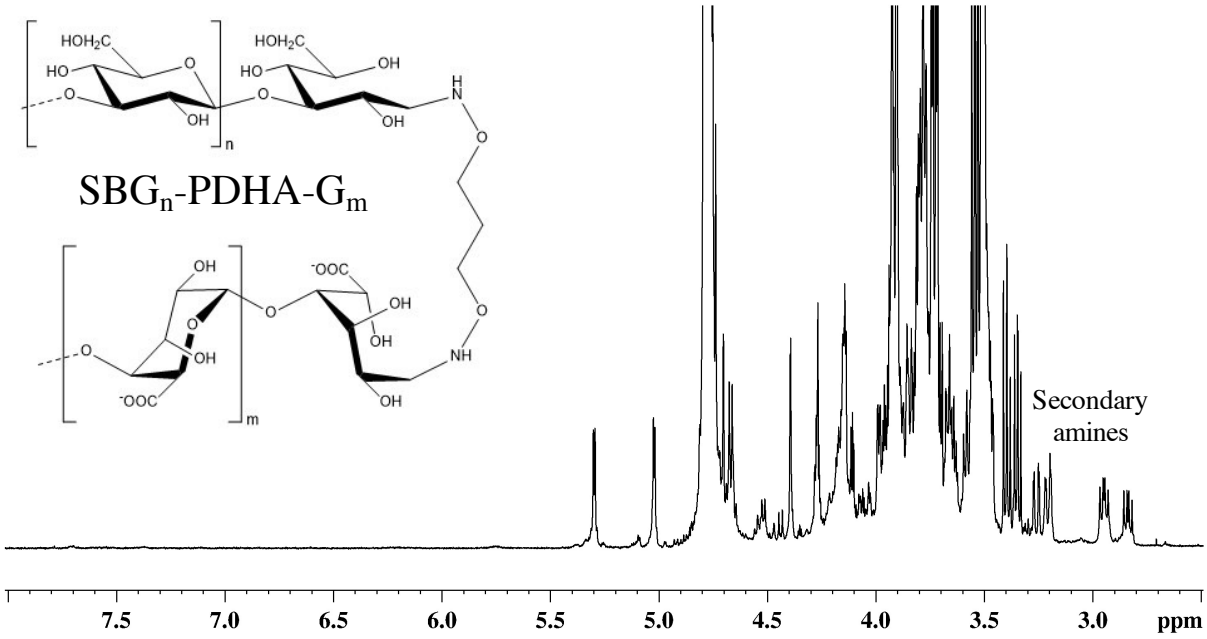

Figure 4.22: ^{1}H-NMR spectrum (600 MHz, 25 °C) of reaction mixture obtained for the preparation of SBG diblock structures by reacting SBG_9-PDHA with G_3 in an equimolar ratio followed by reduction using 3 equivalents PB over a period of 5 days. The general structure of reduced SBG_n-PDHA-G_m diblock are included.

The appearance of secondary amines (2.84-3.26 ppm) and the absence of signals for (*E*)- and (*Z*)-oximes indicated reduction of SBG_9-PDHA-G_3. Complete conversion to the secondary amine was indicated based on integration of resonances from the secondary amine. The absence of resonances from oximes was in good agreement with complete reduction.

4.6.2 Characterization of SBG-*b*-alginate diblocks of high molecular weight using SEC-MALS

Based on the protocol established in the previous section, G_{18} was conjugated to SBG_{133}-PDHA to investigate how the attachment of a polyelectrolyte affected the aggregation of SBG in aqueous solution. SBG_{133}-PDHA was conjugated to 3 equivalents G_{18} and subsequently reduced with PB. G_{18} was added in excess to ensure complete conjugation as the reaction kinetics have shown to be somewhat dependent on DP [unpublished work, Solberg, A.]. The sample was analyzed by SEC-MALLS to evaluate the conjugation and to assess whether the conjugation affected the aggregation of SBG. Unreacted G_{18} was not removed prior to the analysis. The RI profile and the corresponding molecular weight of the diblock sample is presented in Figure 4.23. SBG_{133}-PDHA was included for comparison.

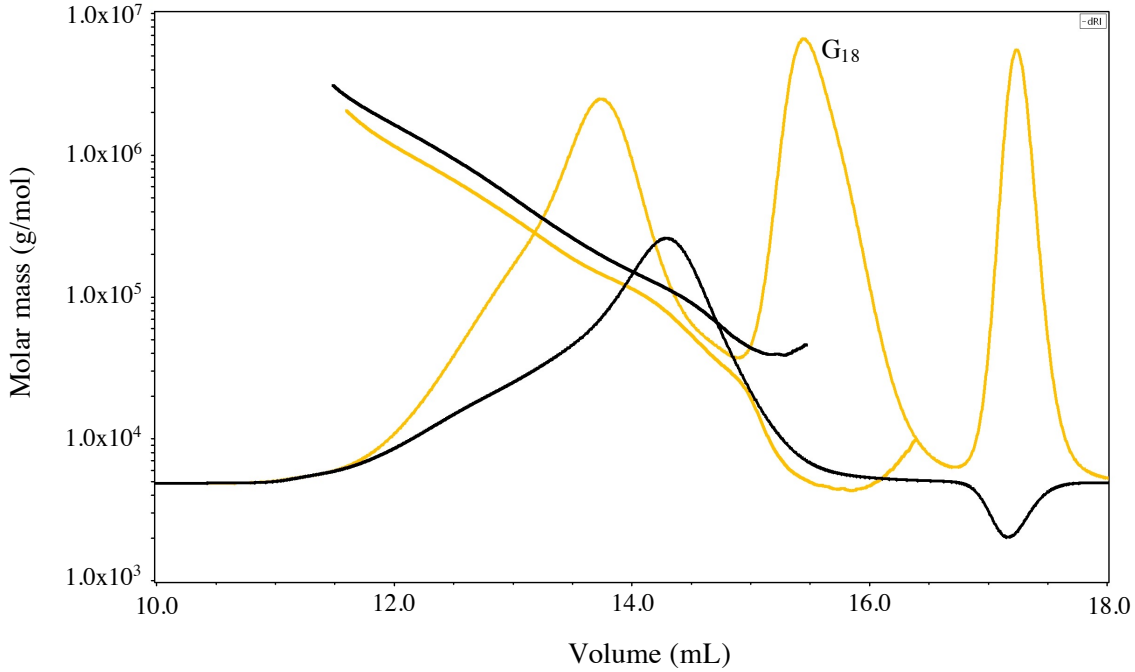

Figure 4.23: SEC-MALLS data for SBG_{133}-PDHA-G_{18} (yellow) and SBG_{133}-PDHA (black) obtained at room temperature. Unreacted G_{18} is marked. Solid lines refer to the RI profile and dotted lines refer to the molecular weights.

As seen for SBG_{133}-PDHA conjugated to $Dext_m$ (section 4.5.2), the diblock sample give rise to two peaks. The broad peak appearing with lower elution volume was largely overlapping with the peak corresponded to SBG_{133}-PDHA while the peak appearing at higher elution volume corresponded to unreacted G_{18}. Also here it should be noted that as the chain length distribution of SBG-PDHA was determined to be 133 after this experiment was carried out, SBG_{133}-PDHA was actually reacted with 5.32 equivalents G_{18}. The broad peak was shifted towards lower elution volumes compared to the peak for free SBG_{133}-PDHA, indicating conjugation to G_{18}. By integration of the chromatogram, the relative yield of SBG_{133}-PDHA-G_{18} diblocks was approximately 100 % (Appendix D, Figure D.3). Notably, as the peaks were not baseline separated, the yield could not be determined accurately by SEC-MALS. However, based on the protocol established in the previous section it could be safe to assume complete conjugation. The molecular weight of SBG_{133}-PDHA-G_{18} was slightly lower than what was observed for free SBG_{133}-PDHA, ranging from 10^4 to 10^6 Da. However, it was still significantly higher than expected for G_{18} conjugated to un-aggregated SBG_{133}-PDHA. This indicated that neither the conjugation of alginate of defined chain length could disrupt the aggregation of SBG_{133}-PDHA in aqueous solution.

5 Discussion

Aggregation of SBG is a known phenomenon present especially in high molecular weight samples [8]. This may be a beneficial property in terms of many biological applications. However, the aggregating behavior complicates both the characterization and general analysis of the polysaccharide. The key aim of this thesis was to prepare samples of fully soluble SBG with defined chain length through terminal modification. Terminal modification allows for optimal retention of the intrinsic properties of the polysaccharide and will therefore better preserve both its chemical and biological properties. This can be valuable for further studies in the biomedical field and for future potential applications.

5.1 Preparation and characterization of PDHA-activated SBG

As a first step, it was of interest to investigate if the conjugation of PDHA to the reducing end of SBG would reduce the aggregation of SBG in aqueous solvent. The pK_a of PDHA is 4.2, thus, PDHA would be positively charged under conditions where pH is close to its pK_a value (50 % charged at pH 4.2). Moreover, conjugation to the bifunctional linker would allow for attachment of a second block (detailed below) for the preparation of SBG-based diblock polysaccharides.

The conjugation of PDHA to the reducing end of SBG_{56} was performed using a large excess of PDHA (10 equivalents) to avoid the formation of di-substituted PDHA as this would prevent the later attachment of a second block. In accordance with literature, the conjugation of an oxyamine with a reducing carbohydrate resulted in a tautomeric mixture of predominantly acyclic and a small quantity of cyclic products [32]. The appearance of acyclic oximes in both (*E*)- and (*Z*)-configuration as well as cyclic *N*-pyranoside in β-configuration was evident from the ^{1}H-NMR spectrum taken after the conjugation of PDHA to SBG_{56}. Due to peak overlap, the combined yield could not be determined accurately by NMR. However, an earlier study performed under equal conditions on the conjugation of SBG (DP 5) to 2 equivalents PDHA reported a combined yield of 94 % after 24 hours reaction [57]. Based on the assumption that reaction kinetics are independent of DP it can be assumed that the combined yield in the present study also was close to 100 % [36]. The absence of resonances from reducing ends was in good agreement with this assumption.

As the reaction between reducing carbohydrates and oxyamines is reversible, SBG_{56}-PDHA was subsequently reduced with PB to obtain stable secondary amines. The reduction was performed at 40 °C to increase the reaction rate as the reduction of SBG-based oximes has been reported to be slow at room temperature [57]. In agreement with literature, the methylene protons of the secondary amines formed after reduction gave proton resonances in the area around 3.00 ppm [36]. By integration, the amount of reduced conjugates were calculated to be 68 % after 48 hours reduction. This indicated incomplete conversion to the secondary amine and that longer reaction time may be required for complete conversion. However, as the signal intensity of the secondary amine resonances became very weak compared to the signal intensity of the internal anomeric protons, accurate determination of reduced SBG_{56}-PDHA was difficult. Using ^{1}H-NMR to determine reaction yield works well for relatively short chains. However, when applied to longer chains which have small terminal anomeric proton peaks, the signal to noise ratio in the spectra becomes low. Hence, the yield of reduced SBG_{56}-PDHA could not be determined accurately by NMR. The absence of signals from the reducing ends and only small amounts of (*E*)-oximes indicated that reduced conjugates had been obtained in high yields.

SBG_{56} activated with PDHA was further separated and fractionated by SEC to obtain samples with a narrower chain length distribution (DP_n). As no study has revealed the aggregation dependency of the DP_n of SBG, the samples could be used to examine the role of chain length in the aggregation process. Evident from the chromatogram obtained from the separation, the sample contained a high concentration of components which were too large to be separated. Data certificates provided by the supplier informs that the SEC system used for this experiment has a separation range of 0.5 to 30 kDa. Notably, these values are based on the separation of dextran which is a much more flexible polysaccharide than SBG hence the exclusion limit for SBG is probably somewhat lower than 30 kDa. However, using these values could indicate that the excluded components of PDHA-activated SBG_{56} had a molecular weight above ~30 kDa. This assumption is in agreement with the weight average (M_w) molecular weight of the initial sample being 35 kDa (Figure 3.1, section 3.1). However, the large amount of excluded components was somewhat unexpected. Knowing that the number average (M_n) molecular weight of the SBG sample was 9.1 kDa it was expected that the amount of un-excluded components would be higher. By assuming an upper exclusion limit of 30 kDa, this could be an indication that SBG_{56}-PDHA was aggregated. However, this was not possible to tell only based on the chromatogram. One thing that was certain based on

the obtained results was that determination of the accurate molar mass distribution of PDHA-activated SBG_{56} was not possible using this system due to the high amount of excluded components. For complete separation, a bigger column with larger pore sizes is necessary.

SBG_{56}-PDHA samples fractionated by SEC was subsequently analyzed by SEC-MALS to determine the molar mass distribution of each collected fraction. According to the separation on SEC, the chromatographic peak of fraction 1-3 appeared with increasing elution volume and decreasing molar mass, respectively. The molecular weight averages (M_w and M_n) of fraction 1 was significantly higher than the corresponding values of fraction 2 and 3. This was expected as fraction 1 comprised the sample components excluded in the SEC separation and would hence have a higher molecular weight distribution. However, M_n corresponded to a DP_n of 775 which was over one order of magnitude above the corresponding value for the parent sample (DP_n 56). This high molecular weight is a prominent characteristic of aggregated SBG preparations in aqueous solutions and it was therefore assumed that fraction 1 was strongly aggregated [8]. Fractions 2 and 3 had M_w and M_n values below 30 kDa which were in accordance with the assumed separation range of the SEC system. However, only based on molecular weight it was difficult to determine whether they also were aggregated.

The aggregation of all three fractions became evident when analyzing the molecular weight dependence of the intrinsic viscosity. All fractions had viscosities below values expected for un-associated SBG chains with corresponding molecular weights [7]. Data for all three fractions also showed some curvature which may suggest that the fractions contained structures of different macromolecular geometries. By line fitting the average slopes of all three fractions ranged between the values of randomly coiled structures and polymers shaped as solid spheres [46]. This indicated very compact structures. Although the nature of SBG aggregates is little described, it could safely be concluded that PDHA-activated SBG is by no means triple-stranded under these conditions [67]. Taken together, the characteristically high molecular weight, especially of fraction 1, and the low intrinsic viscosities clearly indicated aggregation. Thus, the introduction of PDHA at the reducing end does not prevent aggregation of SBG under these conditions. Hence, the preparation of non-aggregated fractions and determination of accurate molecular weight or chain length distribution of SBG-PDHA was not possible using the above-described conditions.

To determine the molecular weight and chain length distributions of the fractionated samples, the samples were analyzed by SEC-MALS using DMAc/LiCl as solvent. The analysis revealed that the M_w of fraction 1 was over one order of magnitude below the value obtained in aqueous solution. The M_w of fraction 2 was also reduced with about ¼. Concurrent reduction in M_n also resulted in reduced values for the chain length distribution of both fractions. The chromatograms showed that the peaks largely overlapped with each other and that the difference in molecular weight was also small. As the fractions were collected after separation by SEC it could be assumed that instead of separating single chains of different length, aggregates of different size containing chains of similar lengths were separated during SEC. Hence, using aqueous SEC for the separation of SBG is inefficient both in terms of analysis of the true molecular weight distribution and in separation based on chain length. Alternative protocols for the separation of SBG by SEC is therefore necessary. Using eluents where SBG is fully soluble would improve the efficiency of the separation significantly. Complete dissolution of the SBG chains during separation can allow for separation based on differences in chain length and not in aggregate size. Thus, this could also be used to examine the DP dependency of the aggregation which were not possible under aqueous conditions. As DMAc/LiCl appeared as suitable solvent for the determination of molar mass distribution of SBG-PDHA by SEC-MALS it may also be an alternative eluent for separation by SEC. Other alternative solvents where β-1,3-glucans are reported to dissociate into single chains are DMSO or dilute alkali [15, 17].

5.2 Effects of thermal treatment on high-molecular weight SBG-PDHA conjugates

Since the SEC-MALS system in DMAc/LiCl was not available in our lab, samples of PDHA-activated SBG were exposed to thermal treatment to explore the possibility of using high temperature as a simple tool to obtain fully dissociated SBG chains. Both the concentrated and diluted sample of activated SBG showed a reduction in molecular weight after heat treatment. Compared to an earlier study where high-molecular weight SBG (DP_n 117) was pre-heated to a temperature of 100 °C for 15 minutes before it was analyzed by SEC-MALS at a column temperature of 80°C, the reduction in molecular weight in the present study was significantly higher [7]. Hence, increased temperature has a greater effect on reducing the aggregation. However, neither in this study did the samples reach a molecular weight equal to that observed for single, un-associated chains. Li et al. reported that the rapid re-association of cereal β-glucan after heat treatment at 90 °C for 3 hours was inevitable in pure water and that this made it nearly

impossible to obtain aggregate-free solutions for evaluation [60]. This may also be the case in the present study as the samples were still clearly aggregated after applied thermal treatment. It has also been reported that the temperature required for complete dissociation of triple stranded *β*-1,3-glucans in aqueous solution are in the range of approximately 130-160 °C [3]. This may suggest that a temperature of 121 °C is not sufficient to disrupt all the hydrogen bonds stabilizing the aggregating SBG chains. However, due to lack of equipment we were not able to reach higher temperatures. Either way, this protocol did not allow for complete dissociation of PDHA-activated SBG in aqueous solution.

5.3 Attaching a second block: SBG-*b*-dextran diblock structures

The motivation for preparing diblock polysaccharides was to prepare a block combining the inherent physicochemical properties of the two block structures. Thus, preparation of diblocks with SBG and highly soluble polysaccharides was hypothesized as a potential route for the preparation of fully soluble, un-associated SBG. Dextran was chosen as the second block due to its high solubility.

To prepare a protocol for the conjugation of dextran to PDHA-activated SBG, the conjugation was first studied by time-course ^{1}H-NMR to estimate the yield and kinetics of the reaction. Formation of oximes in (*E*)- and (*Z*)-configuration and *N*-pyranoside in *β*-configuration was evident after 0.4 hours reaction. The signal intensity of the reaction products increased steadily during the course of the reaction before it started to level of after around 20 hours reaction. Based on a model for first order kinetics, the combined equilibrium yield was estimated to be 53 %. Mo *et al.* studied the conjugation of dextran oligomers (DP 5) to free PDHA using the same approach. Using 2 equivalents PDHA, an equilibrium yield of 90 % was obtained [36]. The equilibrium yield obtained from the conjugation of $Dext_5$ to SBG_4-PDHA in the present study was significantly lower. However, here the two blocks were conjugated in an equimolar ratio, based on the overall need to use minimum amounts of oligomers as well as to simplify following purification steps. Hence it could be assumed that using an excess of SBG_4-PDHA would increase the reaction yield. In another study, Mo *et al.* studied the conjugation of dextran oligomers to PDHA-activated chitin oligomers using equimolar amounts of the two blocks [11]. Here they obtained an equilibrium yield of 66 %. This was more similar to what was obtained in the present study. They used an oligomer concentration twice as high which could be the reason for the slightly higher yield. Hence it

could also be assumed that the conjugation of dextran to PDHA-activated SBG could result in higher yields if higher concentration of reactants is used. An increased reaction rate could also be expected at higher concentrations as the collision frequency between molecules becomes higher.

The reaction mixture was further reduced with 3 equivalent PB to obtain stable diblock structures. Higher yields could be expected after reduction as, according to Le Châteliers principle, the addition of reducing agent will change the equilibrium to counteract the change and hence be shifted towards the formation of reaction products as reaction products are reduced [68]. The reduction in signal for (*E*)-oxime and the disappearance of signals for (*Z*)-oximes and *β*-*N*-pyranoside indicated reduction of the SBG_4-PDHA-$Dext_5$ diblocks. A weak signal for (*E*)-oximes were still detectable as well as signals for reducing end protons after terminated reduction indicating that the diblock structures were not fully reduced. Too early termination of the reduction hence resulted in lower yields than what could have been expected after complete reduction. Due to lack of material, we were not able to repeat the experiment. However, in agreement with literature the reduction of dextran-based oximes by PB at room temperature was very slow. For future studies, the reduction rate could be increased by increasing the temperature.

The protocol established for the conjugation of PDHA-activated SBG to dextran was used for the preparation of SBG-*b*-dextran diblocks of higher DP. SEC-MALS has shown to be useful when evaluating the conjugation of two polysaccharide blocks by other in our research group and was therefore chosen as analysis method. SEC-MALS will also allow for the determination of molecular weight which will reveal if the attachment of dextran can reduce the aggregation of SBG in aqueous solution. As illustrated in Figure 4.19, the reaction mixtures obtained for the preparation of SBG diblock structures by reacting SBG_{133}-PDHA with an excess $Dext_m$ (m = 23, 35, 52) followed by reduction using PB gave rise to two peaks in the chromatograms. In the ideal case when two polysaccharide blocks of different molecular weight are conjugated and one is added in excess, as in the present case, two peaks will appear in the chromatogram if the conjugation is complete (100 %). One peak will correspond to the diblock structures which will have a molecular weight equal to the sum of the two conjugated blocks and be shifted towards lower elution volume, and one peak will correspond to the remains of the block added in excess. However, two peaks will also appear if there is no conjugation between the two blocks. Then the two peaks will appear with a

molecular weight and elution volume equal to that of each unreacted block. The broad peak appearing at lower elution volume was assumed to contain diblock structures as the peak was shifted towards lower elution volume compared to the peak of free SBG_{133}-PDHA. Lower elution volumes indicate larger structures and hence conjugation. By integration of the chromatogram for SBG_{133}-PDHA conjugated to $Dext_{23}$, the area assumed to contain diblock structures was found to account for 93 % of the total area, whereas unreacted dextran accounted for the resisting 7 % of the area. As dextran was added in excess it was expected that the area of unreacted dextran would be larger. If 100 % conjugation the area of dextran would have been accounting for about 27 % of the total area. The weight yield of assumed diblock structures was therefore largely overestimated. The same applied for the chromatogram of SBG_{133}-PDHA conjugated to $Dext_{35}$. The reason for this was not obvious. Some of the unreacted dextran might have been lost during dialysis due to the high flexibility of dextran chains, which increases the probability for the molecules to diffuse through small pores. It could also be speculated whether some of the unreacted dextran associates with SBG_{133}-PDHA in some way. Either way, SEC-MALS under these conditions did not appear to be an optimal analysis tool for the determination of reaction efficiencies between dextran of defined chain lengths and SBG_{133}-PDHA.

Since the degree of conjugation between dextran and SBG_{133}-PDHA could not be determined accurately by SEC-MALS it was difficult to tell whether the conjugation affected the aggregation of SBG. However, by assuming 73 % conjugation (from simulation) the molecular weight of the SBG-*b*-dextran diblock was still essentially the same as SBG_{133}-PDHA by SEC-MALS. This is likely resulting from aggregation. If the attachment of dextran had reduced the aggregation of SBG, it was expected that the molecular weight of the diblock structures would have been reduced. Thus, conjugation to dextran in this case did not appear to increase solubility enough to counter the aggregation of SBG. In other master projects, the conjugation of PDHA-activated dextran oligomers to both alginate, chitosan, and chitin oligomers has revealed to increase their solubility by rendering them soluble under conditions where the unmodified polymer is insoluble. For the alginate case conjugation to dextran has been shown to render the diblock soluble even up on full protonation of alginate (pH 1.0). However, this is only the case for certain chain lengths of dextran [unpublished work, Solberg, A.]. A diblock comprised of G_{14}-*b*-$Dext_{15}$ precipitates similarly to unmodified guluronate under acidic conditions (pH < 3.5) while a diblock comprised of G_{24}-*b*-$Dext_{36}$ was shown to be soluble under the same conditions [unpublished work, Solberg, A.]. For the

chitosan case, a diblock composed of $D_{28}M$-*b*-$Dext_{52}$ (D = D-glucosamine, M = 2,5-anhydro D-mannose) was shown to be soluble under conditions where unmodified chitosan precipitates (pH > 6.5) [69]. Albeit precipitation and aggregation are two different phenomena, it could be hypothesized that dextran could be used to increase the solubility of SBG, but that the chain length of dextran used in the present case was not long enough.

5.4 Attaching a second block: SBG-*b*-Alginate diblock structures

Dextran was chosen as the second block due to its high solubility, but as the conjugation of dextran to SBG did not affect the aggregation it was of interest to examine the effect of preparing a diblock with SBG and a charge polysaccharide. Thus, a second SBG-based diblock was prepared where alginate was chosen as the second block. As opposed to dextran, alginate is a polyelectrolyte with pK_a 3.5 [70]. Thus, SBG-*b*-alginate blocks were prepared and characterized to determine if a charged block could prevent aggregation by charge repulsion.

As the reaction between SBG and alginate had not yet been reported, the conjugation of alginate to PDHA-activated SBG was studied by time-course ^{1}H-NMR to determine an appropriate protocol for the preparation of the diblock. Formation (*E*)- and (*Z*)-oximes was evident after 0.4 hours reaction, and a significant increase was observed after 3 hours reaction. In agreement with literature, no formation of *β*-*N*-pyranoside was observed [unpublished work, Solberg, A.]. The estimated combined equilibrium yield (61 %) was only slightly higher than what was observed for the conjugation of dextran to PDHA-activated SBG. However, the reaction rate was significantly faster. This may be ascribed to the higher reactivity of the reducing end of alginate compared to dextran [unpublished work, Solberg, A.]. The oximes formed under conjugation was further reduced with PB to obtain stable diblock structures. Compared to the reduction of dextran-based oximes, the reduction of alginate-based oximes was very efficient and resulted in complete conversion to the secondary amine. Based on these results, an efficient protocol for the preparation of SBG-*b*-alginate has been developed. By first reacting SBG with an excess of PDHA to prepare PDHA-activated SBG, then attaching alginate as the second block results in high yields of diblock structures.

Based on the protocol developed for the preparation of SBG-*b*-alginate diblock structures, PDHA-activated SBG_{133} was conjugated to G_{18} to examine the effect of terminal attachment of charge on the aggregation behavior of SBG. As observed for the conjugation to dextran, the

elution volume for the peak corresponding to SBG_{133}-PDHA was shifted towards lower elution volumes indicating conjugation to G_{18}. From integration of the chromatogram, the degree of conjugation was calculated to be approximately 100 % which was in good agreement with the established protocol. The molecular weight across the RI profile of the SBG_{133}-PDHA-G_{18} diblocks was slightly lower compared to the molecular weight of free SBG_{133}-PDHA. However, the difference was minimal. Thus, neither the conjugation to alginate in this case appeared to increase the solubility enough to counter the aggregation of SBG. However, since the chain length of the SBG block was much longer than the chain length of the alginate block, it could be assumed that the solubility characteristics of the diblock is determined by the SBG block. It could therefore be hypothesized that alginate could be used to increase the solubility of SBG if the chain length of alginate is increased to that limit in which the solubility characteristics of the diblock are determined by the alginate block.

6 Conclusion

This thesis aimed to prepare fully soluble SBG samples through terminal activation and preparation of SBG-based block polysaccharides. Terminal activation of SBG with the bifunctional dioxyamine PDHA resulted in high yields of SBG-PDHA conjugates with the formation of (*E*)- and (*Z*)-oximes and β-*N*-pyranoside. Stable secondary amines were obtained by reduction with PB. The reduction did not result in complete conversion to secondary amines. However, this was partly ascribed to the low accuracy of integration in the NMR spectrum. As minimal amounts of intermediate products were observed after reduction, this indicated that reduced conjugates had been obtained in high yields.

PDHA-activated SBG was further separated and fractionated by SEC. Complete separation was not obtained as the sample contained a large amount of components too large to be separated. Hence alternative methods are required to achieve complete separation. Analysis of fractionated SBG-PDHA by SEC-MALS with an additional viscosity detector revealed high molecular weights and low intrinsic viscosities of the SBG-PDHA fractions. This indicated that SBG-PDHA was strongly aggregated and could not be dispersed as single chains following terminal activation with PDHA under aqueous conditions. Thermal treatment of SBG-PDHA was also insufficient for the complete dissociation of SBG in aqueous solution. However, aggregating SBG-PDHA could be dispersed as single chains in DMAc containing 0.9 % LiCl, which allowed for determination of accurate molar mass distribution. SEC-MALS analysis in DMAc/LiCl hence appeared as a suitable strategy for studying the molecular weight of SBG.

Block polysaccharide were prepared from PDHA-activated SBG by attaching dextran and alginate as the second block. Kinetic studies for the conjugations revealed that alginate conjugated faster to PDHA-activated SBG compared to dextran. Dextran-based oximes were also slowly reduced by PB at room temperature compared to alginate-based oximes. The slow reduction of dextran-based oximes might be ascribed to the nature of the reducing end residue, as alginate-based oximes were reduced with a much higher rate under the same conditions. The slow reduction of dextran-based oximes may also be attributed to the additional formation of non-reducible cyclic conjugates (β-*N*-pyranoside). A protocol using higher temperatures may improve the reduction of dextran-based oximes significantly.

The protocols established for the preparation of short SBG-*b*-dextran and SBG-*b*-alginate diblock oligosaccharides were further used to prepare diblocks of longer chain lengths. Attachment of dextran and alginate to PDHA-activated SBG in this case did not appear to increase the solubility enough to counter the aggregation of SBG. However, it was hypothesized that dextran and alginate could be used to increase the solubility of SBG if the chain length of the second block is increased to that limit in which the solubility characteristics of the diblock are determined by the second block. Increasing the chain length of the second block may therefore be of interest for future work.

Regarding potential applications, water-soluble SBG activated with PDHA would be ideally suited for conjugation to aldehyde containing particles, surfaces or other macromolecules. As SBG is known to play important roles in activating immune responses, this can be used to study the molecular recognition of SBG by proteins such as immune receptors. Terminally conjugated SBG-based block polysaccharides may also offer a wide range of new and possibly bioactive materials.

References

1. Novoa-Carballal, R. and A.H. Muller, *Synthesis of polysaccharide-b-PEG block copolymers by oxime click.* Chem Commun (Camb), 2012. **48**(31): p. 3781-3.
2. Wang, X., et al., *Multiple Conformation Transitions of Triple Helical Lentinan in DMSO/Water by Microcalorimetry.* The Journal of Physical Chemistry B, 2009. **113**(29): p. 9915-9923.
3. Meng, Y., et al., *Recent Advances in Chain Conformation and Bioactivities of Triple-Helix Polysaccharides.* Biomacromolecules, 2020. **21**(5): p. 1653-1677.
4. Breivik, T., et al., *Soluble β-1,3/1,6-glucan from yeast inhibits experimental periodontal disease in Wistar rats.* Journal of Clinical Periodontology, 2005. **32**(4): p. 347-352.
5. Chan, G.C.-F., W.K. Chan, and D.M.-Y. Sze, *The effects of β-glucan on human immune and cancer cells.* Journal of Hematology & Oncology, 2009. **2**(1): p. 25.
6. Adams, E.L., et al., *Differential high-affinity interaction of dectin-1 with natural or synthetic glucans is dependent upon primary structure and is influenced by polymer chain length and side-chain branching.* J Pharmacol Exp Ther, 2008. **325**(1): p. 115-23.
7. Qin, F., F.L. Aachmann, and B.E. Christensen, *Chain length distribution and aggregation of branched (1-->3)-beta-D-glucans from Saccharomyces cerevisae.* Carbohydr Polym, 2012. **90**(2): p. 1092-9.
8. Qin, F., et al., *Higher order structures of a bioactive, water-soluble (1-->3)-beta-D-glucan derived from Saccharomyces cerevisiae.* Carbohydr Polym, 2013. **92**(2): p. 1026-32.
9. Williams, D.L., et al., *A method for the solubilization of a (1→3)-β-d-glucan isolated from Saccharomyces cerevisiae.* Carbohydrate Research, 1991. **219**: p. 203-213.
10. Qin, F., M. Kes, and B.E. Christensen, *A study of bioactive, branched (1→3)-β-d-glucans in dimethylacetamide/LiCl and dimethyl sulphoxide/LiCl using size-exclusion chromatography with multi-angle light scattering detection.* Journal of Chromatography A, 2013. **1305**: p. 109-113.
11. Mo, I.V., et al., *2,5-Anhydro-d-Mannose End-Functionalized Chitin Oligomers Activated by Dioxyamines or Dihydrazides as Precursors of Diblock Oligosaccharides.* Biomacromolecules, 2020. **21**(7): p. 2884-2895.
12. Gidley, M.J. and K. Nishinari, *Chapter 2.2 - Physico-chemistry of (1,3)-β-Glucans*, in *Chemistry, Biochemistry, and Biology of 1-3 Beta Glucans and Related Polysaccharides*, A. Bacic, G.B. Fincher, and B.A. Stone, Editors. 2009, Academic Press: San Diego. p. 47-118.
13. Nie, S., S.W. Cui, and M. Xie, *Chapter 3 - Beta-Glucans and Their Derivatives*, in *Bioactive Polysaccharides*, S. Nie, S.W. Cui, and M. Xie, Editors. 2018, Academic Press. p. 99-141.
14. Engstad, R.E. and B. Robertsen, *Recognition of yeast cell wall glucan by Atlantic salmon (Salmo salar L.) macrophages.* Dev Comp Immunol, 1993. **17**(4): p. 319-30.
15. Yanaki, T., et al., *Correlation between the antitumor activity of a polysaccharide schizophyllan and its triple-helical conformation in dilute aqueous solution.* Biophysical Chemistry, 1983. **17**(4): p. 337-342.
16. McIntire, T.M. and D.A. Brant, *Observations of the (1→3)-β-d-Glucan Linear Triple Helix to Macrocycle Interconversion Using Noncontact Atomic Force Microscopy.* Journal of the American Chemical Society, 1998. **120**(28): p. 6909-6919.

17. Gawronski, M., et al., *Microfibrillar structure of PGG-Glucan in aqueous solution as triple-helix aggregates by small angle x-ray scattering.* Biopolymers, 1999. **50**(6): p. 569-578.
18. Kenney, J.F., *Properties of block versus random copolymers.* Polymer Engineering & Science, 1968. **8**(3): p. 216-226.
19. Jenkins, A.D., et al., *Glossary of basic terms in polymer science.* Pure and Applied Chemistry, 1996. **68**(12): p. 2287-2311.
20. Schatz, C. and S. Lecommandoux, *Polysaccharide-containing block copolymers: synthesis, properties and applications of an emerging family of glycoconjugates.* Macromol Rapid Commun, 2010. **31**(19): p. 1664-84.
21. Feng, H., et al., *Block Copolymers: Synthesis, Self-Assembly, and Applications.* Polymers (Basel), 2017. **9**(10).
22. Volokhova, A.S., K.J. Edgar, and J.B. Matson, *Polysaccharide-containing block copolymers: synthesis and applications.* Materials Chemistry Frontiers, 2020. **4**(1): p. 99-112.
23. Baudendistel, O.R., et al., *Real-Time NMR Studies of Oxyamine Ligations of Reducing Carbohydrates under Equilibrium Conditions.* Chemistry, 2016. **22**(48): p. 17359-17365.
24. Isono, T., et al., *Self-Assembly of Maltoheptaose-block-polycaprolactone Copolymers: Carbohydrate-Decorated Nanoparticles with Tunable Morphology and Size in Aqueous Media.* Macromolecules, 2016. **49**(11): p. 4178-4194.
25. Pfannemuller, B., et al., *Properties of a Once-Broken Wormlike Chain Based on Amylose Tricarbanilate - Light-Scattering, Viscosity, and Dielectric-Relaxation.* Macromolecules, 1984. **17**(4): p. 710-716.
26. Reibel, L., G. Spach, and C. Dufour, *Etude Phsicochimique des Copolymères Triséquencés Poly(γ-L-glutamate de benzyle)/Poly(oxyéthylène)/Poly(γ-L-glutamate de benzyle). Rŏle de la Polydispersiteé dans la Détermination de la Conformation des Molécules en Solution Diluée.* Biopolymers, 1973. **12**(10): p. 2391-2408.
27. Delas, T., *Formulation and stabilization of colloidal polyelectrolyte complexes of chitosan and siRNA*, in *Chemical science*. 2021, University of Bordeaux.
28. Guerry, A., et al., *Aniline-Catalyzed Reductive Amination as a Powerful Method for the Preparation of Reducing End-"Clickable" Chitooligosaccharides.* Bioconjugate Chemistry, 2013. **24**(4): p. 544-549.
29. Gomez, S., J.A. Peters, and T. Maschmeyer, *The reductive amination of aldehydes and ketones and the hydrogenation of nitriles: Mechanistic aspects and selectivity control.* Advanced Synthesis & Catalysis, 2002. **344**(10): p. 1037-1057.
30. Solomons, G., Fryhle, C., Snyder, S., *Organic Chemistry*. 11 ed. 2014, Singapore: Wiley.
31. Fantoni, N.Z., A.H. El-Sagheer, and T. Brown, *A Hitchhiker's Guide to Click-Chemistry with Nucleic Acids.* Chem Rev, 2021.
32. Kwase, Y.A., M. Cochran, and M. Nitz, *Protecting-Group-Free Glycoconjugate Synthesis: Hydrazide and Oxyamine Derivatives in N-Glycoside Formation*, in *Modern Synthetic Methods in Carbohydrate Chemistry*. 2013. p. 67-96.
33. Coudurier, M., et al., *Reducing-End Functionalization of 2,5-Anhydro-d-mannofuranose-Linked Chitooligosaccharides by Dioxyamine: Synthesis and Characterization.* Molecules, 2020. **25**(5).
34. Dirksen, A. and P.E. Dawson, *Rapid oxime and hydrazone ligations with aromatic aldehydes for biomolecular labeling.* Bioconjug Chem, 2008. **19**(12): p. 2543-8.
35. Munneke, S., et al., *The rapid and facile synthesis of oxyamine linkers for the preparation of hydrolytically stable glycoconjugates.* Org Lett, 2015. **17**(3): p. 624-7.

36. Vikoren Mo, I., et al., *Activation of enzymatically produced chitooligosaccharides by dioxyamines and dihydrazides.* Carbohydr Polym, 2020. **232**: p. 115748.
37. Fang, J., et al., *Quantification of plant cell wall monosaccharides by reversed-phase liquid chromatography with 2-aminobenzamide pre-column derivatization and a non-toxic reducing reagent 2-picoline borane.* J Chromatogr A, 2015. **1414**: p. 122-8.
38. Sato, S., et al., *One-pot reductive amination of aldehydes and ketones with alpha-picoline-borane in methanol, in water, and in neat conditions.* Tetrahedron, 2004. **60**(36): p. 7899-7906.
39. Cosenza, V.A., D.A. Navarro, and C.A. Stortz, *Usage of alpha-picoline borane for the reductive amination of carbohydrates.* Arkivoc, 2011: p. 182-194.
40. Heinze T., L.T., Heublein B., Hornig S. , *Functional polymers based on dextran*, in *Polysaccharides II. Advances in polymer science*. 2006, Springer: Berlin.
41. Draget, K.I. and C. Taylor, *Chemical, physical and biological properties of alginates and their biomedical implications.* Food Hydrocolloids, 2011. **25**(2): p. 251-256.
42. Dalheim, M.Ø., et al., *Efficient functionalization of alginate biomaterials.* Biomaterials, 2016. **80**: p. 146-156.
43. Donati I., P.S., *Material properties of alginates* in *Alginates: Biology and Applications*. 2009, Springer: Berlin, Heidelberg. p. 1-53.
44. Draget, K.I., O. Smidsrød, and G. Skjåk-Bræk, *Alginates from Algae*, in *Biopolymers Online*. 2005.
45. Silverstein, R.M., et al., *Spectrometric Identification of Organic Compounds*. 8th ed. 2014: John Wiley & Sons.
46. Christensen, B.E., *Compendium TBT4135 Biopolymers*. 2018, Trondheim: NTNU.
47. Bubb, W.A., *NMR spectroscopy in the study of carbohydrates: Characterizing the structural complexity.* Concepts in Magnetic Resonance Part A, 2003. **19a**(1): p. 1-19.
48. Yao, H.-Y.-Y., et al., *A review of NMR analysis in polysaccharide structure and conformation: Progress, challenge and perspective.* Food Research International, 2021. **143**: p. 110290.
49. Coskun, O., *Separation techniques: Chromatography.* Northern clinics of Istanbul, 2016. **3**(2): p. 156-160.
50. Poole, C.F.P., S. K., *Chromatography today*. 1991, Amsterdam: Elsevier science publishers B. V.
51. Lundanes, E., L. Reubsaet, and T. Greibrokk, *Cromatography: Basic principles, sample preparations and related methods*. 2014: Wiley-VCH.
52. Mori S., B.H.G., *Fundamental Concepts*, in *Size exclusion chromatography*. 1999, Springer: Berlin, Heidelberg.
53. Poole, C.F., *The essence of chromatography*. 2003, Amsterdam: Elsevier science B.V.
54. Striegel, A.M., *Chapter 10 - Size-exclusion chromatography*, in *Liquid Chromatography (Second Edition)*, S. Fanali, et al., Editors. 2017, Elsevier. p. 245-273.
55. Goodridge, H.S., et al., *Activation of the innate immune receptor Dectin-1 upon formation of a 'phagocytic synapse'.* Nature, 2011. **472**(7344): p. 471-475.
56. Larsen, K., et al., *Solid-phase chemical tools for glycobiology.* Carbohydr Res, 2006. **341**(10): p. 1209-34.
57. Mo, I.V., *Towards block polysaccharides: Terminal activation of chitin and chitosan oligosaccharides by dioxyamines and dihydrazides an the preparation of block structures*, in *Department of Biotechnology and Food Science*. 2021, Norwegian University of Science and Technology.

58. Potthast, A., et al., *The cellulose solvent system N,N-dimethylacetamide/lithium chloride revisited: the effect of water on physicochemical properties and chemical stability.* Cellulose, 2002. **9**(1): p. 41-53.
59. Kivelä, R., et al., *Oxidative and radical mediated cleavage of β-glucan in thermal treatments.* Carbohydrate Polymers, 2011. **85**(3): p. 645-652.
60. Li, W., et al., *Elimination of aggregates of (1→3) (1→4)-β-D-glucan in dilute solutions for light scattering and size exclusion chromatography study.* Food Hydrocolloids, 2006. **20**(2): p. 361-368.
61. Viñarta, S.C., et al., *Effects of thermal, alkaline and ultrasonic treatments on scleroglucan stability and flow behavior.* Carbohydrate Polymers, 2013. **94**(1): p. 496-504.
62. Futatsuyama, H., T. Yui, and K. Ogawa, *Viscometry of Curdlan, a Linear (1→3)-β-D-Glucan, in DMSO or Alkaline Solutions.* Biosci Biotechnol Biochem, 1999. **63**(8): p. 1481-3.
63. Muren, T., *Chitin oligomers and chitin-based polysaccharides: Terminal conjugation of dextran to water insoluble chitin oligomers*, in *Department of Biotechnology and Food Science*. 2021, Norwegian University of Science and Technology.
64. Cló, E., O. Blixt, and K.J. Jensen, *Chemoselective Reagents for Covalent Capture and Display of Glycans in Microarrays.* European Journal of Organic Chemistry, 2010. **2010**(3): p. 540-554.
65. Bordwell, F.G. and D. Algrim, *Nitrogen acids. 1. Carboxamides and sulfonamides.* The Journal of Organic Chemistry, 1976. **41**(14): p. 2507-2508.
66. Cheetham, N.W.H., E. Fialabeer, and G.J. Walker, *Dextran Structural Details from High-Field Proton Nmr-Spectroscopy.* Carbohydrate Polymers, 1990. **14**(2): p. 149-158.
67. Sletmoen, M., B.E. Christensen, and B.T. Stokke, *Probing macromolecular architectures of nanosized cyclic structures of (1-->3)-beta-D-glucans by AFM and SEC-MALLS.* Carbohydr Res, 2005. **340**(5): p. 971-9.
68. Treptow, R.S., *Le Châtelier's principle: A reexamination and method of graphic illustration.* Journal of Chemical Education, 1980. **57**(6): p. 417.
69. Gravdahl, M., *Preparation, characterization, and solution properties of chitosan-b-dextran diblocks*, in *Department of Biotechnology and Food Science*. 2021, Norwegian University of Science and Technology.
70. Haug, A., *Composition and properties of alginates*. 1964, Norwegian Institute of Technology: Trondheim.

Appendix A

The yield of reduced SBG-PDHA was determined by integration of the ^{1}H-NMR spectrum (Figure A.1).

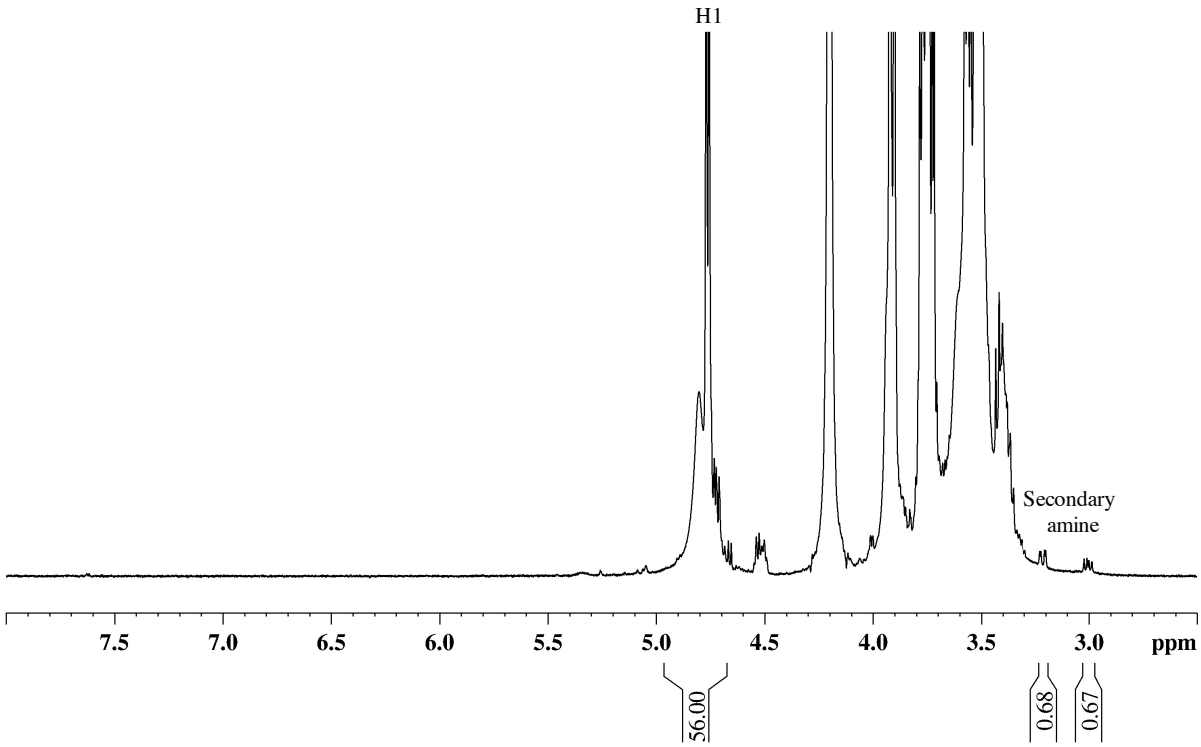

Figure A.1: ^{1}H-NMR spectrum (600 MHz, 82 °C) of reduced PDHA-activated SBG (DP_n 56) with integrated signals.

Appendix B

^{1}H-NMR spectra were obtained throughout the conjugation reactions between SBG_6 and PDHA in DMSO. The relative proportions of reactants and products was calculated using the integrated values of the key resonances. The spectrum taken prior to the addition of PDHA are shown in Figure B.1. The final spectrum obtained after 60 hours reaction is displayed in Figure B.2. Figure B.3 and Figure B.4 shows ^{1}H-NMR spectra for the reaction between SBG_4 and PDHA in DMSO with the addition of 10 % D_2O prior to the addition of PDHA and after 24 hours reaction, respectively.

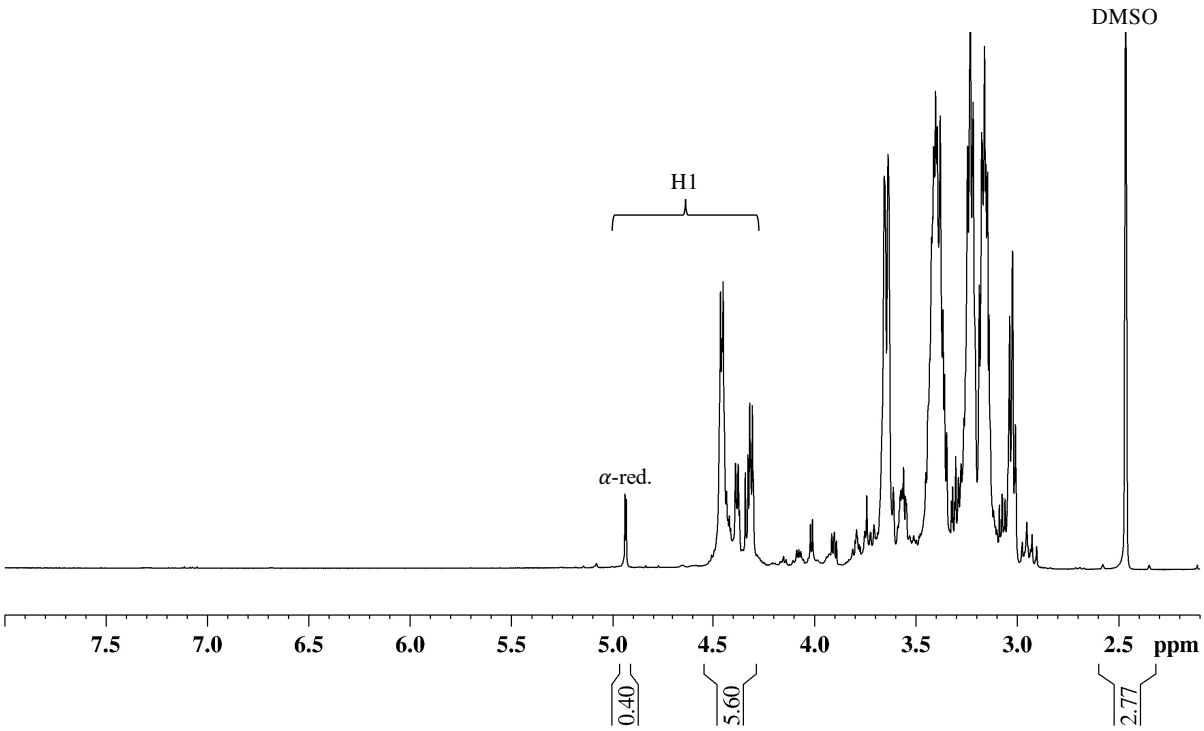

Figure B.1: ^{1}H-NMR spectrum (600 MHz, 25 °C) of SBG_6 prior to the addition of PDHA with integrated signals.

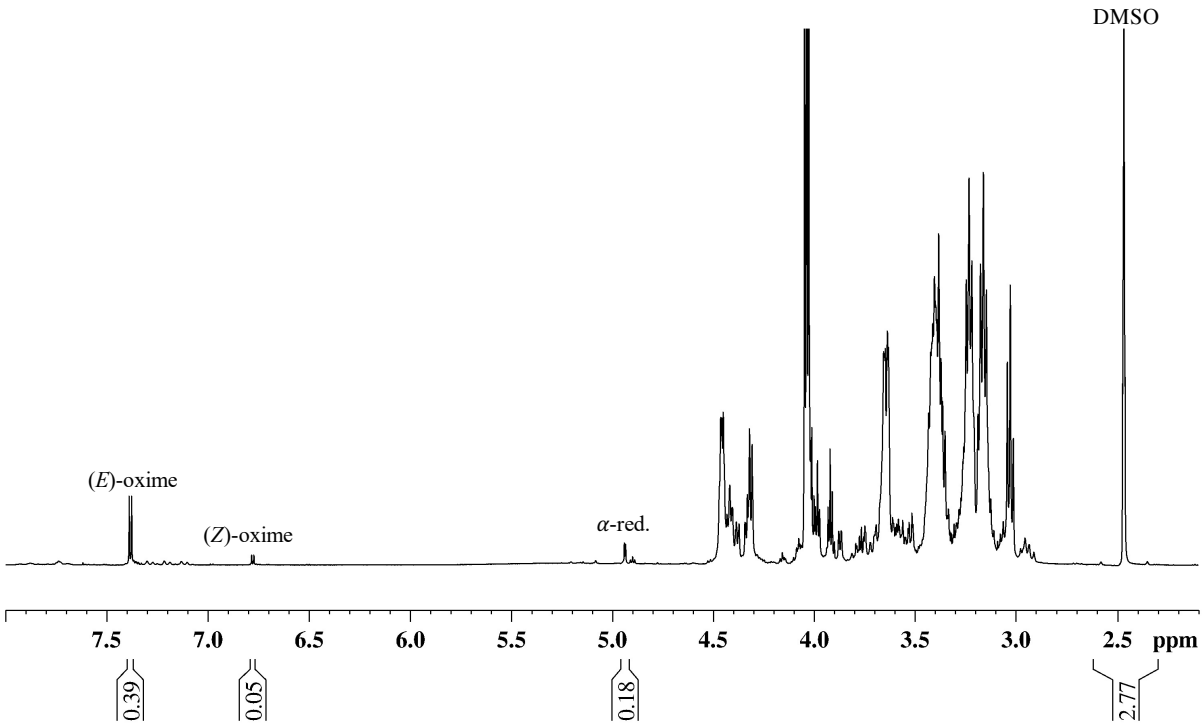

Figure B.2: ^{1}H-NMR spectrum of SBG_6 conjugated to PDHA after 60 hours reaction. Integrated signals for reactant and products are displayed.

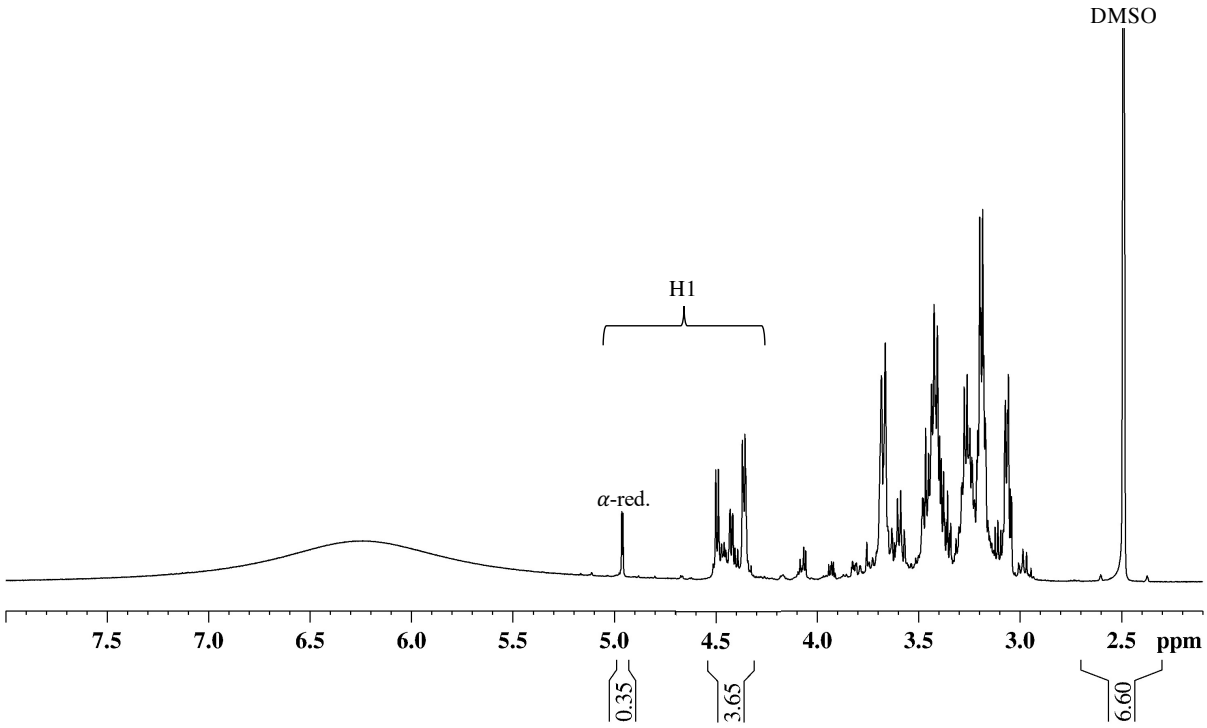

Figure B.3: ^{1}H-NMR spectrum (600 MHz, 25 °C) of SBG_4 prior to the addition of PDHA with integrated signals.

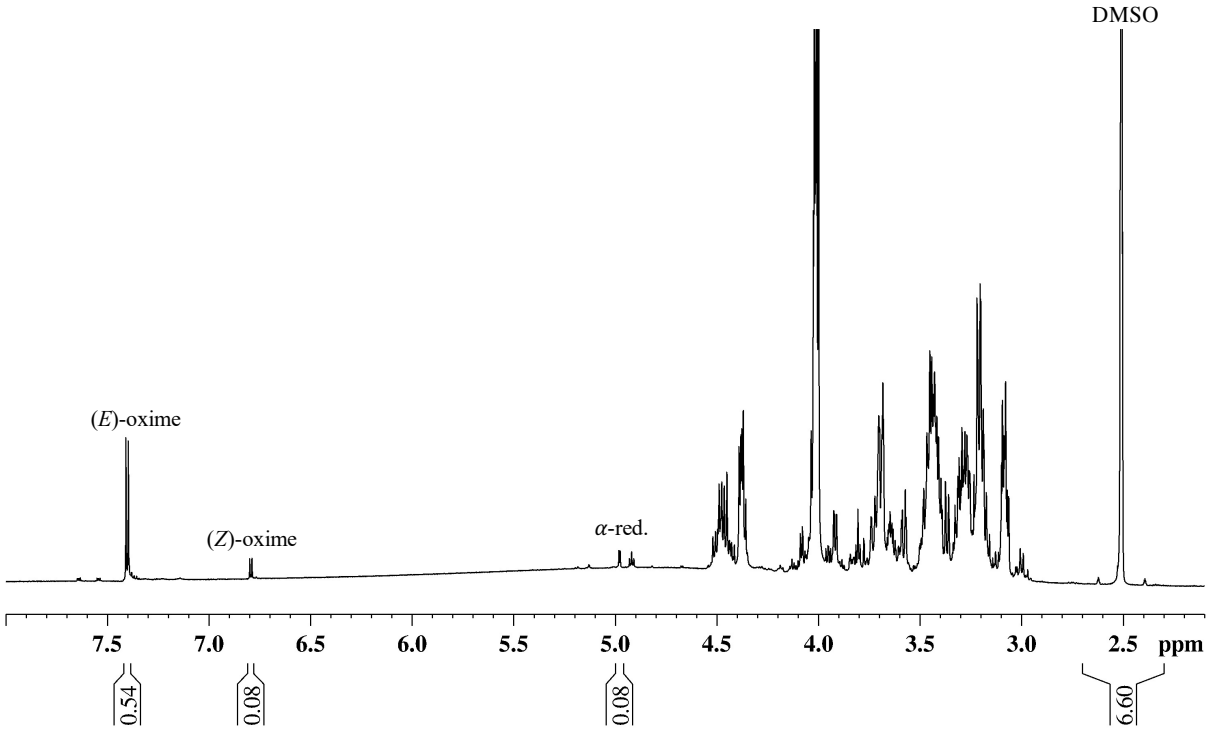

Figure B.4: ^{1}H-NMR spectrum (600 MHz, 25 °C) of SBG_4 conjugated to PDHA after 24 hours reaction. Integrated signals for reactant and products are displayed.

Appendix C

SBG-*b*-dextran diblocks were prepared by reacting SBG_4-PDHA with $Dext_5$ in an equimolar ratio. The conjugation of the second block was monitored by time-course ^{1}H-NMR. Yields were calculated relative to the signal intensity of the methylene proton of SBG_4-PDHA secondary amine at 3.06 ppm before $Dext_5$ was added. TSP was added in a known concentration as an internal standard for calibration of integrals. The spectrum taken prior to the addition of $Dext_5$ is shown in Figure C.1. The final spectrum obtained at equilibrium displayed in Figure C.2.

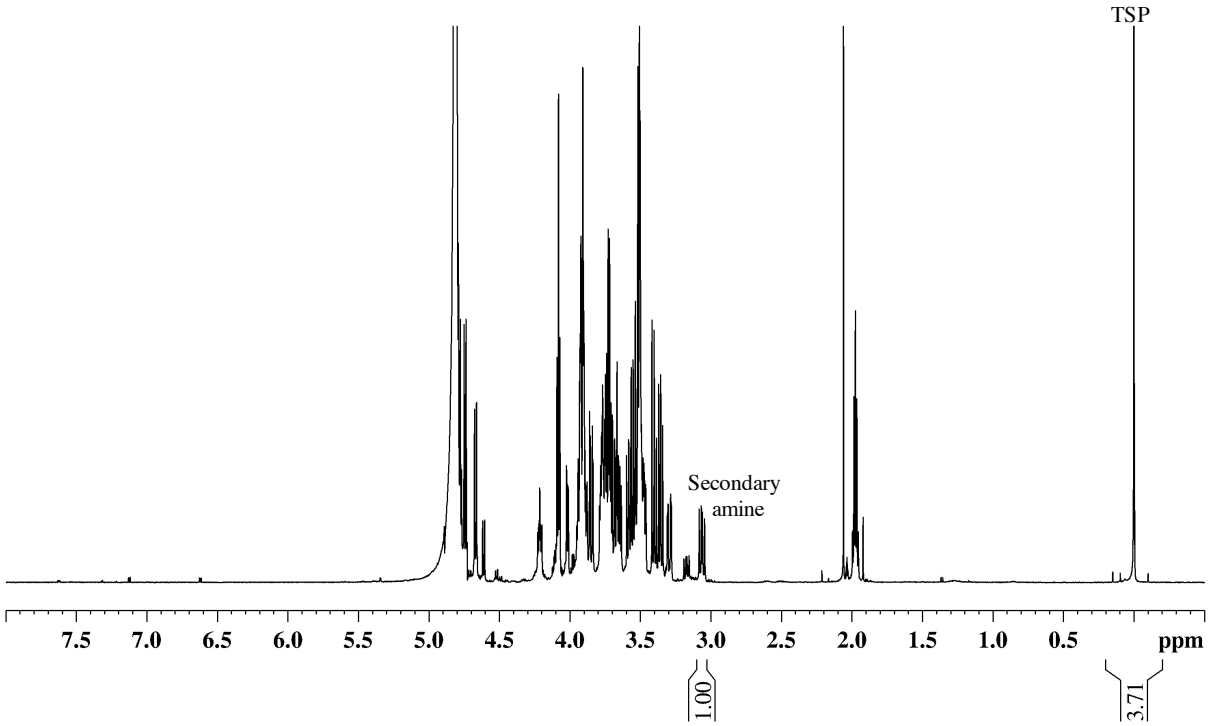

Figure C.1: ^{1}H-NMR spectrum (600 MHz, 25 °C) of SBG_4-PDHA prior to the addition of $Dext_5$ with integrated signals.

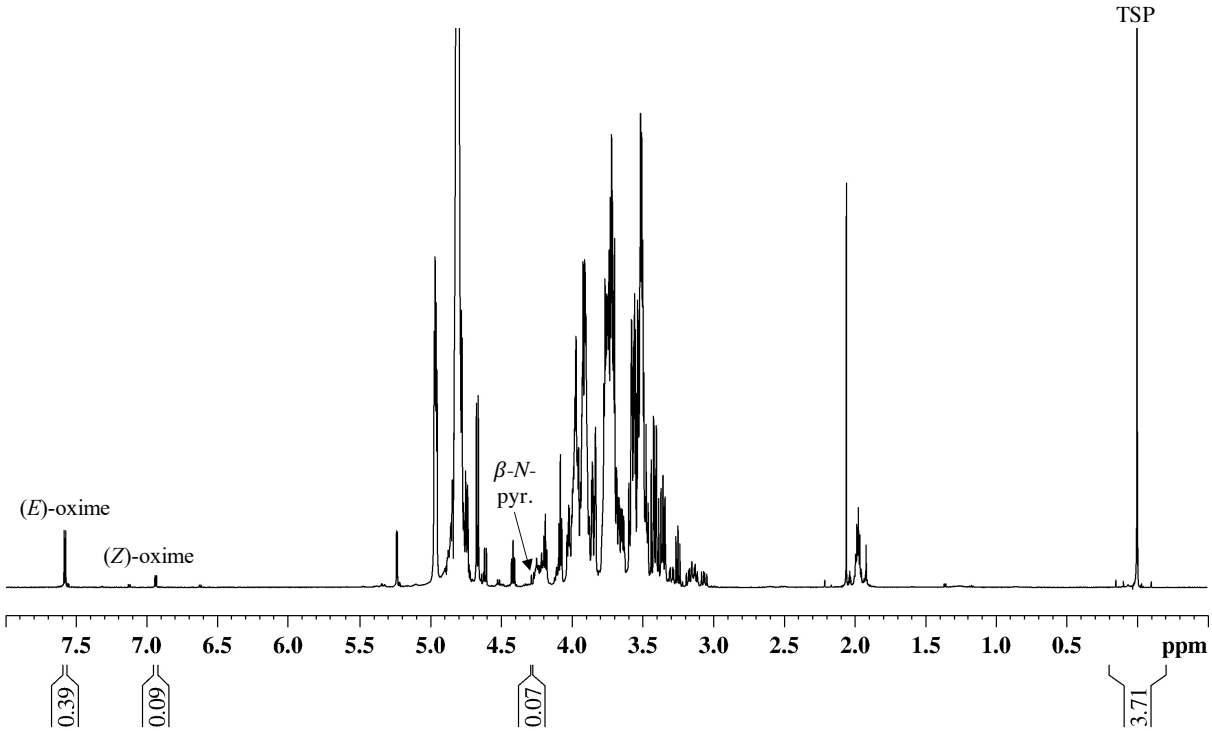

Figure C.2: ^{1}H-NMR spectrum (600 MHz, 25 °C) of SBG_4-PDHA conjugated to $Dext_5$ at equilibrium. Integrated signals for reactant and products are displayed.

The kinetic parameters obtained from the reaction of SBG_4-PDHA with an equimolar proportion of $Dext_5$ are presented in Table C.1. Simulated data for the reaction of SBG_4 to 3 equivalents $Dext_5$ is shown in Figure C.3.

Table C.1: Kinetic parameters obtained from the modelling of the reaction of SBG_4-PDHA to an equimolar proportion of $Dext_5$.

		A + B ↔ E		A + B ↔ Z		E ↔ Pyr		Z ↔ Pyr	
A	B (3x)	k_1 (h^{-1})	k_{-1} (h^{-1})	k_2 (h^{-1})	k_{-2} (h^{-1})	k_3 (h^{-1})	k_{-3} (h^{-1})	k_4 (h^{-1})	k_{-4} (h^{-1})
SBG_4-PDHA	$Dext_5$	4.0×10^{-3}	2.8×10^{-2}	6.0×10^{-4}	2.0×10^{-3}	2.2×10^{-1}	8.8×10^{-1}	2.4×10^{0}	1.8×10^{0}

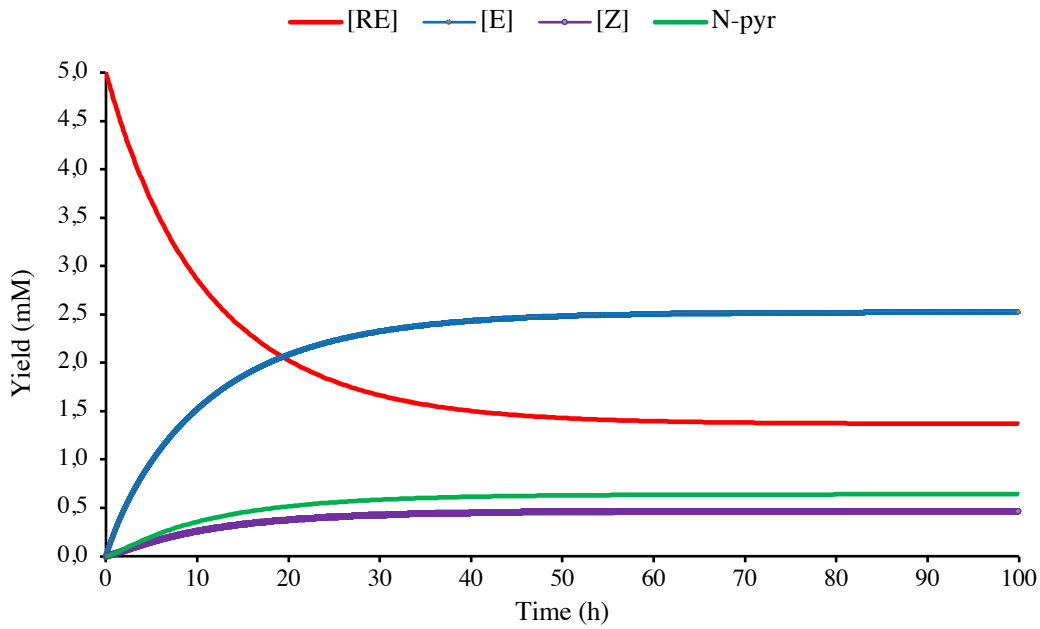

Figure C.3: Simulated data for the reaction of SBG_4 to 3 equivalents $Dext_5$.

The yield of SBG_{133}-PDHA-$Dext_m$ diblock was estimated by integrating the SEC-MALS chromatogram (Figure C.4-C.6). The SBG_{133}-PDHA-$Dext_m$ (m = 23, 35, and 52) diblock and unreacted SBG_{133}-PDHA area was found to account for 93, 74, and 57 % of the total area, respectively. Unreacted $Dext_{23}$, $Dext_{35}$, and $Dext_{52}$ accounted for the resisting 7, 26, and 43 % of the area, respectively. SBG_{133}-PDHA was reacted with $Dext_{23}$ in a molar ratio of 1:3.25. Hence the weight yield of diblock structures in the reaction was calculated to be 501 %. SBG_{133}-PDHA was reacted with $Dext_{35}$ in a molar ratio of 1:3.50. Hence the weight yield of diblock structures in the reaction was calculated to be 156 %. SBG_{133}-PDHA was reacted with $Dext_{52}$ in a molar ratio of 1:2.87. Hence the weight yield of diblock structures in the reaction was calculated to be 73 %.

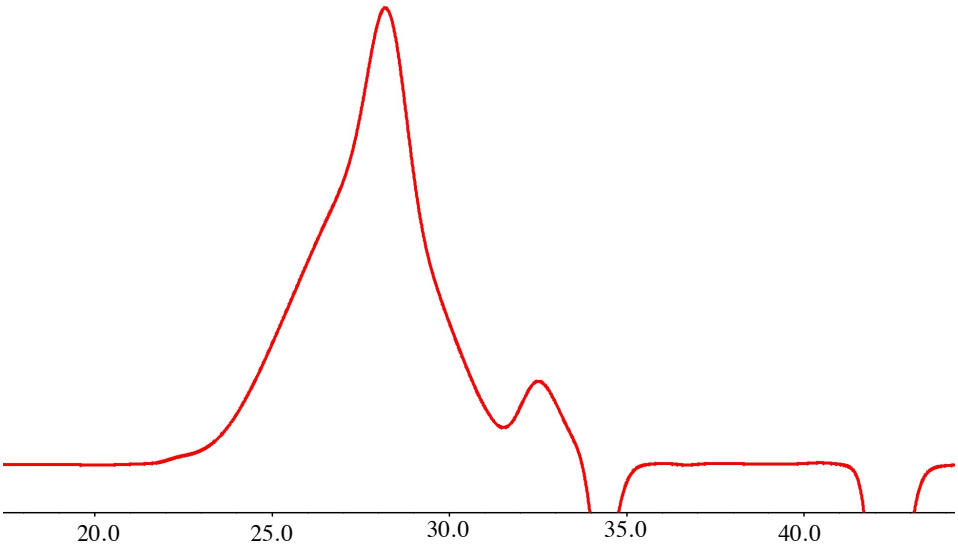

	Diblock/SBG_{133}-PDHA area	Unreacted $Dext_{23}$ area
Time (min)	23.1-31.6	31.6-33.6
Area	$7.1x10^{-5}$	$5.3x10^{-6}$
Area (%)	93	7

Figure C.4: Chromatogram of the reaction mixture obtained for the preparation of SBG diblock structures by reacting SBG_{133}-PDHA with $Dext_{23}$ in molar ratio of 1:3.25.

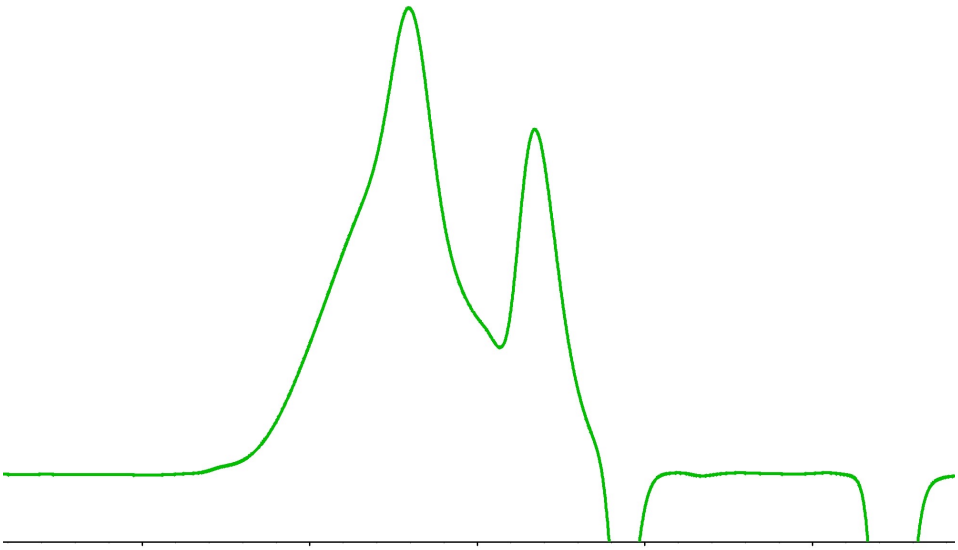

	Diblock/SBG_{133}-PDHA area	Unreacted $Dext_{35}$ area
Time (min)	23.1-30.7	30.7-33.5
Area	$6.1x10^{-5}$	$2.1x10^{-5}$
Area (%)	74	26

Figure C.5: Chromatogram of the reaction mixture obtained for the preparation of SBG diblock structures by reacting SBG_{133}-PDHA with $Dext_{35}$ in molar ratio of 1:3.5.

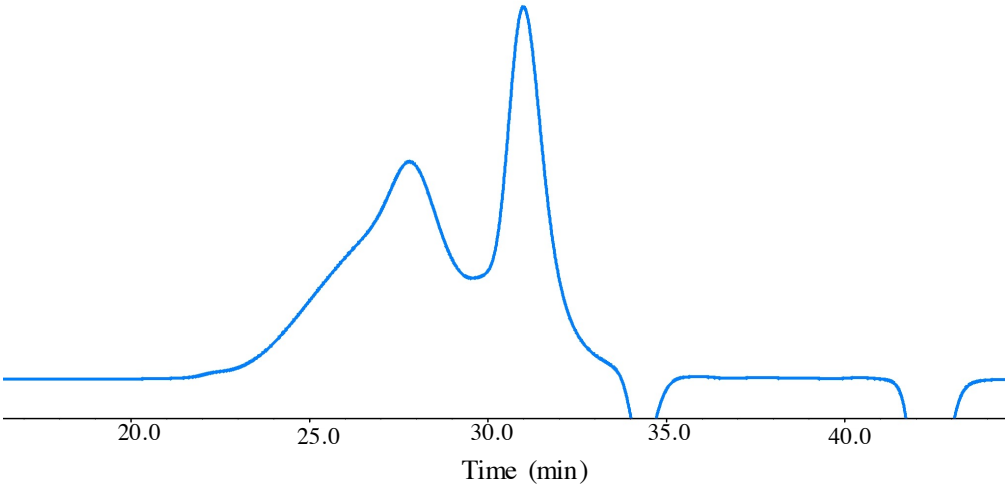

	Diblock/SBG_{133}-PDHA area	Unreacted $Dext_{35}$ area
Time (min)	23.1-29.9	29.9-33.4
Area	$4.4x10^{-5}$	$3.3x10^{-5}$
Area (%)	57	43

Figure C.6: Chromatogram of the reaction mixture obtained for the preparation of SBG diblock structures by reacting SBG_{133}-PDHA with $Dext_{52}$ in molar ratio of 1:2.87.

Appendix D

SBG-*b*-alginate diblocks were prepared by reacting SBG_9-PDHA with G_3 in an equimolar ratio. The conjugation of the second block was monitored by time-course ^{1}H-NMR. Yields were calculated relative to the signal intensity of the methylene proton of SBG_9-PDHA secondary amine at 3.02 ppm before G_3 was added. TSP was added in a known concentration as an internal standard for calibration of integrals. The spectrum taken prior to the addition of G_3 is shown in Figure D.1. The final spectrum obtained at equilibrium displayed in Figure D.2.

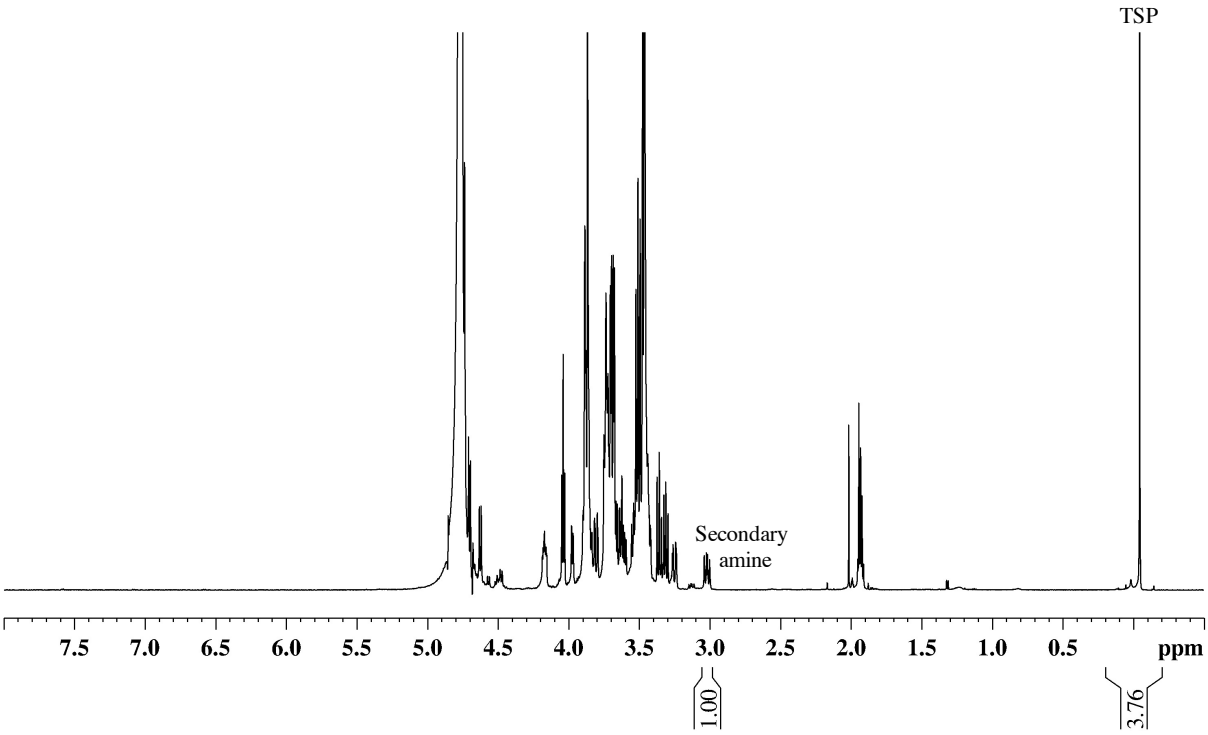

Figure D.1: ^{1}H-NMR spectrum (600 MHz, 25 °C) of SBG_9-PDHA prior to the addition of G_3 with integrated signals.

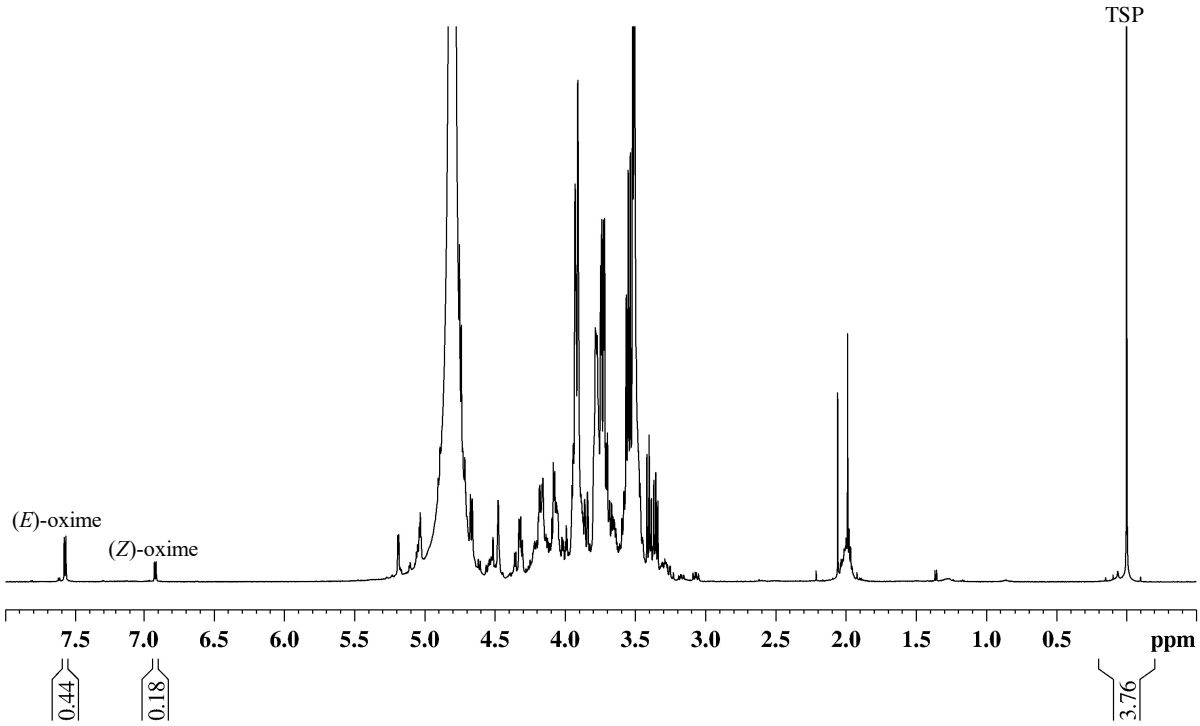

Figure D.2: ^{1}H-NMR spectrum (600 MHz, 25 °C) of SBG_9-PDHA conjugated to G_3 at equilibrium. Integrated signals for reactant and products are displayed.

The yield of SBG_{133}-PDHA-G_{18} diblock was estimated by integrating the SEC-MALS chromatogram (Figure D.3). The SBG_{133}-PDHA-G_{18} diblock area was found to account for 61 % of the total area, whereas unreacted G_{18} accounted for the resisting 39 % of the area. SBG_{133}-PDHA was reacted with G_{18} in a molar ratio of 1:5.32. Hence the weight yield of diblock structures in the reaction was calculated to be approximately 100 %.

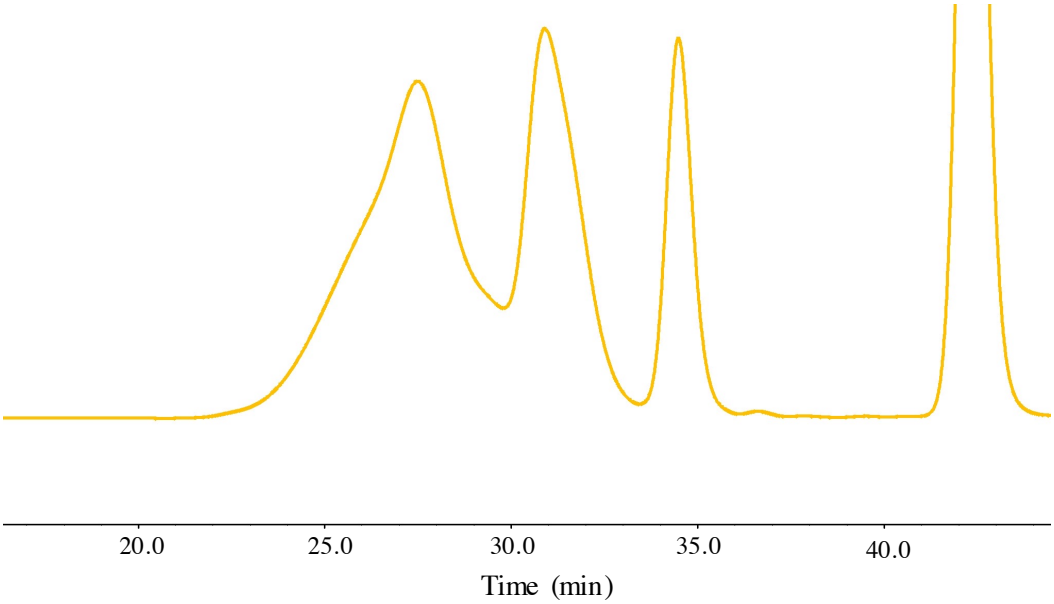

	Diblock/SBG_{133}-PDHA area	**Unreacted G_{18} area**
Time (min)	23.0-29.8	29.8-33.0
Area	$9.1x10^{-5}$	$5.7x10^{-5}$
Area (%)	61	39

Figure D.3: Chromatogram of the reaction mixture obtained for the preparation of SBG diblock structures by reacting SBG_{133}-PDHA with G_{18} in molar ratio of 1:5.32.

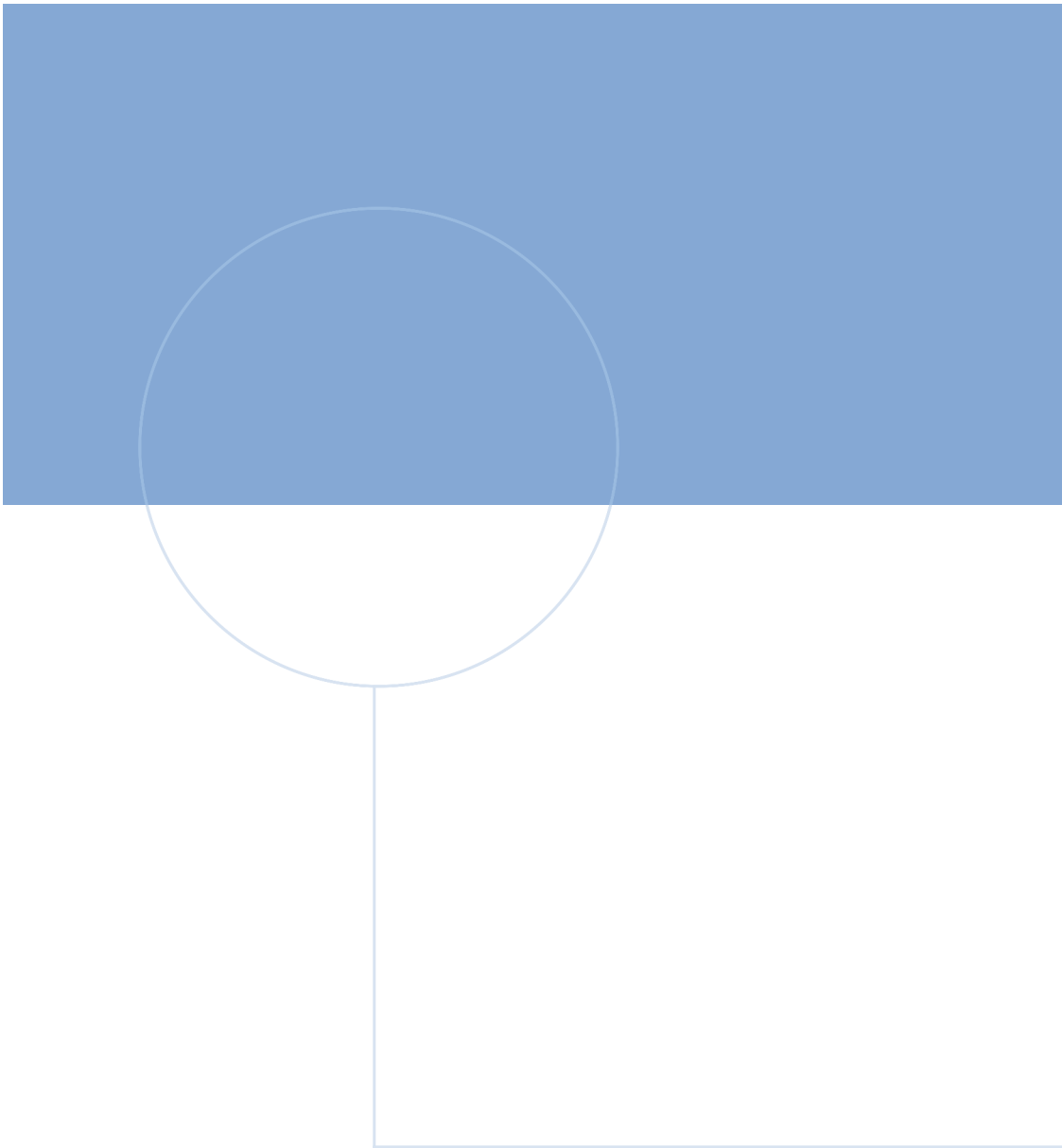

NTNU

Norwegian University of
Science and Technology